

**The Collection 6
MODIS aerosol
products over land
and ocean**

R. C. Levy et al.

The Collection 6 MODIS aerosol products over land and ocean

R. C. Levy^{1,2}, S. Mattoo^{1,2}, L. A. Munchak^{1,2}, L. A. Remer³, A. M. Sayer^{2,4}, and N. C. Hsu²

¹Science Systems and Applications, Inc, Lanham, MD 20709, USA

²Earth Science Division, NASA Goddard Space Flight Center, Greenbelt, MD 20771, USA

³JCET, University of Maryland – Baltimore County, Baltimore, MD 21228, USA

⁴Goddard Earth Sciences Technology And Research (GESTAR), Columbia, MD, USA

Received: 21 November 2012 – Accepted: 27 November 2012 – Published: 4 January 2013

Correspondence to: R. C. Levy (robert.c.levy@nasa.gov)

Published by Copernicus Publications on behalf of the European Geosciences Union.

Title Page

Abstract

Introduction

Conclusions

References

Tables

Figures

⏪

⏩

◀

▶

Back

Close

Full Screen / Esc

Printer-friendly Version

Interactive Discussion



Abstract

The twin Moderate Imaging resolution Spectroradiometer (MODIS) sensors have been flying on Terra since 2000 and Aqua since 2002, creating an incredible dataset of global Earth observations. Here, we introduce the Collection 6 (C6) algorithm to retrieve aerosol optical depth (AOD) and aerosol size parameters from MODIS-observed spectral reflectance. While not a major overhaul from the previous Collection 5 (C5) version, there are enough changes that there is significant impact on the products and their interpretation. The C6 algorithm is comprised of three sub-algorithms for retrieving aerosol properties (1) over ocean (dark in visible and near-IR wavelengths), (2) over vegetated/dark-soiled land (dark in the visible) and (3) over desert/arid land (bright in the visible). Here, we focus on the changes to both “dark target” algorithms (#1 and #2; DT-ocean and DT-land). Affecting both DT algorithms, we have updated assumptions for central wavelengths, Rayleigh optical depths and gas (H₂O, O₃, CO₂, etc.) absorption corrections, and relaxed the solar zenith angle limit (up to $\leq 84^\circ$) to increase pole-ward coverage. For DT-land, we have updated the cloud mask to allow heavy smoke retrievals, fine-tuned the assignments for aerosol type as function of season/location, corrected bugs in the Quality Assurance (QA) logic, and added diagnostic parameters such topographic altitude. For DT-ocean, improvements include a revised cloud mask for thin-cirrus detection, inclusion of wind speed dependence in the retrieval, updates to logic of QA Confidence flag (QAC) assignment, and additions of important diagnostic information. All together, the changes to the DT algorithms result in reduced global AOD (by 0.02) over ocean and increased AOD (by 0.01) over land, along with some changes in spatial coverage. Preliminary validation shows that compared to surface-based sunphotometer data, the C6 DT-products should compare at least as well as those from C5. However, at the same time as we have introduced algorithm changes, we have also been accounting for such “upstream” changes including new instrument calibration, revised land/sea masking and changed cloud masking that has resulted in changes to the coverage and global statistics of the retrieved AOD.

The Collection 6 MODIS aerosol products over land and ocean

R. C. Levy et al.

Title Page

Abstract

Introduction

Conclusions

References

Tables

Figures

⏪

⏩

◀

▶

Back

Close

Full Screen / Esc

Printer-friendly Version

Interactive Discussion



To satisfy users' desires for more complete global aerosol coverage, C6 will include a merged DT/DB product over semi-arid land surfaces. In addition to changes to aerosol retrieval, C6 will include diagnostic information about clouds in the aerosol field, such as an aerosol "cloud mask" at 500 m resolution, and products that describe the "distance to the nearest cloud" from clear pixels. Finally, responding to the needs of the air quality community, in addition to the standard 10 km product, C6 will include a global (DT-land and DT-ocean) aerosol product at 3 km resolution.

1 Introduction

Aerosols, the small, suspended liquid and solid particles in the atmosphere, are important components of Earth's climate system. Among their many roles, they force the global energy budget (IPCC, 2007), drive the hydrological cycle (Koren et al., 2011), and in large concentrations are detrimental to human health (Pope III et al., 2002).

Characterizing aerosol global distribution and changes over time are necessary for understanding present and possible future climate conditions (e.g., IPCC, 2007). Towards these goals, NASA has deployed a suite of satellites known as the Earth Observation System (EOS) to monitor a number of important climate properties, including aerosols. Two of these EOS-era satellite sensors are the twin MODerate resolution Imaging Spectroradiometers (MODIS, Salomonson, 1989), which have been flying in polar orbit on Terra since 2000 and Aqua since 2002 (Remer et al., 2008). MODIS's wide spectral range (0.41 μm to 14.5 μm in 36 channels or *bands*), broad swath (2330 km) and relatively fine spatial resolution (1 km or less depending on band) permit accurate and useful retrieval of aerosol optical depth over land, and aerosol optical depth and particle size parameter over ocean (Remer et al., 2005; Levy et al., 2007a, 2010). Aerosol retrieval is performed operationally (within 1–2 days) of satellite overpass, and is made possible by a large team of scientists and engineers. Retrieved aerosol products include total aerosol optical depth (AOD) at 0.55 μm over land and ocean, and fine mode fraction (FMF) of AOD over ocean.

The Collection 6 MODIS aerosol products over land and ocean

R. C. Levy et al.

Title Page

Abstract

Introduction

Conclusions

References

Tables

Figures

⏪

⏩

◀

▶

Back

Close

Full Screen / Esc

Printer-friendly Version

Interactive Discussion



The Collection 6 MODIS aerosol products over land and ocean

R. C. Levy et al.

Title Page

Abstract

Introduction

Conclusions

References

Tables

Figures

⏪

⏩

◀

▶

Back

Close

Full Screen / Esc

Printer-friendly Version

Interactive Discussion



In addition to providing useful information to the climate community, the instrument's 2330 km swath enables nearly global coverage every day, which makes the operational aerosol product attractive for near real time monitoring of aerosol (Al Saadi et al., 2005; Koren and Kaufman, 2004). The spatial resolution and repeatability lends to ample statistics for a variety of other applications (Stier et al., 2005; Yu et al., 2006; Kaufman et al., 2005).

Because the operational MODIS aerosol product is so important to so many applications, its continued usefulness requires a consistent effort to upgrade (better products) while maintaining its integrity (keeps working) and usability (user relearning not required). Our so-called “maintenance and modest improvement” includes streamlining the science codes, updating the processing environment along with new computer machinery, and improving the user experience when accessing and analyzing the data. It also includes, where possible, making such improvements that will increase the global accuracy and coverage of the product, without severely sacrificing regional and local accuracy.

The last major update of the dark-target aerosol product was implemented in early 2006, marking the start of Collection 5 (C5). Through validation efforts (e.g., Remer et al., 2008; Levy et al., 2010), assimilation studies (e.g., Hyer et al., 2011; Zhang and Reid et al., 2010), and other work since 2006 (e.g., Bréon et al., 2011), the C5 aerosol algorithm and products have been evaluated in detail. We have learned the conditions in which the retrieval and products have performed well, but also conditions in which the product has fallen short of expectations. From our experience when transitioning from Collection 4 (C4) to C5, we learned that we should not apply a new aerosol algorithm without completely understanding the upstream activity (e.g., calibration and cloud masking). At this point in time (fall 2012), as part of the collective MODIS science team, we have a unique opportunity for apply “modest” updates and improvements to the aerosol retrieval algorithm, while also accounting for expected changes to the input. The resulting algorithms and products will be known as Collection 6 (C6), and will be applied to all archived and future data that will be collected from both MODIS

instruments. C6 will represent a continuous consistent data record spanning more than a decade for each satellite.

In addition, in response to the air quality community's need for high resolution aerosol retrieval in urban and suburban locations (e.g., Li et al., 2005), the C6 product will not only include the standard 10 km aerosol retrieval product (Remer et al., 2005) but also global products at 3 km (Remer et al., 2012).

This paper is intended to introduce the community to the C6 aerosol algorithm and products by documenting the changes from C5 to C6. Note that C6 not only represents an update to the aerosol algorithm but also an update to all MODIS algorithms, including the calibration and cloud masking algorithms that produce the inputs to the aerosol algorithm. Even if the aerosol algorithms were to remain unchanged, the global aerosol product will be different because the inputs are different. Therefore, we focus on the changes to the aerosol algorithms, but take into account the expected changes to the inputs. When we say "aerosol algorithm", we mean the union of the "dark target" algorithms, last described by Remer et al. (2005) over ocean, and Levy et al. (2007a, b) over land. In general, the theory and science of the dark-target algorithm is relatively unchanged from C5, however, there are major changes to how data "confidence" or Quality Assurance (QA) is assigned (Hubanks et al., 2012). Obsolete parameters have been deleted from the product files, whereas new diagnostic parameters have been added. The result is more information available to recreate the conditions of the retrieval and for the user to determine what may have gone awry.

This paper can be thought of as a sort of narrative "travel-log", documenting the many changes made in upgrading from C5 to C6. In general, the changes can be separated into four categories: (a) modifications to the retrieval that will produce different values for the same parameters (b) additions and deletions to the list of available parameters (c) completely new products that will be available in separate data files, and (d) changes in the aerosol algorithm or products that were necessitated by expected changes in calibration or other upstream inputs. This paper addresses all four categories of modification.

**The Collection 6
MODIS aerosol
products over land
and ocean**

R. C. Levy et al.

Title Page

Abstract

Introduction

Conclusions

References

Tables

Figures



Back

Close

Full Screen / Esc

Printer-friendly Version

Interactive Discussion



The Collection 6 MODIS aerosol products over land and ocean

R. C. Levy et al.

Title Page

Abstract

Introduction

Conclusions

References

Tables

Figures

⏪

⏩

◀

▶

Back

Close

Full Screen / Esc

Printer-friendly Version

Interactive Discussion



In addition, there are a number of seemingly small details that have been modified or updated for C6 aerosol retrieval, especially in regard to cloud-masking and other issues of pixel selection. However, although these details are small, they may have systematic or even dramatic impacts to the products. It is also important to document these details. However, in the interest of the more casual reader, many of these details can be found in the Appendix.

In Sect. 2, we describe the MODIS Dark Target (DT)-algorithm, its history and our standard methods for evaluation. In Sect. 3, we describe changes to the DT algorithm and products for C6, divided into: changes to the overall assumptions (3.1), changes specifically for DT-land (3.2) and DT-ocean (3.3), changes to combined land and ocean (3.4), new DT products (3.5) and the Deep Blue (DB)-DT merge products (3.6). Section 4 is devoted to the new L3 aggregation protocol. Section 5 introduces a new, parallel aerosol product at higher (3 km) resolution. In Sect. 6, we show how global products are expected to change in relation to intended upgrades to L1B product calibration. In Sect. 7, we discuss how we intend to use the MODIS product to help transition to future satellite data products.

2 MODIS aerosol retrieval

2.1 MODIS terminology, specifications and basic retrieval ideas

This section introduces the MODIS terminology and retrieval methodology, to provide a baseline so we can describe the updates for C6.

MODIS observes a swath approximately 2330 km wide, and makes between 14 and 15 orbits per day. For ease of processing and data storage, MODIS data are organized into 5-minute swath segments called *granules* (288 per day), which are composed of 1354 by 2030 pixels at nominal 1 km resolution (near nadir). The fundamental MODIS file is called Level 0 (L0) and refers to raw counts from the sensor's detectors; when organized into scans, they are known as Level 1A (L1A). Level 1B (L1B) are calibrated

The Collection 6 MODIS aerosol products over land and ocean

R. C. Levy et al.

Title Page

Abstract

Introduction

Conclusions

References

Tables

Figures

⏪

⏩

◀

▶

Back

Close

Full Screen / Esc

Printer-friendly Version

Interactive Discussion

data, providing geolocated radiances or reflectances, and these L1B data are the inputs to the MODIS geophysical retrieval algorithms, including aerosol. The resulting geophysical products (in 5 min granules) are designated as Level 2 (L2). Level 3 (L3) refers to daily and monthly statistics of the geophysical products, organized on to a 1° by 1° latitude/longitude grid (King et al., 2003). Note that these products are processed in a linear fashion (L0 → L1A → L1B → L2 → L3), and that some L2 products are used as inputs for other “downstream” L2 products. This is true in the case of aerosol retrieval, which is a L2 product that requires the existence of other L2 products. All MODIS data products (from L1 onward) are provided in Hierarchical Data Format Files (HDF), and are labeled MODXX for Terra and MYDXX for Aqua. Each HDF file provides meta-data and data in parameters known as Scientific Data Sets (SDSs). SDSs may be multi-dimensional (e.g., length × width × bands).

L2 aerosol product files are known as MOD04 (Terra) and MYD04 (Aqua), collectively denoted here as MxD04 files. Retrieval of the MxD04 product requires input L1B files, L2 files, and ancillary data provided by NOAA/NCEP. L1B files include the nominal 1 km, 0.5 km, and 0.25 km reflectance products (MxD021KM, MxD02HKM and MxD02QKM), and the 1 km geo-location product (MxD03). For L2, both the “cloud-mask” (MxD35.L2) and “atmospheric profile” (MxD07.L2) are required. Ancillary data are at 1° × 1° resolution, and are the closest 6-hourly, meteorological reanalysis from the Global Data Assimilation Model (GDAS) and the daily ozone reanalysis from Total Ozone Analysis using SBUV/2 and TOVS (TOAST). The aerosol retrieval fails if any one of these input files is missing.

MODIS experiences the so-called “bowtie effect” (<http://eoweb.dlr.de:8080/short-guide/D-MODIS.html>), which means that nominal pixel size increases from nadir (1.0 × 1.0 km) to swath edges (4.8 × 2.0 km). Thus, the 1354 pixel-wide granule represents a 2330 km wide swath. Since MxD04 is not gridded, the product spatial resolution also increases toward swath edges. Standard MxD04 files (MxD04.L2) have a nominal spatial resolution of 10 × 10 km at nadir, but increase to 48 × 20 km near the swath edge. L3 products (Hubanks et al., 2008), however, are aggregated to a constant

1° × 1° grid, and are denoted as MxD08_D3 (daily), MxD08_E3 (8-day) and MxD08_M3 (monthly). Note that aerosol products are bundled with other atmospheric products (clouds and water vapor) in these L3 files (King et al., 2003).

The MODIS aerosol retrieval algorithms are maintained and updated by the MODIS aerosol science team. The operational MODIS retrieval data are produced and archived by the MODIS Distribution and Algorithm Development Support (MODAPS; <http://modaps.nascom.nasa.gov/services/>), and are available online (<http://ladsweb.gsfc.nasa.gov>). MODIS calibration is supported by the MODIS Characterization Support Team (MCST; <http://mcst.gsfc.nasa.gov>). The quality and accuracy of downstream retrieved products (including aerosol) is dependent on the accuracy of the calibration of the algorithm's input radiances, which the MCST reports accuracy of ±2–3 % for typical situations (Xiong et al., 2005, 2007).

2.2 Basic concepts of the MODIS aerosol retrieval algorithms

The MODIS aerosol algorithms have been in development for over 20 yr, well before the launch of Terra. These algorithms were designed to capitalize on the wide spectral range of the MODIS instrument. The primary assumption is that in a clear-sky (non cloudy) scene, the solar radiation backscattered from aerosols have different spectral signatures than either the Earth's surface or atmospheric molecules. By using multiple bands in the visible, near-IR, and IR wavelength regions, one can perform a retrieval to back out the aerosol signature, and infer the physical properties of the aerosols within the scene. Of course, the devil is in the details, and since the Earth's surface, molecular atmosphere and aerosols do not have entirely independent spectral signatures, the MODIS retrieval must make observational and physically based assumptions.

To that end, the operational MODIS aerosol retrieval algorithms are actually three separate algorithms; each requires separate assumptions about the Earth's surface and the expected aerosol types above these surfaces. Prior to launch, algorithm concepts were developed for vegetated land surfaces (Kaufman et al., 1997) and remote ocean regions (Tanré et al., 1997). Collectively, we denote these algorithms as the

The Collection 6 MODIS aerosol products over land and ocean

R. C. Levy et al.

Title Page

Abstract

Introduction

Conclusions

References

Tables

Figures

⏪

⏩

◀

▶

Back

Close

Full Screen / Esc

Printer-friendly Version

Interactive Discussion



The Collection 6 MODIS aerosol products over land and ocean

R. C. Levy et al.

Title Page

Abstract

Introduction

Conclusions

References

Tables

Figures

⏪

⏩

◀

▶

Back

Close

Full Screen / Esc

Printer-friendly Version

Interactive Discussion

dark-target (DT) algorithms because they operate best on regions that are “dark” visually. The third algorithm, developed well after launch, is known as the Deep-Blue (DB) algorithm (Hsu et al., 2004, 2006), and was originally designed for application over bright-desert regions. Although these surfaces appear “bright” visually, they are actually fairly dark in the near-UV (Deep Blue band near 0.41 μm), improving the signal for aerosol retrieval relative to the more central visible wavelengths. The DB algorithm is handled by a different science team, and except for a final merge to make a “best-of” product (discussed in Sect. 3.6), this paper focuses only on the development of the C6 DT aerosol product.

Prior to launch, the physical and numerical assumptions that form the basis of the DT algorithms, as well as the proto-algorithms themselves, were tested using mathematical techniques and by using proxy data obtained from aircraft instruments and field experiments (Tanré et al., 1996; Kaufman, 1997; Chu et al., 1998; Remer and Kaufman, 1998; Tanré et al., 1999). Although the details of the DT algorithms have evolved over time, the basic concepts remain unchanged. There are complete descriptions of the C5 DT algorithms in the literature (e.g., Levy et al., 2010; Remer et al., 2005, 2008) and within the online Algorithm Theoretical Basis Documents (ATBD, Levy et al., 2009). Here we provide only a summary.

Tanré et al. (1996) explained that to increase signal-to-noise, the MODIS aerosol retrieval is performed at a lower resolution (e.g., 10 km at nadir) than the inputted spectral reflectance data (e.g., 500 m). Pixels that are non-optimal for aerosol retrieval, for whatever reason, can be screened out yet leave enough “good” pixels to make a successful retrieval. The pixel data are organized into N by N boxes (e.g., 20 by 20), and the geo-location information (e.g., MxD03 or MxD35) are used to determine nominal surface type (water, land or other) of the scene, and which fork of the retrieval to follow. If all (100 %) pixels are considered “water”, then the over-ocean algorithm is performed. If any pixel (at least 1) is considered “land”, then the land retrieval is attempted. If a scene has no land pixels, but has at least one “other” pixel (e.g., coastal or lake shore), then no retrieval is attempted at all. Regardless of which fork is chosen, it is

**The Collection 6
MODIS aerosol
products over land
and ocean**

R. C. Levy et al.

Title Page	
Abstract	Introduction
Conclusions	References
Tables	Figures
⏪	⏩
◀	▶
Back	Close
Full Screen / Esc	
Printer-friendly Version	
Interactive Discussion	

not likely that all pixels are suitable for aerosol retrieval. For example, there is a test to determine if a “land” pixel is in fact contaminated by water (e.g., small stream, puddle). Likewise, there is a test (Li et al., 2003) to filter out shallow “water” pixels contaminated by underwater sediment. Other tests filter out ice/snow pixels (Li et al., 2005), bright land scenes, glint over water, etc. Finally, Martins et al., (2002) describe how to filter out cloudy pixels. Once all unsuitable pixels are removed, the procedure then arbitrarily discards the brightest 25 % and darkest 25 % of remaining pixels over ocean, and the brightest 50 % and darkest 20 % over land. Because the reflectance has been screened for clouds and non-optimal surfaces, and the remaining pixels have been further filtered, residual contamination is minimized over most situations. Furthermore, the retrieval performs corrections for absorption by atmospheric gases, including water vapor, ozone, and carbon dioxide.

The pixels that remain, after all de-selection and gas corrections are applied, are understood to represent the conditions that aerosol retrieval is possible (e.g., Remer et al., 2012). These pixels are averaged, yielding a final set of mean spectral reflectance that is understood to be representative of optimal retrieval conditions, e.g., clear skies, no gases, and low surface variability. The algorithm takes this set of “observed” Top-of-Atmosphere (TOA) spectral reflectance, and tries to match to values within Look Up Tables (LUTs). These LUTs have been pre-computed by using radiative transfer code to simulate spectral TOA reflectance under a variety of aerosol and surface conditions. These LUTs are indexed by aerosol type, aerosol loading (total optical depth at 550 nm), and parameters of sun/satellite geometry. Over ocean, the LUT includes the optical properties of ocean (whitecaps, foam, water-leaving radiance) coupled with the atmosphere (molecular plus aerosol). Over land, the LUT is calculated over a black surface, so that the TOA includes only for molecular (Rayleigh) plus aerosol contributions.

Although both DT algorithms perform inversions to find matches to the LUT, the required assumptions are different. Over the ocean, except for where there is glint, sediments or other surface contamination, surface reflection becomes negligible as



The Collection 6 MODIS aerosol products over land and ocean

R. C. Levy et al.

Title Page

Abstract

Introduction

Conclusions

References

Tables

Figures

⏪

⏩

◀

▶

Back

Close

Full Screen / Esc

Printer-friendly Version

Interactive Discussion

the wavelength increases. This means, that a reflecting aerosol layer provides good contrast over the ocean, and that at least two pieces of aerosol information (loading, size) can be retrieved (Tanré et al., 1996). Spectral reflectance (ρ_λ) observations in six wavelengths (0.55, 0.65, 0.86, 1.24, 1.63, and 2.11 μm) are compared with values in the LUT. It is assumed that the ambient aerosol is composed of a linear combination of *fine* and *coarse* aerosol *modes* from the LUT, where the fine mode is picked from four choices and the coarse mode from five. The retrieved products over ocean are total aerosol optical depth (AOD or τ) at 0.55 μm , fine mode fraction of AOD (FMF or η), which combination of fine and coarse modes, and the least squares spectral fitting error (ε).

On the other hand, over land, the surface is much more variable, and is dark enough only under some conditions. Therefore, many more assumptions need to be made about the surface and aerosol type, in order to accurately determine only one piece of information (aerosol loading). Kaufman et al. (1997) discovered that in many vegetated regions, there is an observed relationship between surface reflectance between 0.47, 0.65 and 2.11 μm (“VISvs2.1”, Levy et al., 2007b). Therefore, observation/LUT comparison is done in only these three wavelength bands. Since the LUT is calculated without surface contributions, the algorithm is constrained by the surface spectral relationships. In addition, the expected aerosol type is prescribed as a linear combination of *fine-dominated model* type, and *coarse-dominated model* types (each having multiple modes themselves). Since the land algorithm tries to deal with larger surface uncertainty with only three spectral bands, both fine and coarse-dominated aerosol types must be prescribed as a function of season and location. The retrieved products over land include total AOD (0.55 μm), fraction of fine-dominated aerosol type (here, also called FMF), constrained surface reflectance, and fitting error.

This means that for both DT algorithms, the primary retrieved products are the total AOD at 0.55 μm (τ), the fractional contribution (η) of the fine aerosol type (mode over ocean, model over land) and the spectral fitting error (ε). Each algorithm reports additional derived and diagnostic parameters. Derived parameters can be calculated

The Collection 6 MODIS aerosol products over land and ocean

R. C. Levy et al.

Title Page

Abstract

Introduction

Conclusions

References

Tables

Figures

⏪

⏩

◀

▶

Back

Close

Full Screen / Esc

Printer-friendly Version

Interactive Discussion



from information contained within the LUT and/or other retrieved products. For example, knowing the resulting total AOD and fine aerosol fraction, it is easy to derive AOD in other wavelengths, and then further calculate Ångström Exponent (AE) based on the spectral dependence of AOD. Diagnostic parameters include information used to perform the retrieval, as well as information about the retrieval itself. Solar zenith angle is an example of information going into the retrieval; the number of pixels used, is an example of information about the retrieval.

This brings us to the concept of Run-Time Quality Assurance (QA) (Hubanks et al., 2012). At each stage in the retrieval an evaluation is made of the situation and a flag switched on or off that describes the results of that evaluation. Input data, the logical flow of the algorithm, and the results are each evaluated in turn. The QA procedure takes note of such information as how many pixels were thrown out during cloud masking, how well the retrieval solution fits the observations, and whether or not the solution characterized realistic physical conditions. Each test triggers its own QA flag. If, during the retrieval, some aspect is less than ideal, the overall accuracy of the retrieval is expected to degrade. Ideal performance is given the highest QA “Confidence” value (QAC = 3), with good, marginal and no confidence retrievals given QAC values of 2, 1 and 0, respectively. The results of the many individual QA tests, plus the final determination of QAC are all coded into a five-byte SDS. Different bits represent the results of individual tests (e.g., Levy et al., ATBD, 2009).

2.3 Evaluation of the C5 MODIS aerosol products

Immediately following Terra launch the first aerosol products were evaluated in a variety of ways that included qualitative examinations and quantitative comparisons of data collected from collocated sunphotometer (SP) data including those from Aerosol Robotic NETwork (AERONET) stations (Holben et al., 1998; Ichoku et al., 2002; Chu et al., 2002; Remer et al., 2002). Evaluation led to modifications of the algorithm to avoid problematic situations and also to add capability, extend range of retrievals and provide new products. Each major change to the algorithm is labeled a “Collection”, although

The Collection 6 MODIS aerosol products over land and ocean

R. C. Levy et al.

Title Page	
Abstract	Introduction
Conclusions	References
Tables	Figures
⏪	⏩
◀	▶
Back	Close
Full Screen / Esc	
Printer-friendly Version	
Interactive Discussion	

5 minor changes had made under the same Collection number. The early Collections were frequently revised. The first set of validated products appeared in Collection 2 (C002), although these were quickly replaced by C003 within the first two years of Terra launch. C004 was the first stable, widely used and well-documented set of MODIS aerosol products (Remer et al., 2005). However, the C004 aerosol product over land produced unacceptable levels of bias (Levy et al., 2005). A second-generation land algorithm was developed and implemented as C5 (Levy et al., 2007a and b) and other changes were implemented at the same time. The MODIS Deep Blue algorithm (Hsu et al., 2006) was added to the Collection 5 processing after the processing had already
10 begun and was thus labeled Collection 5.1 (C51). Since the dark-target algorithms are identical for C5 and C51, we refer to them both as “C5”. Details of the C5 DT algorithms are presented in the literature (Remer et al., 2005, 2008 over ocean; Levy et al., 2007a and b over land) as well as within the online ATBD (Levy et al., 2009).

15 Identical C5 DT aerosol retrieval algorithms have been applied to the entire time series of both MODIS’s data (2000/2002 through 2011). This has allowed time for an exhaustive evaluation process, including numerous papers on global, regional and local MODIS product “validation”. Global validation has been performed by comparing MODIS-retrieved AOD and size parameters to similar parameters observed from Aerosol Robotic Network’s (AERONET; Holben et al., 1998) suite of fixed ground-based sunphotometers, both over land (Levy et al., 2010) and over ocean (Remer et al., 2008). In addition to these global studies, MODIS has also been compared to additional ground based (e.g., Levy et al., 2005), air-borne (e.g., Redemann et al., 2009) and moving ship-borne SPs (e.g., Kleidman et al., 2012).
20

25 Most of the validation studies concluded that, in general, MODIS C5 retrieved aerosol products were comparable to sunphotometer based products, and an expected error (EE) envelope could be defined that contained at least 67 % (approximately one standard deviation) of the matchups. This comparability depended on conditions of the observation scene (location, season, etc.) as well as the estimated QAC of the retrieval. Thus, the EE for total AOD (at 0.55 μm) was described as $\pm(0.03 + 5\%)$ over



of data from both satellites. Large statistical evaluation required processing of multiple months of data across multiple years, nominally all Januarys and Julys from 2003, 2008 and 2010.

To assess the impacts of different algorithm upgrades, our metrics included basic statistics (global mean AOD, number of valid retrievals), histograms, difference maps (e.g., “new-baseline”) and dual collocation with AERONET or other SP data. From these tests, we could determine whether the change had a significant global impact, where it had significant impact, and whether or not it pushed MODIS data closer to or farther from SP values. In addition to the changes that were actually implemented (and described in this paper and appendices) for C6, we note that there were other proposed changes that were abandoned.

3 Changes to the dark-target aerosol retrieval algorithms

In this section, we describe the major changes to the DT (land and ocean) aerosol algorithms and products. Section 3.1 concerns changes that are common to both algorithms, whereas Sects. 3.2 and 3.3 are concerned with changes to the specific algorithms over land and ocean, respectively. Section 3.4 discusses the combined products. New cloud mask products are discussed in Sect. 3.5, whereas a new DT/DB merge is introduced in Sect. 3.6.

3.1 Changes common to both land and ocean algorithms

Since C5 began processing almost six years ago, we have had the opportunity to revisit some of the assumptions that had been implemented even before there was an operational MODIS algorithm. For example, the central wavelengths, Rayleigh optical depth assumptions over ocean, and gas column absorption corrections were all based on MODIS instrument characterization and modeling that was performed prior to Terra launch. What kind of errors might be induced by uncertainties in the exact specifica-

**The Collection 6
MODIS aerosol
products over land
and ocean**

R. C. Levy et al.

Title Page

Abstract

Introduction

Conclusions

References

Tables

Figures



Back

Close

Full Screen / Esc

Printer-friendly Version

Interactive Discussion



The Collection 6 MODIS aerosol products over land and ocean

R. C. Levy et al.

Title Page

Abstract

Introduction

Conclusions

References

Tables

Figures

⏪

⏩

◀

▶

Back

Close

Full Screen / Esc

Printer-friendly Version

Interactive Discussion



The other change affecting both land and ocean is the extension of retrievals to more oblique solar zenith angles that increases coverage at high latitudes. The C5 algorithm did not permit retrieval when the solar zenith angle (θ_0) was larger than 72° . There were no aerosol retrievals made for relatively high latitude regions during low-light seasons, even though interesting aerosol events were seen in MODIS imagery (Crusius et al., 2011). Motivated to increase coverage of these events, we added solar zenith angles of $\theta_0 = 78^\circ$ and $\theta_0 = 84^\circ$ to both ocean and land LUTs, after confirming with the authors of the RT codes (Z. Ahmad, personal communication, 2011) that slant path errors should not be too large at these angles. The Fig. S8 (auxiliary material) within Crusius et al. (2011), demonstrates that relaxing the solar zenith angle threshold ($\theta_0 \leq 84^\circ$) enables retrievals of dust in the Gulf of Alaska. Overall, when applied to multiple months of data (Januarys and Julys, 2003 and 2008), the new threshold adds approximately 1 % and 8 % to the number of valid aerosol retrievals over land and ocean, respectively. Preliminary comparison to AERONET suggests that accuracy is not compromised.

To summarize, this section has introduced only the C6 changes that were intended to homogenize radiative transfer assumptions (wavelength bands, Rayleigh optical depths and gas absorption corrections) and increase satellite retrieval coverage (larger solar zenith angles). Figure 1 shows aggregated Level 2 data from Terra for July 2008, on $1^\circ \times 1^\circ$ gridding, where the aerosol retrieval algorithm and the inputs (L1B and ancillary data) are held constant. Only the LUTs have changed. From “old” (C5) to “new” (homogenized, C5.V6Gas), the overall AOD is reduced by 0.003 over ocean, and increased by 0.008 over land (combined ocean/land decreased by 0.002). The most significant change is additional coverage over the higher latitudes in the winter hemisphere, increasing the number of valid retrievals by 5 %.

3.2 Changes for DT-land

The C5 over land DT retrieval has been carefully validated using collocated sunphotometer measurements (Levy et al., 2010; Bréon et al., 2011). These studies show that

sorption ($SSA < 0.95$) and “dirty” dust days with higher absorption fraction. Sensitivity tests showed that if we could correctly assign the more absorbing coarse model, the MODIS aerosol retrieval might have more sensitivity to FMF. To test, we created an absorbing coarse dust model LUT, and allowed the operational MODIS code to try and retrieve it. However, in practice, the more absorbing dust model did not give the MODIS operational algorithm any new skill. The variability of the surface was still dominating, so that a combination of absorbing dust and non-absorbing fine model was not sufficiently better than a combination of non-absorbing dust and absorbing fine model. Thus, without a clear logic for choosing between absorbing and non-absorbing dust in the MODIS aerosol retrieval, we chose to keep only the single coarse model type (weakly absorbing, non-spherical dust); the coarse model is unchanged from C5.

3.2.2 Land surface assumptions

Levy et al. (2010) clearly showed that the C5 MODIS land product did not compare as well to AERONET in regions with brighter surfaces and/or mountainous terrain (e.g., US southwest, Mongolia, etc.). As the algorithm is tuned towards dark, vegetated targets, this result was not surprising. However, given that the MODIS dataset had doubled since 2005 and AERONET included many new sites, we attempted to reformulate the assumed surface spectral VISvs2.1 relationship (Kaufman et al., 2005; Levy et al., 2007b). Similar to the procedure described by Levy et al. (2007b), atmospheric correction was performed over the entire collection of MODIS/AERONET collocations. There were differences between these results and those using the 2005 data base. However, any attempt to tune a new parameterization relating VIS surface reflectance to $2.11 \mu\text{m}$ reflectance using these new results introduced greater overall uncertainty in the retrieval than had existed for C5. Bright surfaces might improve, but then dark surface retrievals would degrade. The C6 algorithm simply uses the C5 surface reflectance relationships (Levy et al., 2007b) that continue to provide the best overall retrievals.

We also considered alternatives to surface reflectance parameterization. One idea was to abandon the on-the-fly VISvs2.1 assumptions and instead rely on climatology

The Collection 6 MODIS aerosol products over land and ocean

R. C. Levy et al.

Title Page

Abstract

Introduction

Conclusions

References

Tables

Figures



Back

Close

Full Screen / Esc

Printer-friendly Version

Interactive Discussion



**The Collection 6
MODIS aerosol
products over land
and ocean**R. C. Levy et al.

[Title Page](#)[Abstract](#)[Introduction](#)[Conclusions](#)[References](#)[Tables](#)[Figures](#)[⏪](#)[⏩](#)[◀](#)[▶](#)[Back](#)[Close](#)[Full Screen / Esc](#)[Printer-friendly Version](#)[Interactive Discussion](#)

of MODIS albedo (e.g., Moody et al. 2005, 2008; Schaaf et al., 2010). While direct application of gridded MODIS-derived albedo (instead of surface reflectance) introduced significant errors to the aerosol retrieval, we saw promise when using *ratios* of spectral surface albedo in place of assumed VISvs2.1 parameterization. In general, improvements were made (reducing bias compared to AERONET) in the relatively brighter arid regions without harming the comparisons over most vegetated surfaces. However, without discussing details, successful application of the albedo dataset required a huge amount of processing and computer overhead, and we found issues with latitude/longitude registration over highly heterogeneous surfaces (e.g., urban areas). Therefore, while the application of surface albedo climatology may be a good step for the future, we decided to abandon this approach for now. For C6, we continue to use the VISvs2.1 surface reflectance parameterization originally introduced for C5 (Levy et al., 2007b).

3.2.3 Cloud mask and pixel selection

The success of the MODIS dark-target retrieval depends on its ability to throw out unsuitable pixels. At a minimum, the over-land DT algorithm throws out 70% of the observed 500 m resolution data, (darkest 20% and 50% brightest when sorted by 0.66 μm reflectance). However, in most cases, some pixels are completely unsuitable for aerosol retrieval, including clouds, snow and inland water bodies.

The most critical step is accurate cloud masking. Failure to fully remove clouds leads to cloud contamination, and too strong a cloud mask leads to insufficient aerosol coverage. Because the standard MODIS cloud mask (MxD35_L2) is designed to mask pixels that are unsuitable for land-surface retrieval (clouds and heavy aerosol) and at the same time find pixels suitable for cloud product retrieval (not aerosol), it was viewed to be both overly conservative and not conservative enough for aerosol retrieval (Remer et al., 2012). Therefore, based on unpublished work analogous to Martins et al. (2002), the over-land aerosol retrieval applies tests for visible-band (0.47 μm) brightness and spatial variability at 500 m resolution, in conjunction with tests for infrared (1.38 μm ,

The Collection 6 MODIS aerosol products over land and ocean

R. C. Levy et al.

Title Page

Abstract

Introduction

Conclusions

References

Tables

Figures

⏪

⏩

◀

▶

Back

Close

Full Screen / Esc

Printer-friendly Version

Interactive Discussion



the “cirrus” channel) reflectance and spatial variability at 1 km resolution. Values for C5 thresholds were based on visual analyses of multiple granules and statistical analyses of global data, and were documented in the online C5-ATBD (Levy et al., 2009).

However, both Witte et al. (2011) and von Donkelaar et al. (2011) noted that operational MODIS aerosol retrieval failed to capture the extreme Russian fire events of 2010. Although in some cases the retrieval failed because the final value of AOD (> 5.0) was extrapolated outside of the lookup table, there were also many cases where failure occurred because the aerosol cloud mask thresholds were exceeded. Retrieval of the extremely heavy smoke (AOD $\gg 1.0$) in the middle of the plumes required either turning off the cloud mask, or finding a suitable aerosol “call-back” test. Since fine-dominated smoke has weaker signal in $2.11 \mu\text{m}$ than $0.47 \mu\text{m}$, and the region around Moscow has relatively small surface spatial variability at $2.11 \mu\text{m}$, clouds and smoke might be separated by the spectral dependence of their spatial variability. Thus a $2.11 \mu\text{m}$ spatial variability test ($\sigma_{2.11}$) was implemented, such that areas that failed the $0.47 \mu\text{m}$ variability test could be recovered by passing the new $2.11 \mu\text{m}$ test. Aerosol coverage for the Moscow fires was increased by 20 %.

Unfortunately, while successful for the Moscow region, the $2.11 \mu\text{m}$ aerosol recovery test did not end up working globally. Surface variability at $2.11 \mu\text{m}$ is often so much larger than it is at $0.47 \mu\text{m}$, that the combined surface/aerosol variability may be no different than clouds. While looking for alternatives, we found that combining two $0.47 \mu\text{m}$ spatial variability tests sometimes could help. There is the “absolute standard deviation” of the reflectance within a 3×3 box (std_047 or $\sigma_{0.47}$), as well as the “mean weighted standard deviation” (mstd_047 or $\sigma^*_{0.47}$), where

$$\sigma^* = \frac{\sigma \bar{\rho}}{\sqrt{n}}, \quad (1)$$

where $\bar{\rho}$ is the mean reflectance (mean_047) and $n = 9$ (3×3 pixel box). Since the possibility of being flagged as “cloud” increases with both the variability and the magnitude of the reflectance, the σ^* test might be mistaking brighter, less variable smoke

for darker, more variable clouds, which could be called back with regular σ . Therefore, instead of using a $2.11 \mu\text{m}$ test to recover heavy aerosol, C6 will use regular standard deviation ($\sigma_{0.47}$) as an aerosol call back test. This is an addition to the mstd_047 test that is retained from C5.

Thus, the C6 over-land cloud mask is a combination of tests using absolute magnitude and spatial variability at $0.47 \mu\text{m}$ (500 m resolution) and $1.38 \mu\text{m}$ (1 km resolution). Based on analyses of many individual granules, plus statistics of global, monthly data, the C6 cloud detection thresholds are set as follows. A given 500 m pixel is flagged as a cloud if the $0.47 \mu\text{m}$ reflectance exceeds 0.4 ($\rho_{0.47} > 0.4$). For each 3×3 box of 500 m pixels, the center pixel is flagged as cloud if both ($\sigma_{0.47}^* > 0.0025$ and $\sigma_{0.47} > 0.0075$). A given 1 km pixel is flagged as cloud if $\rho_{1.38} > 0.025$. For each 3×3 box of 1 km pixels, the center pixel is flagged if $\sigma_{1.38} > 0.003$. Note there is no $\sigma_{1.38}^*$ test. Finally, if any one 1 km pixel is indicated as cloud then the entire 2×2 box of 500 m pixels are considered cloud. Note that except for addition of the $\sigma_{0.47}$ requirement, all other tests and thresholds are identical to that used for C5. The final result is a binary cloud mask (yes or no) at 500 m resolution, which is saved in memory and used to filter pixels for final aerosol retrieval. Figure 3 is an example of a granule over northeastern South America, where 533 new pixels (5% increase from 10 108) have been retrieved when including the $\sigma_{0.47}$ requirement. Note that the additional pixels retrieved for C6 are located in areas of low optical depth ($\tau < 0.15$) as well as areas of high optical depth ($\tau > 0.75$) within the smoke plume.

3.2.4 Quality assurance

The Run-Time Quality Assurance (QA) Plan (Hubanks et al., 2012) over land is essentially unchanged from C5. There are multiple tests to assess the input data, the logical flow of the algorithm, and then the believability of the results. The results of the many individual QA tests, lead to an estimate of the overall quality confidence (QAC) of the retrieved products. All QA information is coded into a five-byte SDS, such that different

**The Collection 6
MODIS aerosol
products over land
and ocean**

R. C. Levy et al.

Title Page

Abstract

Introduction

Conclusions

References

Tables

Figures



Back

Close

Full Screen / Esc

Printer-friendly Version

Interactive Discussion



bits represent the results of individual tests, and are described in more detail in the Appendix.

For example, one such QA test asks whether there are a sufficient number of non-screened pixels to make a robust aerosol retrieval. If more than 50 pixels remain (out of a possible 120, which is in turn a 70 % exclusion of the original 400), then $QAC = 3$. More than 30, 20 and 12 (10 % of 120) result in $QAC = 2, 1$ and 0, respectively. Fewer pixels suggest increasingly marginal conditions in the retrieval box, and the retrieved AOD is expected to be less accurate.

In addition to explicit cloud masking (determining which pixels to exclude from the aerosol retrieval), the retrieval uses other tests to determine if clouds might be present and possible source of aerosol contamination. One such test is the thin-cirrus test. While pixels with $\rho_{1.38} > 0.025$ are considered to be “cloud” and masked, pixels with $\rho_{1.38} > 0.01$ are used, but flagged as “thin cirrus”. These pixels may have residual contamination, but are included in the aerosol retrieval. If any “thin cirrus” pixels are present, the entire retrieval is tagged and the QAC reduced as 0.

Yet, while this “thin cirrus” test was included within the C5 algorithm, the test was coded in error, such that it the $QAC = 0$ tag could be overwritten. In some of these cases, “thin cirrus” cases were mistakenly assigned $QAC = 3$ (high quality). This coding logic error led to biased AOD statistics, especially over tropical land surfaces. Figur 4 shows a granule with clouds visible to the middle-right of the true-color RGB image over Africa. Without the cirrus coding fix, there were cirrus-present pixels that would have been tagged with $QAC = 3$. With the fix, the high-confidence AOD data stay further from this cloudy area, resulting in a 10 % pixel reduction for this granule. Including both the $\sigma_{0.47}$ call-back test (Sect. 3.2.3) and fixing the ρ_{138} thin-cirrus test, resulted in modest overall increase of the the number of global high-quality pixels.

Other than the changes to logic related to the cirrus flag, the QA plan for C6 over land remains the same as for C5. Table A4 in the Appendix details the QA plan applied for C6.

The Collection 6 MODIS aerosol products over land and ocean

R. C. Levy et al.

Title Page

Abstract

Introduction

Conclusions

References

Tables

Figures

⏪

⏩

◀

▶

Back

Close

Full Screen / Esc

Printer-friendly Version

Interactive Discussion



3.2.5 Deleted and new products

For the Level 2 product (MxD04_L2), the list of over-land SDSs in C6 are compared to those from C5 (Table 1). The most significant change is that the ETA parameter (FMF: Optical_Depth_Ratio_Small_Land) will be the only reported aerosol size characteristic.

5 On a global basis, we and others have found little quantitative skill in MODIS-retrieved aerosol size parameters over land (e.g., Levy et al., 2010; Mishchenko et al., 2010). We have decided to discontinue further attempts at validating Ångström Exponent (AE) and fine-AOD. However, since the ETA parameter is part of the retrieval solution, and a necessary diagnostic, it will continue to be reported for C6. A user can still choose
10 to derive AE (from spectral AOD) or fine-AOD (from product of $\tau\eta$) and evaluate the results themselves.

For C6, there are new, deleted, and renamed products (see Table 1). The diagnostic product, “Topographic_Altitude_Land” is new, and represents the elevation of the land target’s center. We now report dark-target reflectance (“Mean_Reflectance_Land”) and subpixel (1 km resolution) counts in three additional wavelengths (0.41, 0.44 and 0.76 μm). To reduce confusion related to an experimental product that was never properly validated, all SDSs related to calculation of Critical Reflectance and Path Radiance have been deleted. Finally, to reduce confusion between users of the MODIS “Aerosol” cloud mask, and the “Wisconsin” cloud mask (MxD35_L2), our internal cloud mask
20 fraction has been renamed to “Aerosol_Clo_Fraction_Land”. Although the “Corrected_” prefix of “Corrected_Optical_Depth_Land” may be misleading to some users (there is only one retrieval and nothing to correct), a sufficient number of MODIS data users requested the SDS’s name be continued for C6, and thus it remains unchanged.

3.2.6 Comparison with C5 products and AERONET

25 At this point, we have introduced the changes applied to the DT-land aerosol retrieval algorithm, including changes to Rayleigh assumptions, gas correction, aerosol retrieval boundaries, cirrus fix, cloud mask, and QAC revision. How do all these changes affect

The Collection 6 MODIS aerosol products over land and ocean

R. C. Levy et al.

Title Page

Abstract

Introduction

Conclusions

References

Tables

Figures



Back

Close

Full Screen / Esc

Printer-friendly Version

Interactive Discussion



The Collection 6 MODIS aerosol products over land and ocean

R. C. Levy et al.

Title Page

Abstract

Introduction

Conclusions

References

Tables

Figures

⏪

⏩

◀

▶

Back

Close

Full Screen / Esc

Printer-friendly Version

Interactive Discussion

the DT-land aerosol *products* on a global scale? Using a near-final version of the DT-algorithm (referred to as V6.0.13), six full months of aerosol products from Aqua (Januarys and July, from 2003, 2008 and 2010) were processed. Table 2 reports global, Level 2 pixel statistics for January and July 2008, demonstrating the change of QAC distribution from C5 to C6. Also reported are the simple mean of the global AOD for all pixels having sufficient quality of QAC = 3. For these two months, we see that although total coverage (valid count) is increased by 4.6 %, the number of QA filtered retrievals (QAC = 3) are reduced by 2.7 % (8.3 % in January and 0.4 % in July). Global mean AOD of the QA filtered data increased slightly in January (from 0.195 to 0.201), but much more significantly in July (from 0.129 to 0.151).

We can evaluate further the changes from C5 to C6, studying the entire six months of data. Plotted in Fig. 5 are global histograms of the six months of retrieved AOD data for both C5 (red) and C6 (blue), where QAC = 3. We see that, overall, the number of confident retrievals has decreased (2.3 %) and that the C6 data are skewed to higher AOD. The number of negative AOD pixels is reduced by 20 %, presumably as a result of improving the assumptions of molecular optical depth. On the other hand, there is increase of high AOD frequency, which we believe comes from additional retrievals of heavy smoke cases.

Figure 6 plots gridded, monthly means, for the same months (January and July 2008) as summarized in Table 2. Here, one can see where the C6 algorithm produces the largest absolute changes. Large positive changes (~ 0.1) are seen in southeast Asia, central Canada (heavy fire smoke) and equatorial Africa during the summer, with small positive (~ 0.01) changes observed over much of the rest of the land surface. The winter month shows significant positive changes only in southeast Asia. There is small, but systematic negative change in the US Midwest, equatorial Africa and northern Australia, resulting from the updated assumed aerosol model boundaries.

Finally, in Fig. 7, we compare MODIS versus AERONET, for the entire six months of Aqua data. Here, we use the revised protocol developed by Petrenko et al. (2011), where satellite and sunphotometer are compared within a spatial radius of ± 25 km and

**The Collection 6
MODIS aerosol
products over land
and ocean**

R. C. Levy et al.

Title Page	
Abstract	Introduction
Conclusions	References
Tables	Figures
⏪	⏩
◀	▶
Back	Close
Full Screen / Esc	
Printer-friendly Version	
Interactive Discussion	

a temporal interval of ± 30 min. A valid collocation is one where there are at least three MODIS pixels and two sunphotometer measurements within the spatial/temporal window. While there is a decrease in total filtered pixel counts between C5 and C6, there is nearly 20 % increase in the number of valid MODIS/AERONET collocations. Although there might be less MODIS sampling in the cloudy tropics (few or no AERONET sites), there is increased MODIS coverage for larger sun zenith angles, leading to additional AERONET sites being sampled (especially in northern Europe). Although the slope of the regression curve changes slightly between C5 and C6, the high skill at retrieving AERONET-observed AOD is retained. Overall, for C6, the correlation is 0.88, and that 70.8 % of MODIS AOD fall within expected uncertainty of $\pm(0.05 + 15 \%)$.

3.3 Changes for DT-ocean

In several previous studies, good comparability was reported between MODIS and SP data, such that AOD retrieved from MODIS agreed to within $\pm(0.03 + 5 \%)$ (e.g., Remer et al., 2005, 2008). However, the same level of agreement was not achieved at all sites under all conditions. Errors could be traced to the presence of non-spherical dust (e.g., Levy et al., 2003) or absorbing smoke (e.g., Ichoku et al., 2003), instead of the spherical, weakly absorbing aerosol conditions that are assumed in the retrieval. Errors can also result from wrong assumptions of the oceanic surface contributions. Uncertainties in water leaving radiance, glint, and white foam properties would introduce a larger relative error at low AOD cases, but also may have a non-negligible error when AOD is high as well. Considering that optical depths are low over most of the ocean, an error in the surface contribution can have a significant impact on the global AOD. Finally, unlike the DT products over land, the comparability with AERONET was not monotonic with QAC value. Bréon et al. (2011) demonstrated that, statistically, the most accurate MODIS over-ocean dataset required $QAC \geq 1$, not just $QAC = 3$.

In the following subsections, we detail the changes made to the DT-ocean aerosol retrieval algorithm, including assumptions as to surface dependence on wind speed, cloud masking logic, and assignment of QAC.



3.3.1 LUT and wind speed dependence

Zhang and Reid (2011) noted there is uncertainty of the surface boundary condition due to variability of the near-surface wind field. Near-surface wind patterns could significantly influence ocean wave and glint patterns, and wrong assumptions about these patterns would bias the subsequent aerosol retrieval. Since the C5 DT-ocean retrieval assumed a constant wind speed of 6 m s^{-1} , there should be systematic biases all over the globe. Concurrently, Kleidman et al. (2011) compared MODIS C5 DT-ocean data with SP data from the Marine Aerosol Network (MAN) (Smirnov et al., 2009) and found that there were residual MODIS errors related to wind speed. Sensitivity studies suggested that the problem would be enhanced closer to glint. Following other algorithm teams (e.g., Sayer et al., 2012a; Herman et al., 2005), we now introduce wind speed dependence to the MODIS DT-ocean aerosol retrieval. This takes on the form as an additional step in interpolation of the MODIS LUT.

Like the C5 LUT (e.g., Remer et al., 2005), our C6 LUT employs the MODRAD (Ahmad et al., 1991) radiative transfer (RT) code to simulate TOA reflectance for a coupled ocean/atmosphere. Embedded within MODRAD are wind speed dependent models to account for the “roughness” of the sea surface (waves and whitecaps, Cox and Munk, 1954) and the foam fraction (Koepke et al., 1984). In addition to the standard 6 m s^{-1} wind speed having 0.16% foam, the C6 LUT includes simulations for three additional wind speeds, 2 m s^{-1} , 10 m s^{-1} and 14 m s^{-1} , having foam fraction of 0.00%, 1% and 3%, respectively. Note that for the atmospheric contribution, we have installed the slight changes to the MODIS band central wavelengths and assumed Rayleigh optical depths (Sect. 3).

We do not go into the details of the over-ocean aerosol inversion process, as they are described previously (e.g., Remer et al., 2005, 2008). As before, there are nine aerosol modes (four fine, five coarse), and that a solution is the weighted combination fine and coarse modes that best approximates the observed spectral reflectance. The main difference is the addition of the extra interpolation step; that is, the interpolation

The Collection 6 MODIS aerosol products over land and ocean

R. C. Levy et al.

Title Page

Abstract

Introduction

Conclusions

References

Tables

Figures

⏪

⏩

◀

▶

Back

Close

Full Screen / Esc

Printer-friendly Version

Interactive Discussion



of the LUT with respect to actual wind speed. Here, the wind speed comes from the 2-meter wind speed, reported within the NCEP $1^\circ \times 1^\circ$ re-analysis that is already used as inputs to the MODIS processing stream. Wind speeds less than 2 m s^{-1} are assumed to be 2 m s^{-1} , and greater than 14 m s^{-1} are assumed as 14 m s^{-1} ; otherwise the LUT is linearly interpolated between the nearest two indices.

Figure 8 shows an Aqua granule (18 January 2010, 14:40 UTC), where the multiple wind speed LUT was applied. The top left is the true-color (RGB) image, showing a strong glint pattern. The top right and bottom left panels plot at least marginal confidence ($QA \geq 1$) AOD at $0.55 \mu\text{m}$, retrieved from the static 6 m s^{-1} wind speed LUT and the multiple wind speed LUT, respectively. The bottom right shows differences between the two AOD retrievals, with superimposed NCEP 2-meter wind speed contours. Note that these wind speeds are from the nearest six hour interval for GDAS re-analysis, in this case from 12:00 UTC. Clearly, the C6 algorithm will retrieve lower (higher) values of AOD when wind speed is higher (lower) than 6 m s^{-1} . Also, the most significant changes seem to be at the edges of the MODIS glint mask (40° from the specular direction).

Figure 9 plots gridded, global data from one day (1 July 2008), showing how the multiple wind speed LUT tends to reduce global AOD over the ocean, especially near glint, and in the “Roaring Forties” of the southern oceans. Near to the specular direction, increasing wind speed diffuses the glitter pattern. The 40° glint mask was chosen so that under most conditions, the sea surface remains nearly glitter free outside this envelope. However, where wind speed is dramatically higher than 6 m s^{-1} , the glitter pattern can spill outside of the glint mask, causing a positive bias to retrieved AOD. On the other hand, far from glint (e.g., in the “Roaring Forties”), the wind speed is known to be consistently higher than 6 m s^{-1} , so that the main additional contribution from the ocean surface is wind-induced foam.

**The Collection 6
MODIS aerosol
products over land
and ocean**

R. C. Levy et al.

[Title Page](#)[Abstract](#)[Introduction](#)[Conclusions](#)[References](#)[Tables](#)[Figures](#)[⏪](#)[⏩](#)[◀](#)[▶](#)[Back](#)[Close](#)[Full Screen / Esc](#)[Printer-friendly Version](#)[Interactive Discussion](#)

3.3.2 Cloud masking, sediment masking, and pixel selection

As in the over land algorithm, the success of the DT-ocean algorithm is dependent on the ability to discard unsuitable pixels. At a minimum, the over-ocean DT algorithm throws out 50 % of the data (darkest and brightest 25 % when sorted by 0.86 μm reflectance). However, there are many other unsuitable pixels, including those that are cloudy, having visible sediments, or too near the specular angle.

The main problem is to separate “clear” aerosol pixels from “clouds”. We want maximal aerosol coverage with a minimum of cloud contamination. From studies such as Zhang and Reid (2010), cloud contamination remained in C5 data over ocean. Yet, there may “always” be clouds in the scene (e.g., Koren et al., 2008), so that too much screening would result in no valid aerosol data. In general, the methodology of the algorithms for deselecting over-ocean pixels (including cloud masking) has been retained from C5 (ATBD, Levy et al., 2009) to C6. However, in attempt to reduce some of the contamination, we have made some changes that are documented here.

Internal cloud masking depends on spatial variability (within a 3x3 box) and absolute reflectance of visible (VIS) and near-IR (NIR) channels, calculated during aerosol retrieval (Martins et al., 2002). The visible tests make use of absolute and spatial standard deviations of reflectance at 0.55 μm ($\rho_{0.55}$ and $\sigma_{0.55}$), the ratio of 0.47 μm to 0.65 μm ($\rho_{0.47}/\rho_{0.65}$), and the absolute reflectance, $\rho_{0.47}$. These were described within the C5-ATBD (Levy et al., 2009), but we describe here as well. For every ocean pixel (500 m resolution) within the MODIS granule, we have $\rho_{0.47}$, $\rho_{0.55}$ and $\rho_{0.65}$. In addition, $\sigma_{0.65}$ is computed from the 3 \times 3 box having the given center pixel. The VIS test logic is as follows. If there is a large standard deviation ($\sigma_{0.65} > 0.0025$), then the pixel is labeled “cloudy”, unless a color ratio ($\rho_{0.47}/\rho_{0.65} < 0.75$) test suggests it is instead heavy brown dust. The heavy dust test is conservative to limit accidental cloud contamination. In addition, the homogeneous center of thick clouds are labeled “cloudy” if very bright in the visible ($\rho_{0.47} > 0.4$).

The Collection 6 MODIS aerosol products over land and ocean

R. C. Levy et al.

Title Page

Abstract

Introduction

Conclusions

References

Tables

Figures



Back

Close

Full Screen / Esc

Printer-friendly Version

Interactive Discussion



The Collection 6 MODIS aerosol products over land and ocean

R. C. Levy et al.

Title Page

Abstract

Introduction

Conclusions

References

Tables

Figures

⏪

⏩

◀

▶

Back

Close

Full Screen / Esc

Printer-friendly Version

Interactive Discussion

By checking the absolute reflectance at $1.38\ \mu\text{m}$ ($\rho_{1.38}$) and the ratio of that to the reflectance in $1.24\ \mu\text{m}$ ($\rho_{1.38}/\rho_{1.24}$), the NIR tests are designed to detect high thin cirrus (Gao et al., 2002) that would otherwise be non-detectable with visible reflectance tests. These tests are performed concurrently with the visible tests. However, since $1.38\ \mu\text{m}$ is at 1 km resolution, results of the tests apply to all four 500 m pixels within. At the same time, due to high amounts of water vapor over the tropical ocean, the internal NIR cirrus detection algorithm is not always sufficient to mask out high, thin cirrus. Therefore, three infrared (IR) test results are selected from the upstream MODIS cloud mask file (MxD35_L2, Ackerman et al., 1998). Each IR test result is encoded into the MxD35 product as one “Bit”, having the value of 0 (“not applied”) or 1 (“applied”) (Hubanks et al., 2012).

The three IR tests are the “Thin Cirrus (IR) Test” (Bit 11), the “High Cloud ($6.7\ \mu\text{m}$) Test” (Bit 15), and the “IR Temperature Difference Test” (Bit 18). If any of these three tests register as “applied”, then the 2×2 box of 500 m pixels (1 km MxD35 pixel) is denoted as “cloudy”, and none of these pixels are retained for aerosol retrieval. This was documented in the C5-ATBD (Levy et al., 2009). However, during C6 development, the MODIS cloud mask team also made changes to the MxD35 algorithm. Specifically, the Bit 18 test was relaxed in order to reduce the number of falsely identified tropical cirrus cases. The goal was to prevent ambiguous cirrus clouds from being targeted for cloud retrieval, but it also resulted in additional cirrus contamination for the aerosol retrieval.

To undo the extra cirrus continuation, we strengthened the internal NIR cirrus-masking test. As before, it is applied in a three-step process, but the logic is changed. If ($\rho_{1.38} > 0.03$) then the 1 km pixel (and four 500 m pixels) is considered “cloudy”. If ($0.005 < \rho_{1.38} \leq 0.03$) then apply the ratio, which means if ($\rho_{1.38}/\rho_{1.24} > 0.30$), then the pixel is cloudy. If the pixel survives as “not cloudy”, then the algorithm checks if there still might be residual cirrus, which means if ($0.005 < \rho_{1.38} \leq 0.03$ AND $0.10 < \rho_{1.38}/\rho_{1.24} \leq 0.30$ AND $\rho_{0.65} > 1.5 \cdot \rho_{0.65}^{\text{ray}}$) then the presence of cirrus is ambiguous and the pixel will be included, but the entire MODIS retrieval box will have degraded

QAC value. Note that the extra “AND” statement makes sure that there is enough visible signal (in the 0.65 μm channel compared to Rayleigh-only reflectance) to care about residual cirrus contamination.

The overall effect of a weakened MxD35 test and strengthened internal NIR test tends is to slightly reduce aerosol coverage (compared to C5) in the midlatitude oceans. This is demonstrated with the granule plotted in Fig. 10, observed over the Pacific, by Aqua on 1 January 2010.

To this point, a 500 m pixel will be deselected from aerosol retrieval if any of the following tests are failed: (1) within glint mask of 40°, (2) any of the three MxD35 IR tests, (3) any internal NIR test, (4) any internal VIS test. An ocean pixel may be also deselected if it fails the ocean sediment test. The ocean sediment test is designed to identify ocean scenes that are contaminated by river or other coastal sediments (Li et al., 2002), by comparing expected VIS (0.55 μm) reflectance with that fitted (in log-log space) from measurements at 0.47, 1.24, 1.63 and 2.11 μm . If it is a dark water scene ($\rho_{2.11} < 0.10$), and there is significant extra reflectance in the visible ($\rho_{0.55} = \rho_{0.55} - \rho_{0.55}^{\text{expect}} < 0.015$), then that pixel is considered to be “sediment” and deselected.

Finally after de-selection of individual 500 m pixels, and 1 km groups of 500 m pixels, the ocean algorithm makes final pixel selection. Here, as documented previously (e.g., Remer et al., 2005, 2012) the data within a 10 km box are sorted by 0.86 μm reflectance. The brightest 25 % and darkest 25 % are removed, leaving at most 200 pixels (out of original 400) to be averaged for final retrieval.

3.3.3 Quality assurance

During the retrieval process, there are a number of tests that infer the “satisfaction” of the retrieval. This is known as the Quality Assurance (QA) plan, and its ultimate product is the assignment of the QA Confidence (QAC), having values between “0” (no confidence) and “3” (high confidence). The detailed tests of the DT-ocean QA plan are reported in the Appendix. For the most part, the general methodology of QA assignment

The Collection 6 MODIS aerosol products over land and ocean

R. C. Levy et al.

Title Page

Abstract

Introduction

Conclusions

References

Tables

Figures

⏪

⏩

◀

▶

Back

Close

Full Screen / Esc

Printer-friendly Version

Interactive Discussion



is the same as for C5. However, there are some changes that are described in this section.

Bréon et al. (2011) and Sayer et al. (2012b) noted that for C5 over ocean, that MODIS comparability with AERONET was not monotonic with QAC value. It was shown that cases with QAC = 3 were no better than cases where QAC = 1, and in some statistics (fraction within EE), the higher QAC cases compared worse. Looking closer at the data, we determined that the cases with low confidence tended to have lower retrieved AOD. In other words, lower QAC was assigned even when it was obvious that the scene was clear (no aerosol). We also noted that there were many cases where QAC = 0 (no confidence) and the AOD was reported as exactly zero.

In retrieval operation, there are two places where the observed reflectance in the 0.86 μm channel ($\rho_{0.86}$) is compared to that modeled for a Rayleigh-only atmosphere ($\rho_{0.86}^{\text{Ray}}$). For the C5 algorithm, the logic was if ($\rho_{0.86} < 1.1\rho_{0.86}^{\text{Ray}}$) then there was not enough aerosol signal to do a retrieval. As a result, AOD was assigned to 0.0, and the QAC was assigned to zero. This meant that all of these extremely clean ocean retrievals were discarded when daily and monthly statistics were computed, thus biasing results. Another test was such that if ($\rho_{0.86} < 1.5\rho_{0.86}^{\text{Ray}}$), then the retrieval would be attempted, but the QAC value assigned to 1. These retrievals would be included in global statistics but would be weighted less heavily than higher AOD cases. In either situation, the result forced the under-sampling of clean cases ($\tau < 0.05$) and produced a high bias to global AOD. There should be more confidence given to obviously “clean” aerosol cases.

For C6, QA logic has been redesigned, so that the extremely clean cases receive higher QAC weighting. Cases where there is no retrieval (and AOD assigned to 0.0) are given QAC = 1, where cases where there could be AOD retrieval (but not robust retrieval of size parameter) are given QAC = 2.

The Collection 6 MODIS aerosol products over land and ocean

R. C. Levy et al.

Title Page

Abstract

Introduction

Conclusions

References

Tables

Figures

⏪

⏩

◀

▶

Back

Close

Full Screen / Esc

Printer-friendly Version

Interactive Discussion



3.3.4 New and changed SDSs

Table 3 lists the over-ocean aerosol SDSs within the Level 2 (MxD04) product. There are no deleted SDSs over ocean, however there is one new SDS, three SDSs with larger dimensions, and two renamed SDSs. The new SDS, “Wind_Speed_NCEP_Ocean”, represents the wind speed used in the retrieval (as reported by the NCEP 1° re-analysis). The SDSs representing reflectance and the number of pixels used have been increased to ten wavelengths (adding values for 0.41, 0.44 and 0.76 μm). The cloud fraction variable now has the prefix “Aerosol_”, to reduce confusion between cloud fraction for the cloud retrievals and cloud masking for aerosol. Finally, what used to be “Cloud_Condensation_Nuclei” in C5, is now “PSML003_Ocean” (Particles of the Small Mode Larger than 0.03 μm), which better denotes the physical meaning of the parameter.

3.3.5 Comparison with C5 products and AERONET

At this point, we have introduced the changes applied to the DT-ocean aerosol retrieval algorithm and Level 2 product listing. Updates include changes to Rayleigh assumptions, gas correction, wind speed interpolation, cloud mask, and QAC revision. What do we expect to be the change to the DT-ocean aerosol *products* on a global scale? As described in Sect. 3.2.6, six full months of aerosol products from Aqua (Januarys and Julys, from 2003, 2008 and 2010) were processed with a near-final version of the retrieval algorithms.

Table 4 reports global, Level 2 pixel statistics for January and July 2008, demonstrating the change of QAC distribution when going from C5 to C6 retrieval algorithms. The number of retrievals having QAC = 3 has increased by 49%, with an overall 6% increase in the “filtered” retrievals having QAC ≥ 1 . As a result of the new protocol in assigning QAC for low signal cases, the Mean AOD (filtered for QAC ≥ 1) has dropped by 0.025 in both months. Analogous to our DT-land description in Sect. 3.2.6, we evaluate C5 \rightarrow C6 algorithm changes by studying the entire six months of Aqua data. Plotted in

Title Page

Abstract

Introduction

Conclusions

References

Tables

Figures

⏪

⏩

◀

▶

Back

Close

Full Screen / Esc

Printer-friendly Version

Interactive Discussion



Fig. 11 are global histograms of the six months of retrieved AOD data for both C5 (red) and C6 (blue), filtered for $QAC \geq 1$. We see that, overall, the number of retrievals has increased (7%) and that there is a significant increase in low AOD cases with a slight decrease in the number of high AOD cases.

Figure 12 (top six panels and colorbars) plots $1^\circ \times 1^\circ$ monthly mean AOD for January and July 2008, showing C5, C6 and differences (C6-C5) between the two algorithms. Each monthly mean value is the average of all filtered ($QAC \geq 1$) L2 values, within the latitude/longitude grid box, collected during the month. There is no change in the overall spatial patterns, although there is a consistent decrease in ocean AOD. As indicated in Table 4, the average decrease for both months is about 0.025, although there are regions of larger decrease and regions of little decrease (or slight increase). For the most part, the large decreases (~ 0.04 or more) are the midlatitudes of both summer hemispheres (e.g., the Roaring Forties), where there are systematically higher wind speeds. The smallest changes are in the tropics, and may be due to cloud mask differences.

Figure 12 (bottom six panels and colorbars) plots $1^\circ \times 1^\circ$ Ångström exponent, AE, calculated from 0.55 and 0.86 μm . Like the AOD plotted in the top panels, these are simple averages of L2 AE values collected within each latitude/longitude box. Although this is not necessarily a preferred way of deriving a mean AE value, the plots clearly show how mean AE is expected to increase for C6, especially where AOD is expected to decrease when accounting for wind speed. This indicates that C6 may derive generally smaller-sized aerosol over the global ocean.

Finally, in Fig. 13, we compare products derived from MODIS and SP, for the entire six months of Aqua data. The top two panels plot AOD from C5 and C6, respectively, whereas the bottom two panels show comparisons of AE. As explained in Sect. 3.2.6, we use the modified collocation protocol of Petrenko et al. (2011), where the MODIS radius is ± 25 km and the sunphotometer time interval is ± 30 minutes of satellite overpass. In addition to plotting MODIS versus AERONET, we also display comparisons for MODIS versus the ship-based sunphotometers of

**The Collection 6
MODIS aerosol
products over land
and ocean**

R. C. Levy et al.

[Title Page](#)[Abstract](#)[Introduction](#)[Conclusions](#)[References](#)[Tables](#)[Figures](#)[⏪](#)[⏩](#)[◀](#)[▶](#)[Back](#)[Close](#)[Full Screen / Esc](#)[Printer-friendly Version](#)[Interactive Discussion](#)

the Maritime Aerosol Network (MAN; http://aeronet.gsfc.nasa.gov/new_web/maritime_aerosol_network.html). For each panel, the square symbols (grey and colored) represent frequency of MODIS/AERONET collocations at each ordered pair (0.01 intervals), whereas the black circles are collocations for MODIS versus the Maritime Aerosol Network (MAN). Comparison statistics in all panels are for MODIS versus AERONET only.

While there was a 6% increase in total filtered ($QAC \geq 1$) pixel counts between C5 and C6, there is nearly a 12% increase in the number of valid MODIS/AERONET AOD collocations. The percentage within EE $\pm(0.03+5\%)$ increases slightly (from 64 to 67%), along with a slight improvement in regression slope (from 0.92 to 0.95). There is an increase of MAN collocations from 34 to 38, and a small improvement (slightly less scatter) for comparisons with MAN in C6.

When comparing AE with AERONET, there are 2% fewer collocated points in C6. This is due to not reporting size parameters when the AOD signal is too small to retrieve size robustly. Here, the EE is set at ± 0.4 , which is where we see nearly 66% match for C6. While there is no significant overall improvement for AE comparability in C6, there are fewer cases where MODIS is retrieving the limiting values for AE, and fewer cases where MODIS is very far from AERONET values. This is suggesting that improved pixel screening or other corrections (Rayleigh, gas) may be providing the DT-ocean retrieval with more consistent information. The same reasoning may be responsible for the decrease in the scatter with relation to MAN-derived AE; that allows the C6 retrieval to make better use of the information. Again, since C6 will not report AE for small AOD, the number of MODIS/MAN collocations drops from 34 to 18.

3.4 Combined DT-land and DT-ocean products

In Sects. 3.2 and 3.3, we described changes to the algorithm and products related to the separate DT-land and DT-ocean retrievals. At the completion of either algorithm, some parameters are merged into a joint dark-target aerosol product. Some of the parameters are filtered by QAC, meaning that the joint named SDS will only report values

The Collection 6 MODIS aerosol products over land and ocean

R. C. Levy et al.

Title Page

Abstract

Introduction

Conclusions

References

Tables

Figures



Back

Close

Full Screen / Esc

Printer-friendly Version

Interactive Discussion



with sufficiently high confidence. This enables a “best-of” product that we consider to be useful for most quantitative purposes.

We expect that the primary product for most users is the SDS named “Optical_Depth_Land_And_Ocean”. This SDS contains only AOD values for the filtered, quantitatively useful retrievals over dark targets. Specifically, this SDS includes any DT-ocean retrieval having $QAC \geq 1$, and any DT-land retrieval having $QAC = 3$. On the other hand, the C6 product continues to offer the SDS named “Image_Optical_Depth_Land_And_Ocean” which contains all AOD values, regardless of QAC value. This SDS is intended for more qualitative purposes, such as imagery and data continuity. Because Levy et al. (2010) demonstrated there is not even significant “qualitative” value for the ratio product (FMF) over land, the joint ratio SDS has been deleted for C6.

At the same time, we have added two new “diagnostic” SDSs to the product list. These are the “Land_Sea_Flag”, reported directly from the MxD35_L2 file used for land/ocean decision making, and the “Land_Ocean_Quality_Flag”, which is simply reporting the QAC value contained within the top bytes of the separate “Quality_Assurance_Land” and “Quality_Assurance_Ocean” SDSs. Both of these flags are short integers, and are intended for making it easier for users (and our own algorithm development team) to interpret retrieval results. However, if the user wants to delve into more depth as to why a particular quality was assigned to the retrieval, the separate (bit-packed) QA products are still available.

3.5 New cloud-diagnostic products

For C6, there will be a new array of cloud diagnostics reported in the MxD04 file, including two products offered at 500 m resolution (Table 6). During the cloud masking operations (separate for land and ocean), the algorithm keeps track of whether a given 500 m pixel is considered to be “cloudy” or “clear”. This information is carried along, in an array of bits (0 = cloudy, 1 = clear) and reported as “Aerosol_Cldmsk_Land_Ocean”. As this cloud mask is created, the algorithm also determines the distance from every

The Collection 6 MODIS aerosol products over land and ocean

R. C. Levy et al.

Title Page

Abstract

Introduction

Conclusions

References

Tables

Figures



Back

Close

Full Screen / Esc

Printer-friendly Version

Interactive Discussion



pixel to the nearest “cloud” pixel. This is “Cloud_Distance_Land_Ocean”. The intention is that users concerned about aerosol retrievals affected by cloud adjacency effects (3-D effects) or by humidified aerosols and cloud fragments in cloud fields (twilight zone) can trace exactly which pixels were used in the retrieval or plot the retrievals as a function to the nearest cloud. There is also a 10 km product that offers the average distance to the nearest cloud of all the pixels within the 10 km box used by the retrieval, i.e., “Average_Cloud_Distance_Land_Ocean”. An example of the 500 m parameters is shown in Fig. 14.

3.6 Deep blue/dark target merged products

The dark target algorithm over land (e.g., Levy et al., 2007a and b) is not designed to retrieve aerosol over bright surfaces, including desert. This leaves significant holes in global aerosol sampling. However, in recent years, Hsu et al. (2004, 2006) have developed an algorithm that retrieves aerosol properties over brighter surfaces. This algorithm, known as Deep Blue (DB), makes use of the observation that even visually bright desert scenes are relatively “dark” and relatively stable in the deep-blue wavelengths (e.g., 0.41 and 0.47 μm). The DB algorithms have also been revised for C6, and notably will now also provide coverage over vegetated land surfaces, although not over oceans (Sayer et al., 2012c; Hsu et al., 2012).

Here, we do not discuss the DB-land algorithm and product validation. We note, however, that the DB algorithm was applied to MODIS data and included as part of Collection 5.1 (C51). Rather than create an entirely new MODIS product, DB products were provided as appended SDSs onto the existing (C5) MxD04_L2 product. For C6, DB products will continue to be reported within MxD04_L2.

Unlike the clear separation between land and ocean within the DT framework, there are land areas that may be retrieved by both DB and DT algorithms. Essentially, all vegetated terrain falls into this category, as DT excludes bright desert surfaces (e.g., the Sahara desert) and both the DT and DB algorithms exclude snow-covered surfaces.

The Collection 6 MODIS aerosol products over land and ocean

R. C. Levy et al.

[Title Page](#)

[Abstract](#)

[Introduction](#)

[Conclusions](#)

[References](#)

[Tables](#)

[Figures](#)

[⏪](#)

[⏩](#)

[◀](#)

[▶](#)

[Back](#)

[Close](#)

[Full Screen / Esc](#)

[Printer-friendly Version](#)

[Interactive Discussion](#)



Both algorithms report AOD at 0.55 μm , and both may report with high QA confidence. How should a user decide which one to use and under what conditions?

As only DB data are available for bright arid regions, there is no choice to be made in this case. Conversely, in the areas with densest vegetation, the DT algorithm is more mature and better characterized than the comparatively new expanded DB algorithm, and performs well; thus, a sensible choice is to use DT in these areas. This leaves a number of transition regions which comparatively low vegetation cover but are sufficiently dark for the DT algorithm to be applied; perhaps most notable are the African Sahel, which is a transition region between desert and tropical forest, and the arid southwest of the United States of America. Although there have been multiple validation efforts, there are insufficient number of AERONET sites in these transition zones to conclude clear superiority of one retrieval or another. It is known that the DT algorithm tends to be biased high in brighter regions (e.g., Levy et al., 2010). It has also had been shown that DB (C51) was biased low in some of the same regions. The algorithms are built for different assumptions, and it is not obvious how to create an algorithm that leverages only the strengths of both.

For C6, the solution is to simply merge the products from the two algorithms in these transition regions, thus creating a “best-of” AOD product that combines DB, DT-land and DT-ocean. This will be reported by the SDS named “Dark_Target_Deep_Blue_Optical_Depth_550_Combined”. Essentially, a climatology from the MODIS-derived, monthly, gridded NDVI product (MYD13C2, Huete et al., 2011) is used as a map for assigning which algorithm takes precedence. This database is a set of 12 multiannual monthly means, gap-filled using the nearest month. If ($\text{NDVI} > 0.3$) then use the results from DT (τ_{DT}). If ($\text{NDVI} < 0.2$) then use results from DB (τ_{DB}). For the transition areas ($0.2 \leq \text{NDVI} \leq 0.3$), the routine considers the confidence as indicated by QAC values (Q_{DT} and Q_{DB}), where high confidence means $Q_{\text{DT}} = 3$ or $Q_{\text{DB}} \geq 2$. If both are high confidence, the AOD is the average of the two, i.e.,

$$\tau = (\tau_{\text{DT}} + \tau_{\text{DB}})/2. \quad (2)$$

**The Collection 6
MODIS aerosol
products over land
and ocean**R. C. Levy et al.

[Title Page](#)[Abstract](#)[Introduction](#)[Conclusions](#)[References](#)[Tables](#)[Figures](#)[⏪](#)[⏩](#)[◀](#)[▶](#)[Back](#)[Close](#)[Full Screen / Esc](#)[Printer-friendly Version](#)[Interactive Discussion](#)

The Collection 6 MODIS aerosol products over land and ocean

R. C. Levy et al.

Title Page

Abstract

Introduction

Conclusions

References

Tables

Figures

◀

▶

◀

▶

Back

Close

Full Screen / Esc

Printer-friendly Version

Interactive Discussion



If only one has high confidence, then the AOD is assigned to that one. However, if neither has high confidence, then the combined AOD remains undefined. Table 7 reports the new SDSs referring to the DT/DB merging. Figure 15 shows this combined product for January 2010, demonstrating that DT/DB increases coverage over both dark and bright surfaces (except snow and clouds).

Although these new “Combined” products are offered for C6, we note that they are not yet validated (although by definition should be as least as good as the poorer-performing of DT and DB for any given location and time). It is expected that there may be changes in the NDVI thresholds and/or the exact protocol in which the merging occurs.

4 Protocol for L3

Until this point, our discussion has focused on describing changes to L2 (along-orbit) algorithm and products. Since many applications rely on gridded aerosol data (e.g., L3), here we describe updates for the L3 product. As reported on the MODIS-Atmosphere website (<http://modis-atmos.gsfc.nasa.gov>), there are daily (MxD08_D3), eight-day (MxD08_E3) and monthly (MxD08_M3) data products. The D3 files contain roughly 600 statistical datasets that are derived from approximately 80 scientific parameters from four different L2 product files, including the MxD04_L2 aerosol product. Statistics are sorted into $1^\circ \times 1^\circ$ cells on an equal-angle grid that spans a 24 h (00:00 to 23:59 Greenwich Mean Time) interval. There is a range of different statistical summaries that are computed, depending on the parameter being considered. For example, from any derived L2 aerosol parameter, the daily (D3) product may include:

- Simple (mean, minimum, maximum, standard deviation, pixel counts) statistics.
- Histograms of the quantity within each grid box.
- Histograms of the confidence placed in each measurement.

– Confidence weighted statistics (QA mean, QA standard deviation).

As explained by Levy et al. (2009), “how” one derives the gridded, global product is very important. Analogous to selection process when going from L1B to L2 (cloud masking, pixel selection, whether N pixels are sufficient for retrieval, etc.), there is a selection process when going from L2 to L3 and then from D3 to M3. Here the questions involve retrieved pixel selection, QAC filtering, and again, whether N retrievals are sufficient. We have considered many assumptions and the changes from C5 to C6 are reported here.

For the D3 product, there is no significant change in how it is computed. For many of the individual, separately retrieved (DT-land, DT-ocean, DB-land) aerosol SDSs, other than the addition of a median statistic, the set of statistics will be the same as in C5. However, the prefix “Aerosol_” has been prepended to all D3 aerosol statistics. Also, many SDSs have been removed from the product list. These include the deleted L2 SDSs over DT-land (Sect. 3.2.5) as well as aggregations based on products with intensive properties. Intensive aerosol properties do not depend on the amount of aerosol material. Intensive properties such as Ångström exponent do not add. Mixing aerosols with AE of 0.6 with an equal number of particles with AE of 1.5, does not result in a mixture with AE of 2.1. In contrast, extensive aerosol properties are directly proportional to the amount of material and do add. For example, mixing an air parcel containing particles with AOD of 0.5 with another air parcel with AOD of 1.0 does result in a mixture of AOD of 1.5. Because of the different additive properties of intensive and extensive variables, their aggregations must be made differently. Extensive variables, such as AOD and mass, can be simply accumulated and averaged. Intensive variables, such as AE and FMF, must be weighted by the total AOD, but this becomes too complicated within the standard L3 algorithm framework. Therefore, we have removed all intensive variables from L3 files, and all SDSs with “ratio” in the title have been discontinued. For the combined AOD products (e.g., “Optical_Depth_Land_And_Ocean”, and “Dark_Target_Deep_Blue_Optical_Depth_550_Combined”) it is assumed that QAC

The Collection 6 MODIS aerosol products over land and ocean

R. C. Levy et al.

[Title Page](#)

[Abstract](#)

[Introduction](#)

[Conclusions](#)

[References](#)

[Tables](#)

[Figures](#)

[⏪](#)

[⏩](#)

[◀](#)

[▶](#)

[Back](#)

[Close](#)

[Full Screen / Esc](#)

[Printer-friendly Version](#)

[Interactive Discussion](#)



filtering has been done within the L2 algorithm, so no additional Confidence weighted statistics are produced.

As explained by Levy et al. (2009), instead of going back to L2 data, the M3 (and E3) products are computed from D3 products. There are two paths from L2 to D3 to M3 products, one that includes confidence weighting (“_QA_Mean” in D3 and “QA_Mean_Mean” in M3) and the other, which does not (“_Mean” in D3 and “_Mean_Mean” in M3). For C5, both of the M3 products were also “pixel weighted” where contribution from each day is weighted by the number of pixels for the day.

Pixel weighting has the effect of biasing the global statistics toward the sampling of the sensor. This means that pixel weighting may be appropriate for describing statistics of cloud properties (e.g., Platnick et al., 2006). Clouds are retrieved whether or not aerosol is present, so that days with more retrieved cloud pixels should have greater weight than days with fewer cloud pixels. Aerosol properties, however, are only retrieved by MODIS under clear (not cloudy) skies. Statistics of aerosol are inherently clear-sky biased, so that pixel weighting makes it even more so.

Therefore, for C6, the monthly (M3) and eight-day (E3) aerosol SDSs computations have dropped the pixel weighting step. Now, as long as a given day has sufficient number of clear pixels ($N \geq 6$) in the grid box, its value is counted equally as any other day. This reduces the clear-sky bias in the multi-day aerosol products. As seen from Fig. 16, the change to equal day weighting will tend to increase gridded, mean AOD, especially in regions of the globe already dominated by higher AOD.

As of this writing, although we have a fairly firm understanding of expected changes in L3 products, at least as related to aerosol, the full suite of L3 changes is still in development. A detailed list of all L3-atmosphere SDSs (D3, E3 and M3) will be available soon (<http://modis-atmos.gsfc.nasa.gov>).

The Collection 6 MODIS aerosol products over land and ocean

R. C. Levy et al.

Title Page

Abstract

Introduction

Conclusions

References

Tables

Figures



Back

Close

Full Screen / Esc

Printer-friendly Version

Interactive Discussion



5 New MODIS 3 km product (MxD04_3K)

Since before Terra launch, the MODIS aerosol algorithms have been designed to retrieve aerosol at 10 km resolution (at nadir). This, in part, was seen as a compromise between signal-to-noise of the instrument, of surface variability, and expected aerosol variability. The 10 km was reasonable for deriving global aerosol climatology, and yet produce manageable volumes of information.

One unexpected application of the MODIS aerosol product was its use as a proxy for estimating surface-level particulate pollution (Chu et al., 2003; Wang and Christopher, 2003; Engel-Cox et al., 2004). However, some studies (e.g, Li et al., 2005) indicated that the 10 km resolution was not fine enough to resolve local variability, especially near and within cities where most of the human population lives. Therefore, in recent years, the air quality community in particular has been advocating for higher resolution aerosol retrieval data to monitor and model pollution threats to our human population. Other research applications for a higher resolution data product include, but are not limited to, efforts in characterizing smoke plumes from fires, resolving aerosol loading in complex terrain and studying aerosol-cloud processes.

Because the MODIS 10 km aerosol algorithms were designed with climate applications in mind, they were constructed in such a way to suppress noise in the retrieval. The danger in producing a higher-resolution dataset is that there is the possibility of introducing noise into the product. The standard DT aerosol retrieval throws out at least 50 % (over ocean) and 70 % (over land) of its available 500 m pixels. This has been proven to reduce noise due to land surface variability, cloud contamination and other non-aerosol signals. Blindly going to a 500 m (or 1 km) resolution global retrieval will lead to retrieval errors.

However, because there is such a strong need for a global fine resolution aerosol product, we have developed a compromise algorithm that retains sufficient pixel screening and statistics. For C6, this will take the form of a separate Level 2 aerosol data product at 3 km resolution. (Remer et al., 2012), archived as “MOD04_3K” for

The Collection 6 MODIS aerosol products over land and ocean

R. C. Levy et al.

Title Page

Abstract

Introduction

Conclusions

References

Tables

Figures



Back

Close

Full Screen / Esc

Printer-friendly Version

Interactive Discussion



The Collection 6 MODIS aerosol products over land and ocean

R. C. Levy et al.

Title Page

Abstract

Introduction

Conclusions

References

Tables

Figures

⏪

⏩

◀

▶

Back

Close

Full Screen / Esc

Printer-friendly Version

Interactive Discussion



Terra and “MYD04_3K” for Aqua (i.e., MxD04_3K). Compared to the standard 10 km algorithm, the 3 km algorithm will have the same methodology and structure, and use the same inversion method, surface optical property assumptions, and lookup tables. The differences arise only in the manner in which pixels are selected and grouped for retrieval. Since global 3 km product file dimensions will be so much larger, the new MxD04_3KM file will provide only a subset of the SDSs offered by the standard MxD04_L2 file.

Plotted in Fig. 17 are two examples of granules retrieved by both 10 km and 3 km retrieval algorithms. Both are located over Maryland during July 2010. Cloud masking is the same for both algorithms. However, the sorting and discarding processes are slightly different, meaning that the input reflectances (from L1B) are organized into groups of 6×6 pixels for the 3 km algorithm, versus 20×20 pixels for the 10 km algorithm. Therefore, pixels that might be discarded during the sorting and discarding procedure at 10 km might be kept at 3 km. This has the potential to make the 3 km product noisier than at 10 km. On the other hand, if sufficient pixels escape the masking and discarding procedure at 10 km, then an entire 10 km box might appear to have inaccurate AOD, which is given substantial weight in an areal weighting of a spatial average. In the 3 km product these outlying AOD retrievals can be confined to a smaller area and play a lesser role in an areal weighting of a regional average. Figure 17 shows both situations.

The formal validation of the 3 km product is currently underway, both globally (Remer et al., 2012) and locally (Munchak et al., 2012). Note, that initially for C6, the 3 km product includes only DT retrievals (over land and ocean). There are not DB retrievals, but these could be added later. Note also, that there is no operational Level 3 product derived from this 3 km dataset.

6 Geolocation and calibration issues

Sections 3, 4 and 5 discussed changes we have made to the aerosol retrieval algorithms and products. Except for changes in cloud masking over ocean, where the change was warranted by upstream modifications, all other changes have been independent of the algorithm inputs.

However, for C6 processing, in addition to cloud mask changes (Level 2 data), there have been numerous changes with regard to the L1B dataset. As described in Sect. 2.2, the MODIS aerosol retrieval requires information as to whether “ocean” or “land” fork should be attempted. Although the information is read from the MxD35 data file, it is originally determined and reported for MxD03. However, as Carroll et al. (2011) explains, there are sometimes significant and rapid changes in land/sea cover, especially in the Arctic. Also, there are coastal and lakeshore regions with complicated, fractal-like structure. Therefore, MODIS C6 will be relying on a 250 m-resolution water mask (Carroll et al., 2009), convolved with a determination of possible water present, which will result in more 500 m and 1 km pixels with “possible” water contamination. This means that any area with complicated coastal or lakeshore structure, including the Arctic, there will be more pixels that are neither “ocean” nor “land”. To compensate for this, the aerosol retrieval code will accept as “possible land” any pixel that is not explicitly tagged as a water pixel. The DT-land algorithm can then go through its normal steps of inland water (NDVI tests) and snow/ice masking without introducing significant contamination. At the time of this writing, the algorithm modifications due to land/sea flag issues have not been finalized.

When the MODIS algorithm was upgraded from C4 to C5, all testing was performed based on C4 inputs. Remer et al. (2008) showed that for C4, global monthly mean AOD from Terra (M_T) and Aqua (M_A) agreed along the one-to-one line. However, in C5, M_T suddenly “jumped” so that $M_T > M_A$. In hindsight, we learned that while individual MODIS science teams are making changes to retrieval algorithms, the MCST has also

The Collection 6 MODIS aerosol products over land and ocean

R. C. Levy et al.

Title Page

Abstract

Introduction

Conclusions

References

Tables

Figures

⏪

⏩

◀

▶

Back

Close

Full Screen / Esc

Printer-friendly Version

Interactive Discussion



been making changes to MODIS calibration coefficients, and these basic calibration changes affect the aerosol product significantly.

For C5, over land, global AOD from Terra tends to decrease, while Aqua remains constant. In other words, Terra and Aqua diverge, such that $M_T > M_A$ prior to 2004, switching to $M_T < M_A$ after. These tendencies are seen in Levy et al. (2010), where $M_T > AERONET$ prior to 2004 and $M_T < AERONET$ afterwards. Wang et al. (2011) performed sensitivity tests and showed how it was possible for systematic changes in Terra's blue-channel calibration could lead to artificial trends in retrieved NDVI. Our own sensitivity tests demonstrated that the same issues would lead to artificial aerosol trends.

It short, the redundancies of MODIS on-orbit calibration are not sufficient to characterize all changing aspects of the mirrors and on-board solar diffuser. This was a known problem, and the ocean-color team had been handling it with vicarious calibration (Franz et al., 2007). However, until recently, the problem was thought to be confined to the shortest blue wavelengths (0.41 and 0.44 μm), and was not believed to be a significant problem in the land/aerosol blue channel (0.47 μm) and longer wavelengths. The results of our dark-target aerosol product, as well as the NDVI product, clearly indicated that the issues in the longer wavelengths could not be ignored any longer. As a result of collaboration with members of many science teams, the MCST has developed an improved method for long-term MODIS calibration. The correction, based on reflectance of pseudo-invariant "bright" desert targets, has been applied to the calibration coefficients for each channel. Details about the calibration adjustments are given in Sun et al. (2012), and will not be repeated here.

What should happen to the MODIS DT-aerosol product after calibration adjustment? In the same way we have been working with MODAPS to test entire months of data with revised aerosol retrieval algorithms, we have also tested entire months with revised L1B calibration. Figure 18 demonstrates that for July 2008 (Terra), expected L1B changes will result in a significant increase (~ 0.02) for AOD at 0.55 μm over DT-land, with only a very slight (~ 0.002) change over ocean. At this point, since the Deep Blue product

The Collection 6 MODIS aerosol products over land and ocean

R. C. Levy et al.

Title Page

Abstract

Introduction

Conclusions

References

Tables

Figures

⏪

⏩

◀

▶

Back

Close

Full Screen / Esc

Printer-friendly Version

Interactive Discussion



for C51 already included some correction for calibration (e.g., Jeong et al., 2011), we cannot provide a similar C6 to C5 comparison for the DB-land product.

Work is in progress to determine how the revised calibration efforts will impact global trends and divergence of Terra and Aqua. However, preliminary results show that, in fact, the trending differences will most likely be mitigated by the new calibration effort. The point is, that unlike the situation in 2007 when the C5 aerosol algorithms were put into operation after testing only on C4 inputs, we have supplied some information to characterize C6 algorithms on C6 inputs before C6 becomes operational.

7 Discussion, including transition to NPP-VIIRS

To this point, we have described the many improvements and updates to the MODIS along-orbit, dark-target aerosol algorithms and products. Except for introducing wind speed dependence over ocean, we have made only minor adjustments to the actual DT retrieval procedures. The theoretical basis of the DT-algorithms is solid, at least over the intended DT-land and ocean surfaces. The more interesting and substantive adjustments have been related to characterizing boundary conditions (center wavelengths, gas absorption correction, instrument calibration) as well as pixel selection (e.g., cloud masking) and quality assurance (including assigning confidence). In addition, we have discussed aggregation to Level 3, and introduced a new high-resolution (3 km) global product. Finally, we are now providing a merged product that theoretically takes the “best of” alternative algorithms over transitionally bright regions.

Thus, the MODIS DT-algorithm is a mature algorithm, and we expect that the MODIS-derived DT products will continue to be useful for research and applications. Specifically, after corrections for Terra calibration, we believe that the MODIS retrievals can be a reliable “standard” for an aerosol climate data record.

A climate data record (CDR) is an elusive quality. It is defined by the National Research Council (NRC, 2004) as “a time series of measurements of sufficient length, consistency, and continuity to determine climate variability and change”. While we have

The Collection 6 MODIS aerosol products over land and ocean

R. C. Levy et al.

Title Page

Abstract

Introduction

Conclusions

References

Tables

Figures

⏪

⏩

◀

▶

Back

Close

Full Screen / Esc

Printer-friendly Version

Interactive Discussion



taken many steps with the MODIS instrument, calibration, and retrieval algorithms to attain consistency, it is debatable whether ten or twelve years is sufficient length and continuity. While MODIS may orbit for another few years, it will not have provided a multi-decade data record.

5 On 25 October 2011, the Visible Infrared Imaging Radiometer Suite (VIIRS) was launched by the National Polar-orbiting Partnership (NPP) aboard the Suomi-NPP satellite. Suomi-NPP is a joint NASA/NOAA mission that is intended to provide continuity for the environmental data that has been produced by existing Earth-observing missions. Suomi-NPP will also act as a bridge between NASA's EOS program, and the
10 Joint Polar Satellite System (JPSS) program.

Specifically, VIIRS was designed to have similar capabilities as MODIS, and Suomi-NPP is flying with a similar equator crossing time as Aqua, but at a much higher orbit (825 km versus 705 km). In terms of aerosol retrieval, the standard VIIRS algorithm is based on the joint heritage of the MODIS DT-retrieval algorithms and the MODIS atmospheric correction algorithms to derive land surface properties (Vermote and Kotchenova, 2008). Sensitivity tests and radiative transfer studies indicate that the VIIRS algorithm for VIIRS should provide at least as good of an aerosol product as MODIS retrieval on MODIS. However, there are many small differences between VIIRS and MODIS (satellite altitude, spatial resolution, exact wavelength bands, etc.) as well as
15 differences in retrieval algorithms (cloud masking, pixel selection, fitting algorithm, etc.) that ensure that the VIIRS aerosol record will be different than that has been provided by MODIS.

In many of the subsections of Sects. 3, 4 and 5, we described new diagnostic SDSs reported within the aerosol product file. These include the wind speed information over ocean, the topographic elevation over land, and land-sea masks, cloud distances and other parameters over both land and ocean. We also added three wavelengths to reflectance and pixel count information (noted in Tables 1 and 3), specifically for 0.41, 0.44 and 0.76 μm wavelengths (Bands 8, 9 and 12). Since similar wavelength bands are used by the aerosol retrieval on VIIRS, we expect that this expanded diagnostic
25

**The Collection 6
MODIS aerosol
products over land
and ocean**

R. C. Levy et al.

Title Page

Abstract

Introduction

Conclusions

References

Tables

Figures



Back

Close

Full Screen / Esc

Printer-friendly Version

Interactive Discussion



information can help to quantify how to transition from MODIS to VIIRS in the global aerosol climate data record.

8 Conclusions

Four years ago, the MODIS DT-aerosol team proposed to provide maintenance and modest improvement to the aerosol dark-target target algorithms and products. This has resulted in some minor adjustments to the DT-retrieval algorithms, themselves, but more significant advances in doing cloud masking, assigning quality assurance, and implementing new diagnostic products like cloud distance. The theoretical basis of the DT-algorithms is solid, at least over the intended DT-land and ocean surfaces. It is a mature algorithm, and we expect that the MODIS-derived DT products will continue to be useful for research and applications.

However, no matter how much energy is put into improved DT assumptions (surface characterization, aerosol model, pixel selection, quality assurance, etc.), we find that there is little or no additional information within the MODIS shortwave channels that can be used for on-orbit aerosol retrieval. Because desert surfaces are relatively dark in the UV (and Deep-Blue, near-UV) wavelengths, the DB-land algorithm is a useful alternative, particularly for regions where traditional DT algorithms cannot work. To take advantage of this coverage, we have created a new “best-of” combined aerosol product that merges results from both algorithms. Nonetheless, because of the inherent uncertainties of the surface reflectance, as well as to all other assumptions, there is probably a theoretical limit to the accuracy and precision of these along-orbit (independent retrieval) algorithms.

There are alternatives to along-orbit algorithms. One very promising alternative is the temporal/spatial MAIAC algorithm (Lyapustin et al., 2011). MAIAC adds the knowledge that land surfaces change very little over a short time scale. Using multi-day measurements from MODIS, coupled with some constraints about surface spectral BRDF, one can retrieve land surface and aerosol properties simultaneously. MAIAC

The Collection 6 MODIS aerosol products over land and ocean

R. C. Levy et al.

Title Page

Abstract

Introduction

Conclusions

References

Tables

Figures

⏪

⏩

◀

▶

Back

Close

Full Screen / Esc

Printer-friendly Version

Interactive Discussion



**The Collection 6
MODIS aerosol
products over land
and ocean**

R. C. Levy et al.

Title Page	
Abstract	Introduction
Conclusions	References
Tables	Figures
⏪	⏩
◀	▶
Back	Close
Full Screen / Esc	
Printer-friendly Version	
Interactive Discussion	

has been proven to provide accurate AOD over many surface types, including vegetated and desert surfaces. The main problem with MAIAC is its practicality – multi-day inversions require more computer resources than the DT or DB algorithms, and cannot be performed in near-real time. There have been no alternative algorithms proposed that improve on the traditional DT cloud-free over ocean retrieval. However, another avenue of improvement that may prove viable in the future is the retrieval of aerosol optical depth above clouds, in certain situations (Jethva et al., 2012).

Therefore, even though there are promising new algorithms for retrieving aerosol from MODIS, they are not yet capable of producing global information, quickly and reliably. In addition to running as standard products in the MODAPS environment, the MODIS DT-algorithm is operating in near real time (Rapid Response, <http://earthdata.nasa.gov/data/near-real-time-data/rapid-response>). MODIS DT data are reliably being used in operational applications of data assimilation (e.g., Zhang et al., 2008; Benedetti et al., 2009; Reid et al., 2011), weather forecasting (e.g., Carmona et al., 2008), fire monitoring (Kaufman et al., 2003) and air quality applications (e.g., Hoff et al., 2009). After corrections for Terra calibration, we expect that the MODIS retrievals can be a reliable “standard” for an aerosol climate data record (NRC, 2004). This is especially important as we use and evaluate NPP-VIIRS data as continuation for the aerosol data record.

Acknowledgements. We thank Bill Ridgway (SSAI/GSFC) and the MODAPS team for facilitating our testing needs. We are grateful to Zia Ahmad for helping us create and interpret the new over-ocean LUTs. Finally, we thank the AERONET team for their quality controlled, easy-access data.



MODIS instrument characteristics, LUT assumptions and gas absorption corrections

Computation of the MODIS lookup tables (LUTs) over both land and ocean, in addition to requiring knowledge about surface and aerosol optical properties, also require inputs of center wavelength values and assumptions of sea-level Rayleigh optical depths (ROD). During the aerosol retrieval and pixel selection, the inputted Level 1B (L1B) require correction for the presumed absorption of gases in the atmospheric column. For MODIS, the central wavelengths, Rayleigh optical depth (ROD) assumptions, and gas column absorption corrections are all based on presumed knowledge about the MODIS instrument's band-by-band filter response functions (<http://mcst.gsfc.nasa.gov/>).

By weighting the online response functions with assumed top-of-atmosphere solar spectra, we determined weighted center wavelengths for each MODIS band. All response values from all detectors and both mirror sides were weighted equally, and that out-of-band filter response was included only if greater than 1 %. We applied the empirical formula (Eq. 30, from Bodhaine et al., 1999), with λ wavelength in nm, to calculate sea level molecular ROD values:

$$\tau_R(\text{sealevel}, 45^\circ \text{N}) = 0.0021520 \left(\frac{1.0455996 - 31.29061 \lambda^{-2} - 0.90230850 \lambda^2}{1 + 0.002759889 \lambda^{-2} - 85.968563 \lambda^2} \right) \quad (\text{A1})$$

The band central wavelengths and calculated RODs are presented in Table A1. As compared to ROD assumed for the C5 LUT (over ocean), C6 ROD values differ by -0.0028 , -0.0015 , -0.0012 and -0.0003 , for Bands #3, 4, 1 and 2, respectively. For the other bands, differences from C5 were in the fifth digit or smaller.

Accurate aerosol retrieval also requires appropriate correction for the absorption of atmospheric gases, denoted as the total gas transmission correction factor (T_λ^{gas}). While the aerosol retrieval is performed in bands that are centered in atmospheric

The Collection 6 MODIS aerosol products over land and ocean

R. C. Levy et al.

Title Page

Abstract

Introduction

Conclusions

References

Tables

Figures

⏪

⏩

◀

▶

Back

Close

Full Screen / Esc

Printer-friendly Version

Interactive Discussion



The Collection 6 MODIS aerosol products over land and ocean

R. C. Levy et al.

Title Page

Abstract

Introduction

Conclusions

References

Tables

Figures

⏪

⏩

◀

▶

Back

Close

Full Screen / Esc

Printer-friendly Version

Interactive Discussion



windows, the non-trivial width of these bands (nominally 20 nm) contains absorption lines of water vapor (H_2O), ozone (O_3), carbon dioxide (CO_2), methane (CH_4), oxygen (O_2), nitrous oxide (N_2O), nitrogen dioxide (NO_2), and other trace gases. The MODIS aerosol retrieval requires gas-free spectral reflectance (ρ_λ^m), which is obtained by multiplying the L1B values ($\rho_\lambda^{\text{L1B}}$) with the total gas transmission correction factor (T_λ^{gas}).

$$\rho_\lambda^m = T_\lambda^{\text{gas}} \rho_\lambda^{\text{L1B}} \quad (\text{A2})$$

The MODIS retrieval is designed to compute total gas transmission correction as the product of the individual gases, i.e.,

$$T_\lambda^{\text{gas}} = T_\lambda^{\text{O}_3} T_\lambda^{\text{H}_2\text{O}} T_\lambda^{\text{CO}_2} T_\lambda^{\text{other}} \quad (\text{A3})$$

Depending on the wavelength band, the sum of gas absorption optical depths ($\tau_\lambda^{\text{gas}}$) can be as large as 0.05. Since

$$T_\lambda^{\text{gas}} \approx \exp(M\tau_\lambda^{\text{gas}}) \approx 1 + M\tau_\lambda^{\text{gas}}, \quad (\text{A4})$$

where M is air mass factor, neglect of (or errors in) gas absorption can lead to significant errors for TOA reflectance that is in turn matched with the aerosol LUTs.

For C5, the online ATBD (Levy et al., 2009) reports spectral coefficients for correcting the H_2O column (w in cm) and the O_3 column (O in Dobson units) corrections. In fact there are two sets of corrections for each of these gases: one formula for when there is valid ancillary NCEP data, the second for when the NCEP data are missing and mid-latitude summer climatology is applied. The formula in case of valid H_2O is quadratic with respect to $\ln(w)$ i.e.,

$$T_\lambda^{\text{H}_2\text{O}} = \exp(\exp(K_{0,\lambda}^{\text{H}_2\text{O}} + K_{1,\lambda}^{\text{H}_2\text{O}} \ln(Mw) + K_{2,\lambda}^{\text{H}_2\text{O}} (\ln(Mw))^2)) \quad (\text{A5})$$

whereas the formula for valid O_3 is linear (slope only) with respect to O . In case of climatology, fixed spectral optical depths are given for each gas ($\tau_\lambda^{\text{H}_2\text{O}}$ and $\tau_\lambda^{\text{O}_3}$). For

other gases, the ATBD reports only a correction for global average CO₂ optical depth ($\tau_{\lambda}^{\text{CO}_2}$), with no reference or indication of the CO₂ column concentration assumed for this computation. It is clear that aside from CO₂, H₂O and O₃, there are no other gas corrections.

Unfortunately, the C5 MODIS gas absorption correction factors were calculated well prior to Terra launch, and there is no known documentation of the assumptions made for these calculations. Therefore, for C6, we have recalculated MODIS gas absorption coefficients using the 6S-Vector (6sV, Kotchenova et al., 2006). We varied the types of atmospheres, gas concentrations, and air mass factors, and computed coefficients for regressions. Not surprisingly, results differed from the values documented within the ATBD. The revised C6 gas correction coefficients are reported in Table A2.

For H₂O, we made insignificant changes to the quadratic coefficients for valid NCEP value, yet the climatological values for mid-latitude summer optical depths were modified significantly for the 1.63 and 2.11 μm bands. For O₃, the climatology optical depths were close to that assumed for C5, but much better linear fits were attained when including a slope and offset. For other gases, instead of CO₂ only, we took climatology to be the sum of all gases that are not H₂O and O₃. While most of the absorbing gases are relatively well mixed throughout the atmosphere, we had to make some reasonable assumptions for NO₂. NO₂ is concentrated close to sources (usually urban/industrial) so we assumed a global mean column concentration of $3 \times 10^{15} \text{ cm}^{-2}$, and applied the table 9.5 of Jacobson, (2005). Thus, the total optical depth for “other” gases is the sum of that reported by 6sV plus our assumptions for NO₂.

AMTD

6, 159–259, 2013

The Collection 6 MODIS aerosol products over land and ocean

R. C. Levy et al.

Title Page

Abstract

Introduction

Conclusions

References

Tables

Figures

⏪

⏩

◀

▶

Back

Close

Full Screen / Esc

Printer-friendly Version

Interactive Discussion



Appendix B

List of C6 SDSs in MxD04_L2

Table B1 lists the SDSs found within the C6 MxD04_L2 file. Properties given include units, scale factor, and valid range (min = 1, max = 2). Also listed are the dimensions of the parameter, and the descriptive “long name”, given as an SDS attribute. SDSs marked with * are aggregated further into L3 data and # are included in the C6 MxD04_3K file.

Appendix C

Run time QA flags for MxD04 (.L2)

The Aerosol (dark target) run time *Quality Assurance* (QA) flags are stored as Scientific Data Sets (SDSs), *Quality_Assurance_Land*, and *Quality_Assurance_Ocean*. The Deep Blue retrieval has its own QA flag but is not discussed here. Each of the two dark-target QA flags are five bytes that provide information on the processing (logic) path taken during the aerosol retrieval. The aerosol QA includes product quality flags, retrieval processing flags, and input data resource flags which are designed separately for land and ocean because of the differences of retrieval algorithms. Particular flags may indicate: (a) conditions why retrieval was not attempted at all (e.g., input data outside of boundary conditions), (b) cases where input data quality may be poor (e.g., large cloud fraction), so that the retrieval is performed with lower confidence, or (c) cases where retrieval may have been performed but the results were poor (e.g., results outside of realistic conditions). Aerosol QA arrays are produced at product resolution and for daytime only.

The Quality Assurance confidence (QAC) flags summarize the QA logic, and are referred to in the main text of this paper. The QAC flags are the “Estimated quality flag

[Title Page](#)

[Abstract](#)

[Introduction](#)

[Conclusions](#)

[References](#)

[Tables](#)

[Figures](#)

[⏪](#)

[⏩](#)

[◀](#)

[▶](#)

[Back](#)

[Close](#)

[Full Screen / Esc](#)

[Printer-friendly Version](#)

[Interactive Discussion](#)



of aerosol optical thickness” for land and the “Estimated quality of aerosol parameter of average solution” for ocean retrievals. These flags appear embedded in the bits of the 5-byte “Quality_Assurance_Land” and “Quality_Assurance_Ocean”, but they also appear as straightforward integers in “Land_Ocean_Quality_Flag”.

The following tables describe the byte decoding of the MxD04 “Quality_Assurance_Land”, and “Quality_Assurance_Ocean” SDSs. Each flag corresponds to a certain number of bits, and bit values corresponding to results of certain tests. Note that the flags representing the case of valid retrieval but lower confidence is known as “Part I” over land, but “Part II” over ocean. Similarly the flags representing the case of no valid retrieval are known as Part II over land, but Part I over ocean. Under the column “Comments”, we describe possible flag cascades. For example, if Part I over land receives value = 8 (less than optimal clear sky pixels) then the QAC would be set to 2 (good quality).

References

- Ackerman, S. A., Strabala, K. I., Menzel, W. P., Frey, R. A., Moeller, C. C., and Gumley, L. E.: Discriminating clear sky from clouds with MODIS, *J. Geophys. Res.*, 103, 32141–32157, 1998.
- Ahmad, Z. and Fraser, R. S.: An Iterative Radiative Transfer Code For Ocean-Atmosphere Systems, *J. Atmos. Sci.*, 39, 656–665, doi:10.1175/1520-0469, 1982.
- Al-Saadi, J., Szykman, J., Pierce, R., Kittaka, C., Neil, D., Chu, D., Remer, L., Gumley, L., Prins, E., Weinstock, L., MacDonald, C., Wayland, R., Dimmick, F., and Fishman, J.: Improving national air quality forecasts with satellite aerosol observations, *B. Am. Meteorol. Soc.*, 86, 1249–1261, doi:10.1175/BAMS-86-9-1249, 2005.
- Anderson, T., Charlson, R., Winker, D., Ogren, J., and Holmen, K.: Mesoscale variations of tropospheric aerosols, *J. Atmos. Sci.*, 60, 119–136, 2003.
- Benedetti, A., Morcrette, J. J., Boucher, O., Dethof, A., Engelen, R. J., Fisher, M., Flentje, H., Huneeus, N., Jones, L., Kaiser, J. W., Kinne, S., Mangold, A., Razingerg, M., Simmons, A. J., and Suttie, M.: Aerosol analysis and forecast in the European Centre for Medium-Range

The Collection 6 MODIS aerosol products over land and ocean

R. C. Levy et al.

Title Page

Abstract

Introduction

Conclusions

References

Tables

Figures

⏪

⏩

◀

▶

Back

Close

Full Screen / Esc

Printer-friendly Version

Interactive Discussion



The Collection 6 MODIS aerosol products over land and ocean

R. C. Levy et al.

Title Page

Abstract

Introduction

Conclusions

References

Tables

Figures

⏪

⏩

◀

▶

Back

Close

Full Screen / Esc

Printer-friendly Version

Interactive Discussion



Weather Forecasts Integrated Forecast System: 2, Data assimilation, *J. Geophys. Res.*, 114, D13205, doi:10.1029/2008JD011115, 2009.

Bodhaine, B., Wood, N., Dutton, E., and Slusser, J.: On Rayleigh optical depth calculations, *J. Atmos. Ocean. Tech.*, 16, 1854–1861, 1999.

5 Breon, F.-M., Vermeulen, A., and Descloitres, J.: An evaluation of satellite aerosol products against sunphotometer measurements, *Remote Sens. Environ.*, 115, 3102–3111, doi:10.1016/j.rse.2011.06.017, 2011.

Carmona, I., Kaufman, Y. J., and Alpert, P.: Using numerical weather prediction errors to estimate aerosol heating, *Tellus B*, 60, 729–741, doi:10.1111/j.1600-0889.2008.00371.x, 2008.

10 Carroll, M. L., Townshend, J. R., DiMiceli, C. M., Noojipady, P., and Sohlberg, R. A.: A new global raster water mask at 250 m resolution, *International Journal of Digital Earth*, 2, 291–308, doi:10.1080/17538940902951401, 2009.

Carroll, M. L., Townshend, J. R. G., DiMiceli, C. M., Loboda, T., and Sohlberg, R. A.: Shrinking lakes of the Arctic: Spatial relationships and trajectory of change, *Geophys. Res. Lett.*, 38, 20406, doi:10.1029/2011GL049427, 2011.

15 Chu, D. A.: Global monitoring of air pollution over land from the Earth Observing System-Terra Moderate Resolution Imaging Spectroradiometer (MODIS), *J. Geophys. Res.*, 108, 4661, doi:10.1029/2002JD003179, 2003.

20 Chu, D., Kaufman, Y., Ichoku, C., Remer, L., Tanre, D., and Holben, B.: Validation of MODIS aerosol optical depth retrieval over land, *Geophys. Res. Lett.*, 29, 1617, doi:10.1029/2001GL013205, 2002.

Cox, C. and Munk, W.: measurement of the roughness of the sea surface from photographs of the sun's glitter, *J. Opt. Soc. Am.*, 44, 838–850, 1954.

25 Crusius, J., Schroth, A. W., Gasso, S., Moy, C. M., Levy, R. C., and Gatica, M.: Glacial flour dust storms in the Gulf of Alaska: Hydrologic and meteorological controls and their importance as a source of bioavailable iron, *Geophys. Res. Lett.*, 38, L06602, doi:10.1029/2010GL046573, 2011.

30 Dubovik, O., Sinyuk, A., Lapyonok, T., Holben, B. N., Mishchenko, M., Yang, P., Eck, T. F., Volten, H., Munoz, O., Veihelmann, B., van der Zande, W. J., Mangold, A., Razingerg, M., Simmons, A. J., and Suttie, M.: Application of spheroid models to account for aerosol particle nonsphericity in remote sensing of desert dust, *J. Geophys. Res.*, 111, 11208, doi:10.1029/2005JD006619, 2006.

The Collection 6 MODIS aerosol products over land and ocean

R. C. Levy et al.

[Title Page](#)
[Abstract](#)
[Introduction](#)
[Conclusions](#)
[References](#)
[Tables](#)
[Figures](#)
[⏪](#)
[⏩](#)
[◀](#)
[▶](#)
[Back](#)
[Close](#)
[Full Screen / Esc](#)
[Printer-friendly Version](#)
[Interactive Discussion](#)


Engel-Cox, J., Holloman, C., Coutant, B., and Hoff, R.: Qualitative and quantitative evaluation of MODIS satellite sensor data for regional and urban scale air quality, *Atmos. Environ.*, **38**, 2495–2509, 2004.

Evans, K. and Stephens, G.: A new polarized atmospheric radiative-transfer model, *J. Quant. Spectrosc. and Ra.*, **46**, 413–423, 1991.

Franz, B. A. B., Bailey, S. W. S., Werdell, P. J. P., and McClain, C. R. C.: Sensor-independent approach to the vicarious calibration of satellite ocean color radiometry, *Appl. Optics*, **46**, 5068–5082, doi:10.1364/AO.46.005068, 2007.

Gao, B., Yang, P., Han, W., Li, R., and Wiscombe, W.: An algorithm using visible and 1.38 μm channels to retrieve cirrus cloud reflectances from aircraft and satellite data, *IEEE T. Geosci. Remote*, **40**, 1659–1668, doi:10.1109/TGRS.2002.802454, 2002.

Giles, D. M., Holben, B. N., Eck, T. F., Sinyuk, A., Smirnov, A., Slutsker, I., Dickerson, R. R., Thompson, A. M., and Schafer, J. S.: An analysis of AERONET aerosol absorption properties and classifications representative of aerosol source regions, *J. Geophys. Res.*, **117**, 17203, doi:10.1029/2012JD018127, 2012.

Herman, M., Deuze, J., Marchand, A., Roger, B., and Lallart, P.: Aerosol remote sensing from POLDER/ADEOS over the ocean: Improved retrieval using a nonspherical particle model, *J. Geophys. Res.-Atmos.*, **110**, D10S02, doi:10.1029/2004JD004798, 2005.

Hoff, R., Zhang, H., Jordan, N., Prados, A., Engel-Cox, J., Huff, A., Weber, S., Zell, E., Kondragunta, S., Szykman, J., Johns, B., Dimmick, F., Wimmers, A., Al-Saadi, J., and Kittaka, C.: Applications of the Three-Dimensional Air Quality System to Western US Air Quality, IDEA, Smog Blog, Smog Stories, AirQuest, and the Remote Sensing Information Gateway, *J. Air and Waste Manage.*, **59**, 980–989, doi:10.3155/1047-3289.59.8.980, 2009.

Holben, B. N., Eck, T. F., Slutsker, I., Tanre, D., Buis, J. P., Setzer, A., Vermote, E., Reagan, J. A., Kaufman, Y. J., Nakajima, T., Lavenu, F., Jankowiak, I., and Smirnov, A.: AERONET – A federated instrument network and data archive for aerosol characterization, *Remote Sens. Environ.*, **66**, 1–16, doi:10.1016/S0034-4257(98)00031-5, 1998.

Holben, B. N., Eck, T. F., Slutsker, I., Smirnov, A., Sinyuk, A., Schafer, J., Giles, D., and Dubovik, O.: Aeronet’s Version 2.0 quality assurance criteria, in: *Remote Sensing of the Atmosphere and Clouds*, edited by: Tsay, S.-C., **16**, 6408, doi:10.1117/12.706524, 2006.

Hsu, N. C., Tsay, S. C., King, M. D., and Herman, J. R.: Aerosol Properties Over Bright-Reflecting Source Regions, *IEEE T. Geosci. Remote*, **42**, 557–569, doi:10.1109/TGRS.2004.824067, 2004.

The Collection 6 MODIS aerosol products over land and ocean

R. C. Levy et al.

Title Page

Abstract

Introduction

Conclusions

References

Tables

Figures

◀

▶

◀

▶

Back

Close

Full Screen / Esc

Printer-friendly Version

Interactive Discussion



- Hsu, N. C., Tsay, S. C., King, M. D., and Herman, J. R.: Deep blue retrievals of Asian aerosol properties during ACE-Asia, *IEEE T. Geosci. Remote.*, 44, 3180–3195, 2006.
- Hubanks, P. A.: MODIS Atmosphere QA Plan for Collection 005, Greenbelt, MD USA, NASA Goddard Space Flight Center, 57, 2012.
- 5 Hubanks, P. A., King, M. D., Platnick, S., and Pincus, R.: MODIS atmosphere L3 gridded product algorithm theoretical basis document, ATBD Reference Number: ATBD-MOD-30, http://modis-atmos.gsfc.nasa.gov/MOD08_M3/atbd.html, 2008.
- Huete, A., Didan, K., van Leeuwen, W., Miura, T., and Glenn, E.: MODIS Vegetation Indices, *Land Remote Sensing and Global Environmental Change*, 1, 579, doi:10.1007/978-1-4419-6749-7_26, 2011.
- 10 Hyer, E. J., Reid, J. S., and Zhang, J.: An over-land aerosol optical depth data set for data assimilation by filtering, correction, and aggregation of MODIS Collection 5 optical depth retrievals, *Atmos. Meas. Tech.*, 4, 379–408, doi:10.5194/amt-4-379-2011, 2011.
- Ichoku, C., Chu, D., Mattoo, S., Kaufman, Y., Remer, L., Tanre, D., Slutsker, I., and Holben, B.: A spatio-temporal approach for global validation and analysis of MODIS aerosol products, *Geophys. Res. Lett.*, 29, 1616, doi:10.1029/2001GL013206, 2002.
- 15 Ichoku, C., Remer, L., Kaufman, Y., Levy, R., Chu, D., Tanre, D., and Holben, B.: MODIS observation of aerosols and estimation of aerosol radiative forcing over southern Africa during SAFARI 2000, *J. Geophys. Res.-Atmos.*, 108, 8499–8499, doi:10.1029/2002JD002366, 2003.
- Jacobson, M. Z.: *Fundamentals of Atmospheric Modeling*, Cambridge University Press, 2005.
- Jeong, M.-J., Hsu, N. C., Kwiatkowska, E. J., Franz, B. A., Meister, G., and Salustro, C. E.: Impacts of Cross-Platform Vicarious Calibration on the Deep Blue Aerosol Retrievals for Moderate Resolution Imaging Spectroradiometer Aboard Terra, *IEEE T. Geosci. Remote.*, 49, 4877–4888, doi:10.1109/TGRS.2011.2153205, 2011.
- 25 Jethva, H., Satheesh, S. K., and Srinivasan, J.: Assessment of second-generation MODIS aerosol retrieval (Collection 005) at Kanpur, India, *Geophys. Res. Lett.*, 34, L19802, doi:10.1029/2007GL029647, 2007.
- Jethva, H., Torres, O., Remer, L. A., and Bhartia, P. K.: A color ratio method for the simultaneous retrieval of aerosol and cloud optical thickness of above-cloud absorbing aerosols from passive sensors: Application to MODIS measurements, *IEEE Trans. Geosci. Rem. Sens.*, 2012.
- 30

The Collection 6 MODIS aerosol products over land and ocean

R. C. Levy et al.

[Title Page](#)
[Abstract](#)
[Introduction](#)
[Conclusions](#)
[References](#)
[Tables](#)
[Figures](#)
[⏪](#)
[⏩](#)
[◀](#)
[▶](#)
[Back](#)
[Close](#)
[Full Screen / Esc](#)
[Printer-friendly Version](#)
[Interactive Discussion](#)


- Kaufman, Y., Ichoku, C., Giglio, L., Korontzi, S., Chu, D., Hao, W., Li, R., and Justice, C.: Fire and smoke observed from the Earth Observing System MODIS instrument – products, validation, and operational use, *Int. J. Remote Sens.*, 24, 1765–1781, 2003.
- 5 Kaufman, Y. J., Koren, I., Remer, L. A., Rosenfeld, D., and Rudich, Y.: The effect of smoke, dust, and pollution aerosol on shallow cloud development over the Atlantic Ocean, *P. Natl. Acad. Sci. USA*, 102, 11207–11212, doi:10.1073/pnas.0505191102, 2005.
- Kaufman, Y., Tanre, D., Remer, L., Vermote, E., Chu, A., and Holben, B.: Operational remote sensing of tropospheric aerosol over land from EOS moderate resolution imaging spectroradiometer, *J. Geophys. Res.*, 102, 17051–17067, 1997a.
- 10 Kaufman, Y., Wald, A., Remer, L., Gao, B., Li, R., and Flynn, L.: The MODIS 2.1 μm channel – Correlation with visible reflectance for use in remote sensing of aerosol, *IEEE T. Geosci. Remote*, 35, 1286–1298, 1997b.
- King, L. V.: On the Complex Anisotropic Molecule in Relation to the Dispersion and Scattering of Light, *Proceedings of the Royal Society of London, Series A, P. R. Soc. Lond. A.-Conta.*, 104, 333–357, 1923.
- 15 King, M., Menzel, W., Kaufman, Y., Tanre, D., Gao, B., Platnick, S., Ackerman, S., Remer, L., Pincus, R., and Hubanks, P.: Cloud and aerosol properties, precipitable water, and profiles of temperature and water vapor from MODIS, *IEEE T. Geosci. Remote*, 41, 442–458, 2003.
- Kinne, S., Lohmann, U., Feichter, J., Schulz, M., Timmreck, C., Ghan, S., Easter, R., Chin, M., Ginoux, P., Takemura, T., Tegen, I., Koch, D., Herzog, M., Penner, J., Pitari, G., Holben, B., Eck, T., Smirnov, A., Dubovik, O., Slutsker, I., Tanré, D., Torres, O., Mishchenko, M., Geogedzhayev, I., Chu, D.-A., and Kaufman, Y.: Monthly averages of aerosol properties: A global comparison among models, satellite data, and AERONET ground data, *J. Geophys. Res.-Atmos.*, 108, 4634–4634, doi:10.1029/2001JD001253, 2003.
- 20 Kishcha, P., Starobinets, B., and Alpert, P.: Latitudinal variations of cloud and aerosol optical thickness trends based on MODIS satellite data, *Geophys. Res. Lett.*, 34, L05810, doi:10.1029/2006GL028796, 2007.
- Kleidman, R. G., O'Neill, N. T., Remer, L. A., Kaufman, Y. J., Eck, T. F., Tanré, D., Dubovik, O., and Holben, B. N.: Comparison of moderate resolution Imaging spectroradiometer (MODIS) and aerosol robotic network (AERONET) remote-sensing retrievals of aerosol fine mode fraction over ocean, *J. Geophys. Res.-Atmos.*, 110, D22205, doi:10.1029/2005JD005760, 2005.
- 30

The Collection 6 MODIS aerosol products over land and ocean

R. C. Levy et al.

[Title Page](#)
[Abstract](#)
[Introduction](#)
[Conclusions](#)
[References](#)
[Tables](#)
[Figures](#)
[⏪](#)
[⏩](#)
[◀](#)
[▶](#)
[Back](#)
[Close](#)
[Full Screen / Esc](#)
[Printer-friendly Version](#)
[Interactive Discussion](#)


Kleidman, R. G., Smirnov, A., Levy, R. C., Mattoo, S., and Tanre, D.: Evaluation and Wind Speed Dependence of MODIS Aerosol Retrievals Over Open Ocean, *IEEE T. Geosci. Remote Sensing*, 50, 429–435, doi:10.1109/TGRS.2011.2162073, 2012.

Koepke, P.: Effective reflectance of oceanic whitecaps, *Appl. Optics*, 23, 1816–1824, 1984.

5 Koren, I. and Feingold, G.: Aerosol-cloud-precipitation system as a predator-prey problem, *P. Natl. Acad. Sci. USA*, 108, 12227–12232, doi:10.1073/pnas.1101777108, 2011.

Koren, I. and Kaufman, Y. J.: Direct wind measurements of Saharan dust events from Terra and Aqua satellites, *Geophys. Res. Lett.*, 31, L06122, doi:10.1029/2003GL019338, 2004.

10 Koren, I., Oreopoulos, L., Feingold, G., Remer, L. A., and Altaratz, O.: How small is a small cloud?, *Atmos. Chem. Phys.*, 8, 3855–3864, doi:10.5194/acp-8-3855-2008, 2008.

Kotchenova, S. Y. S., Vermote, E. F. E., Matarrese, R. R., and Klemm, F. J. F.: Validation of a vector version of the 6S radiative transfer code for atmospheric correction of satellite data, Part I, path radiance, *Appl. Optics*, 45, 6762–6774, 2006.

15 Kotchenova, S. Y., Vermote, E. F., Levy, R., and Lyapustin, A.: Radiative transfer codes for atmospheric correction and aerosol retrieval: intercomparison study, *Appl. Optics*, 47, 2215–2226, doi:10.1364/AO.47.002215, 2008.

Levy, R., Remer, L., Tanré, D., Kaufman, Y. J., Ichoku, C., Holben, B. N., Livingston, J. M., Russell, P. B., and Maring, H.: Evaluation of the Moderate-Resolution Imaging Spectroradiometer (MODIS) retrievals of dust aerosol over the ocean during PRIDE, *J. Geophys. Res.-Atmos.*, 20 108, 8594, doi:10.1029/2002JD002460, 2003.

Levy, R. C., Remer, L. A., Martins, J. V., Kaufman, Y. J., Plana-Fattori, A., Redemann, J., and Wenny, B.: Evaluation of the MODIS aerosol retrievals over ocean and land during CLAMS, *J. Atmos. Sci.*, 62, 974–992, doi:10.1175/JAS3391.1, 2005.

25 Levy, R. C., Remer, L. A., and Dubovik, O.: Global aerosol optical properties and application to Moderate Resolution Imaging Spectroradiometer aerosol retrieval over land, *J. Geophys. Res.-Atmos.*, 112, doi:10.1029/2006JD007815, 2007a.

Levy, R. C., Remer, L. A., Mattoo, S., Vermote, E. F., and Kaufman, Y. J.: Second-generation operational algorithm: Retrieval of aerosol properties over land from inversion of Moderate Resolution Imaging Spectroradiometer spectral reflectance, *J. Geophys. Res.-Atmos.*, 112, D13211, doi:10.1029/2006JD007811, 2007b.

30 Levy, R. C., Leptoukh, G. G., Kahn, R., Zubko, V., Gopalan, A., and Remer, L. A.: A Critical Look at Deriving Monthly Aerosol Optical Depth From Satellite Data, *IEEE T. Geosci. Remote*, 47, 2942–2956, doi:10.1109/TGRS.2009.2013842, 2009a.

The Collection 6 MODIS aerosol products over land and ocean

R. C. Levy et al.

Title Page

Abstract

Introduction

Conclusions

References

Tables

Figures

⏪

⏩

◀

▶

Back

Close

Full Screen / Esc

Printer-friendly Version

Interactive Discussion



- Levy, R. C., Remer, L. A., Tanré, D., Mattoo, S., and Kaufman, Y. J.: Algorithm for remote sensing of tropospheric aerosol over dark targets from modis: Collections 005 and 051: Revision 2, MODIS Algorithm Theoretical Basis Document, 2009b.
- 5 Levy, R. C., Remer, L. A., Kleidman, R. G., Mattoo, S., Ichoku, C., Kahn, R., and Eck, T. F.: Global evaluation of the Collection 5 MODIS dark-target aerosol products over land, *Atmos. Chem. Phys.*, 10, 10399–10420, doi:10.5194/acp-10-10399-2010, 2010.
- Li, C., Lau, A., Mao, J., and Chu, D.: Retrieval, validation, and application of the 1 km aerosol optical depth from MODIS measurements over Hong Kong, *IEEE T. Geosci. Remote*, 43, 2650–2658, 2005.
- 10 Li, R.-R., Kaufman, Y. J., Gao, B.-C., and Davis, C. O.: Remote sensing of suspended sediments and shallow coastal waters, *IEEE T. Geosci. Remote*, 41, 559–566, doi:10.1109/TGRS.2003.810227, 2003.
- Li, R.-R., Remer, L., Kaufman, Y., Mattoo, S., Gao, B., and Vermote, E.: Snow and ice mask for the MODIS aerosol products, *IEEE Geosci. Remote Sens. Lett.*, 2, 306–310, doi:10.1109/LGRS.2005.847755, 2005.
- 15 Lyapustin, A., Wang, Y., Laszlo, I., Kahn, R., Korkin, S., Remer, L., Levy, R., and Reid, J. S.: Multiangle implementation of atmospheric correction (MAIAC), 2, *Aerosol algorithm, J. Geophys. Res.-Atmos.*, 116, D03211, doi:10.1029/2010JD014986, 2011.
- Martins, J., Tanre, D., Remer, L., Kaufman, Y., Mattoo, S., and Levy, R.: MODIS Cloud screening for remote sensing of aerosols over oceans using spatial variability, *Geophys. Res. Lett.*, 29, 1619, doi:10.1029/2001GL013252, 2002.
- 20 Mishchenko, M. I., Liu, L., Geogdzhayev, I. V., Travis, L. D., Cairns, B., and Lacis, A. A.: Toward unified satellite climatology of aerosol properties, *J. Quant. Spectrosc. & Ra.*, 111, 540–552, doi:10.1016/j.jqsrt.2009.11.003, 2010.
- Moody, E. G., King, M. D., Platnick, S., Schaaf, C. B., and Feng G.: Spatially complete global spectral surface albedos: value-added datasets derived from Terra MODIS land products, *IEEE T. Geosci. Remote.*, 43, 144–158, doi:10.1109/TGRS.2004, 2005.
- 25 Moody, E. G., King, M. D., Schaaf, C. B., and Platnick, S.: MODIS-Derived Spatially Complete Surface Albedo Products: Spatial and Temporal Pixel Distribution and Zonal Averages, *J. Appl. Meteorol. Clim.*, 47, 2879–2894, doi:10.1175/2008JAMC1795.1, 2008.
- 30 Munchak, L.A., Levy, R. C., Mattoo, S., Remer, L. A., Holben, B. N., Shafer, J. S., Hostetler, C. A., and Ferrare, R. A.: MODIS 3km aerosol product: Applications over land in an urban/suburban region, submitted to *Atmos. Meas. Tech.*, 2012.

The Collection 6 MODIS aerosol products over land and ocean

R. C. Levy et al.

Title Page

Abstract

Introduction

Conclusions

References

Tables

Figures

◀

▶

◀

▶

Back

Close

Full Screen / Esc

Printer-friendly Version

Interactive Discussion



National Research Council (US): Committee on Climate Data Records from NOAA Operational Satellites: Climate Data Records from Environmental Satellites, National Academy Press, 2004.

Oo, M. M., Jerg, M., Hernandez, E., Picón, A., Gross, B. M., Moshary, F., and Ahmed, S. A.: Improved MODIS Aerosol Retrieval Using Modified VIS/SWIR Surface Albedo Ratio Over Urban Scenes, *IEEE T. Geosci. Remote*, 48, 983–1000, doi:10.1109/TGRS.2009.2028333, 2010.

Petrenko, M., Ichoku, C., and Leptoukh, G.: Multi-sensor Aerosol Products Sampling System (MAPSS), *Atmos. Meas. Tech.*, 5, 913–926, doi:10.5194/amt-5-913-2012, 2012.

Platnick, S., King, M. D., Ackerman, S. A., Menzel, W. P., Baum, B. A., Riedi, J. C., and Frey, R. A.: The MODIS cloud products: algorithms and examples from terra, *IEEE T. Geosci. Remote*, 41, 459–473, doi:10.1109/TGRS.2002.808301, 2003.

Pope, III, C. A., Burnett, R. T., Thun, M. J., Calle, E. E., Krewski, D., Ito, K., and Thurston, G. D.: Lung Cancer, Cardiopulmonary Mortality, and Long-term Exposure to Fine Particulate Air Pollution, *JAMA*, 287, 1132–1141, doi:10.1001/pubs.JAMA-ISSN-0098-7484-287-9-joc11435, 2002.

Redemann, J., Zhang, Q., Livingston, J., Russell, P., Shinozuka, Y., Clarke, A., Johnson, R., and Levy, R.: Testing aerosol properties in MODIS Collection 4 and 5 using airborne sunphotometer observations in INTEX-B/MILAGRO, *Atmos. Chem. Phys.*, 9, 8159–8172, doi:10.5194/acp-9-8159-2009, 2009.

Reid, J. S., Benedetti, A., Colarco, P. R., and Hansen, J. A.: International Operational Aerosol Observability Workshop, *B. Am. Meteorol. Soc.*, 92, 21–24, doi:10.1175/2010BAMS3183.1, 2011.

Remer, L. A. and Kaufman, Y. J.: Dynamic aerosol model: Urban/industrial aerosol, *J. Geophys. Res.*, 103, 13859–13871, doi:10.1029/98JD00994, 1998.

Remer, L., Kaufman, Y., Holben, B., Thompson, A., and McNamara, D.: Biomass burning aerosol size distribution and modeled optical properties, *J. Geophys. Res.-Atmos.*, 103, 31879–31891, 1998.

Remer, L., Tanre, D., Kaufman, Y., Ichoku, C., Mattoo, S., Levy, R., Chu, D., Holben, B., Dubovik, O., Smirnov, A., Martins, J. V., Li, R. R., and Ahmad, Z.: Validation of MODIS aerosol retrieval over ocean, *Geophys. Res. Lett.*, 29, 8008–8008, doi:10.1029/2001GL013204, 2002.

Remer, L. A., Kaufman, Y. J., Tanre, D., Mattoo, S., Chu, D. A., Martins, J. V., Li, R. R., Ichoku, C., Levy, R. C., Kleidman, R. G., Eck, T. F., Vermote, E., and Holben, B. N.:

The Collection 6 MODIS aerosol products over land and ocean

R. C. Levy et al.

[Title Page](#)
[Abstract](#)
[Introduction](#)
[Conclusions](#)
[References](#)
[Tables](#)
[Figures](#)
[⏪](#)
[⏩](#)
[◀](#)
[▶](#)
[Back](#)
[Close](#)
[Full Screen / Esc](#)
[Printer-friendly Version](#)
[Interactive Discussion](#)

The MODIS aerosol algorithm, products, and validation, *J. Atmos. Sci.*, 62, 947–973, doi:10.1175/JAS3385.1, 2005.

Remer, L. A., Kleidman, R. G., Levy, R. C., Kaufman, Y. J., Tanre, D., Mattoo, S., Martins, J. V., Ichoku, C., Koren, I., Yu, H., and Holben, B. N.: Global aerosol climatology from the MODIS satellite sensors, *J. Geophys. Res.-Atmos.*, 113, D14S07, doi:10.1029/2007JD009661, 2008a.

Remer, L. A., Kleidman, R. G., Levy, R. C., Kaufman, Y. J., Tanré, D., Mattoo, S., Martins, J. V., Ichoku, C., Koren, I., Yu, H., and Holben, B. N.: Global aerosol climatology from the MODIS satellite sensors, *J. Geophys. Res.-Atmos.*, 113, D14S07, doi:10.1029/2007JD009661, 2008b.

Remer, L. A., Mattoo, S., Levy, R. C., Heidinger, A., Pierce, R. B., and Chin, M.: Retrieving aerosol in a cloudy environment: aerosol product availability as a function of spatial resolution, *Atmos. Meas. Tech.*, 5, 1823–1840, doi:10.5194/amt-5-1823-2012, 2012.

Remer, L.A., Mattoo, S., Levy, R.C, and Munchak, L.A.: MODIS 3 km product: Algorithm and global perspective, submitted to *Atmos. Meas. Tech.*, in press, 2012.

Salomonsen, V., Barnes, W., Maymon, P., Montgomery, H., and Ostrow, H.: MODIS – Advanced facility instrument for studies of the earth as a system, *IEEE T. Geosci. Remote.*, 27, 145–153, 1989.

Sayer, A. M., Hsu, N. C., Bettenhausen, C., Ahmad, Z., Holben, B. N., Smirnov, A., Thomas, G. E., and Zhang, J.: SeaWiFS Ocean Aerosol Retrieval (SOAR): Algorithm, validation, and comparison with other data sets, *J. Geophys. Res.*, 117, D03206, doi:10.1029/2011JD016599, 2012a.

Sayer, A. M., Smirnov, A., Hsu, N. C., Munchak, L. A., and Holben, B. N.: Estimating marine aerosol particle volume and number from Maritime Aerosol Network data, *Atmos. Chem. Phys.*, 12, 8889–8909, doi:10.5194/acp-12-8889-2012, 2012b.

Sayer, A. M., Hsu, N. C., Bettenhausen, C., Jeong, M. J., Holben, B. N., and Zhang, J.: Global and regional evaluation of over-land spectral aerosol optical depth retrievals from SeaWiFS, *Atmos. Meas. Tech.*, 5, 1761–1778, doi:10.5194/amt-5-1761-2012, 2012c.

Schaaf, C. B., Liu, J., Gao, F., and Strahler, A. H.: Aqua and Terra MODIS Albedo and Reflectance Anisotropy Products, *Land Remote Sensing and Global Environmental Change*, 1, 549, doi:10.1007/978-1-4419-6749-7_24, 2011.

Schafer, J. S., Eck, T. F., Holben, B. N., Artaxo, P., and Duarte, A. F.: Characterization of the optical properties of atmospheric aerosols in Amazonia from long-term

**The Collection 6
MODIS aerosol
products over land
and ocean**

R. C. Levy et al.

[Title Page](#)[Abstract](#)[Introduction](#)[Conclusions](#)[References](#)[Tables](#)[Figures](#)[⏪](#)[⏩](#)[◀](#)[▶](#)[Back](#)[Close](#)[Full Screen / Esc](#)[Printer-friendly Version](#)[Interactive Discussion](#)

AERONET monitoring (1993–1995 and 1999–2006), *J. Geophys. Res.-Atmos.*, 113, D04204, doi:10.1029/2007JD009319, 2008.

Smirnov, A., Holben, B. N., Slutsker, I., Giles, D. M., McClain, C. R., Eck, T. F., Sakerin, S. M., Macke, A., Croot, P., Zibordi, G., Quinn, P. K., Sciare, J., Kinne, S., Harvey, M., Smyth, T. J., Piketh, S., Zielinski, T., Proshutinsky, A., and Goes, J. I., Nelson, N. B., Larouche, P., Radionov, V. F., Goloub, P., Krishna Moorthy, K., Matarrese, R., Robertson, E. J., and Jourdin, F.: Maritime Aerosol Network as a component of Aerosol Robotic Network, *J. Geophys. Res.*, 114, 06204, doi:10.1029/2008JD011257, 2009.

Stier, P., Feichter, J., Kinne, S., Kloster, S., Vignati, E., Wilson, J., Ganzeveld, L., Tegen, I., Werner, M., Balkanski, Y., Schulz, M., Boucher, O., Minikin, A., and Petzold, A.: The aerosol-climate model ECHAM5-HAM, *Atmos. Chem. Phys.*, 5, 1125–1156, doi:10.5194/acp-5-1125-2005, 2005.

Sun, J., Xiong, X., Angal, A., Chen, H., Geng, X., and Wu, A.: On-orbit performance of the MODIS reflective solar bands time-dependent response versus scan angle algorithm, edited by: Butler, J. J., Xiong, X. J., and Gu, X., *Proc. of SPIE*, 8510, 85100J-1-9, doi:10.1117/12.930021, 2012.

Takemura, T., Nakajima, T., Dubovik, O., Holben, B., and Kinne, S.: Single-scattering albedo and radiative forcing of various aerosol species with a global three-dimensional model, *J. Climate*, 15, 333–352, 2002.

Tanre, D., Herman, M., and Kaufman, Y.: Information on aerosol size distribution contained in solar reflected spectral radiances, *J. Geophys. Res.-Atmos.*, 101, 19043–19060, 1996.

Tanre, D., Kaufman, Y. J., Herman, M., and Mattoo, S.: Remote sensing of aerosol properties over oceans using the MODIS/EOS spectral radiances, *J. Geophys. Res.-Atmos.*, 102, 16971–16988, 1997.

Tanre, D., Remer, L. A., Kaufman, Y. J., Mattoo, S., Hobbs, P. V., Livingston, J. M., Russell, P. B., and Smirnov, A.: Retrieval of aerosol optical thickness and size distribution over ocean from the MODIS airborne simulator during TARFOX, *J. Geophys. Res.*, 104, 2261–2278, doi:10.1029/1998JD200077, 1999.

van Donkelaar, A., Martin, R. V., Levy, R. C., da Silva, A. M., Krzyzanowski, M., Chubarova, N. E., Semutnikova, E., and Cohen, A. J.: Satellite-based estimates of ground-level fine particulate matter during extreme events: A case study of the Moscow fires in 2010, *Atmos. Environ.*, 45, 6225–6232, doi:10.1016/j.atmosenv.2011.07.068, 2011.

The Collection 6 MODIS aerosol products over land and ocean

R. C. Levy et al.

[Title Page](#)
[Abstract](#)
[Introduction](#)
[Conclusions](#)
[References](#)
[Tables](#)
[Figures](#)
[Back](#)
[Close](#)
[Full Screen / Esc](#)
[Printer-friendly Version](#)
[Interactive Discussion](#)


- Vermote, E. F. and Kotchenova, S.: Atmospheric correction for the monitoring of land surfaces, *J. Geophys. Res.*, 113, D23S90, doi:10.1029/2007JD009662, 2008.
- Vermote, E. F., Tanre, D., Deuze, J. L., Herman, M., and Morcette, J. J.: Second Simulation of the Satellite Signal in the Solar Spectrum, 6S: an overview, *IEEE T. Geosci. Remote*, 35, 675–686, doi:10.1109/36.581987, 1997.
- Wang, J. and Christopher, S. A.: Intercomparison between satellite-derived aerosol optical thickness and PM 2.5mass: Implications for air quality studies, *Geophys. Res. Lett.*, 30, 2095, doi:10.1029/2003GL018174, 2003.
- Wang, D., Morton, D., Masek, J., Wu, A., Nagol, J., Xiong, X., Levy, R., Vermote, E., and Wolfe, R.: Impact of sensor degradation on the MODIS NDVI time series, *Remote Sens. Environ.*, 119, 55–61, 2012.
- Witte, J. C., Douglass, A. R., da Silva, A., Torres, O., Levy, R., and Duncan, B. N.: NASA A-Train and Terra observations of the 2010 Russian wildfires, *Atmos. Chem. Phys.*, 11, 9287–9301, doi:10.5194/acp-11-9287-2011, 2011.
- Xiong, X., Sun, J.-Q., Wu, A., Chiang, K.-F., Esposito, J., and Barnes, W. L.: Terra and Aqua MODIS Calibration Algorithms and Uncertainty Analysis, SPIE: Sensors, Systems, and Next-Generation Satellites IX, 2005.
- Xiong, X., Sun, J., Barnes, W., Salomonson, V., Esposito, J., Erives, H., and Guenther, B.: Multiyear on-orbit calibration and performance of Terra MODIS reflective solar bands, *IEEE T. Geosci. Remote*, 45, 879–889, doi:10.1109/TGRS.2006.890567, 2007.
- Young, A. T.: Revised depolarization corrections for atmospheric extinction, *Appl. Optics*, 19, 3427–3428, doi:10.1364/AO.19.003427, 1980.
- Yu, H., Kaufman, Y. J., Chin, M., Feingold, G., Remer, L. A., Anderson, T. L., Balkanski, Y., Belloouin, N., Boucher, O., Christopher, S., DeCola, P., Kahn, R., Koch, D., Loeb, N., Reddy, M. S., Schulz, M., Takemura, T., and Zhou, M.: A review of measurement-based assessments of the aerosol direct radiative effect and forcing, *Atmos. Chem. Phys.*, 6, 613–666, doi:10.5194/acp-6-613-2006, 2006.
- Yu, H., Remer, L. A., Chin, M., Bian, H., Tan, Q., Yuan, T., and Zhang, Y.: Aerosols from Overseas Rival Domestic Emissions over North America, *Science*, 337, 566–569, doi:10.1126/science.1217576, 2012.
- Zhang, J. and Reid, J. S.: A decadal regional and global trend analysis of the aerosol optical depth using a data-assimilation grade over-water MODIS and Level 2 MISR aerosol products, *Atmos. Chem. Phys.*, 10, 10949–10963, doi:10.5194/acp-10-10949-2010, 2010.

Zhang, J., Reid, J. S., Westphal, D. L., Baker, N. L. and Hyer, E. J.: A system for operational aerosol optical depth data assimilation over global oceans, *J. Geophys. Res.-Atmos.*, 113, D10208, doi:10.1029/2007JD009065, 2008.

AMTD

6, 159–259, 2013

The Collection 6 MODIS aerosol products over land and ocean

R. C. Levy et al.

Title Page

Abstract

Introduction

Conclusions

References

Tables

Figures



Back

Close

Full Screen / Esc

Printer-friendly Version

Interactive Discussion



The Collection 6 MODIS aerosol products over land and ocean

R. C. Levy et al.

Title Page

Abstract

Introduction

Conclusions

References

Tables

Figures

⏪

⏩

◀

▶

Back

Close

Full Screen / Esc

Printer-friendly Version

Interactive Discussion



Table 1. C6 DT-land data products and changes from C51.

C5 SDS	C6 SDS	C6 dimension	Noted changes from C5 to C6
Corrected_Optical_Depth_Land	Corrected_Optical_Depth_Land	X, Y, 3a λ	
Corrected_Optical_Depth_Land_wav2p1	Corrected_Optical_Depth_Land_wav2p1	X, Y: (at 2.11 μm)	
Optical_Depth_Ratio_Small_Land	Optical_Depth_Ratio_Small_Land	X, Y: (at 0.55 μm)	
Surface_Reflectance_Land	Surface_Reflectance_Land	X, Y, 3a λ	
Fitting_Error_Land	Fitting_Error_Land	X, Y: (at 0.65 μm)	
Quality_Assurance_Land	Quality_Assurance_Land	X, Y, 5B	
Aerosol_Type_Land	Aerosol_Type_Land	X, Y	
Angstrom_Exponent_Land			deleted
Mass_Concentration_Land	Mass_Concentration_Land	X, Y	
Optical_Depth_Small_Land		X, Y, 4 λ	deleted
Mean_Reflectance_Land	Mean_Reflectance_Land	X, Y, 10 λ	Added 3 wavelengths
STD_Reflectance_Land	STD_Reflectance_Land	X, Y, 10 λ	Added 3 wavelengths
Cloud_Fraction_Land	Aerosol_Cloud_Fraction_Land	X, Y	Renamed
Number_Pixels_Used_Land	Number_Pixels_Used_Land	X, Y, 10 λ	Separate tally each λ
Path_Radiance_Land			deleted
Error_Path_Radiance_Land			deleted
Critical_Reflectance_Land			deleted
Error_Crit_Reflectance_Land			deleted
Error_Critical_Reflectance_Land			deleted
Quality_Weight_Path_Radiance_Land			deleted
Quality_Weight_Crit_Reflectance_Land			deleted
	Topographic_Altitude_Land	X, Y	New diagnostic

X,Y refers to a 2-dimensional array along/across the swath (at a particular wavelength λ)

Some parameters have a third dimension.

A dimension of “# λ ” refers to # wavelengths

= 3a: 0.47, 0.55 and 0.65 μm

= 3b: 0.47, 0.55 and 2.11 μm .

= 4: 0.47, 0.55, 0.65 and 2.11 μm

= 7: 0.47, 0.55, 0.65, 0.86, 1.24, 1.63 and 2.11 μm .

= 10: 0.47, 0.55, 0.65, 0.86, 1.24, 1.63, 2.11, 0.41, 0.44 and 0.76 μm .

A dimension of “5B” refers to the number of bytes (5) of the QA Flags.

The Collection 6 MODIS aerosol products over land and ocean

R. C. Levy et al.

Table 2. C5/C6 Comparison of DT-land statistics for Aqua, January and July 2008.

Month: C	Granule count	Pixel count	Valid count	QA0	QA1	QA2	QA3	QA-Filtered count	Mean AOD QA-Filtered
Jan: C5	4158	114005610	3187427	521093	365787	469646	1830901	1830901	0.1952
Jan: C6	4158	114005070	3325960	943250	310386	395245	1677079	1677079	0.2009
Jul: C5	4132	113292675	7454199	1032086	885926	1146430	4389757	4389757	0.1293
Jul: C6	4132	113292000	7838947	1511884	854003	1099299	4373761	4373761	0.151

Title Page

Abstract

Introduction

Conclusions

References

Tables

Figures

◀

▶

◀

▶

Back

Close

Full Screen / Esc

Printer-friendly Version

Interactive Discussion



The Collection 6 MODIS aerosol products over land and ocean

R. C. Levy et al.

[Title Page](#)[Abstract](#)[Introduction](#)[Conclusions](#)[References](#)[Tables](#)[Figures](#)[⏪](#)[⏩](#)[◀](#)[▶](#)[Back](#)[Close](#)[Full Screen / Esc](#)[Printer-friendly Version](#)[Interactive Discussion](#)**Table 3.** C6 DT-ocean data products and changes from C51.

C6 SDS	C6 dimensions	Noted changes from C51 to C6
Effective_Optical_Depth_Average_Ocean	X, Y, 7 λ	
Effective_Optical_Depth_Best_Ocean	X, Y, 7 λ	
Optical_Depth_Ratio_Small_Ocean_0.55micron	X, Y, 2S	
Solution_Index_Ocean_Small	X, Y, 2S	
Solution_Index_Ocean_Large	X, Y, 2S	
Least_Squares_Error_Ocean	X, Y, 2S	
Effective_Radius_Ocean	X, Y, 2S	
Optical_Depth_Small_Best_Ocean	X, Y, 7 λ	
Optical_Depth_Small_Average_Ocean	X, Y, 7 λ	
Optical_Depth_Large_Best_Ocean	X, Y, 7 λ	
Optical_Depth_Large_Average_Ocean	X, Y, 7 λ	
Mass_Concentration_Ocean	X, Y, 2S	
Cloud_Condensation_Nuclei_Ocean	X, Y, 2S	
Asymmetry_Factor_Best_Ocean	X, Y, 7 λ	
Asymmetry_Factor_Average_Ocean	X, Y, 7 λ	
Backscattering_Ratio_Best_Ocean	X, Y, 7 λ	
Backscattering_Ratio_Average_Ocean	X, Y, 7 λ	
Angstrom_Exponent_1_Ocean (0.55/0.86 micron)	X, Y, 2S	
Angstrom_Exponent_2_Ocean (0.86/2.1 micron)	X, Y, 2S	
PSML003_Ocean	X, Y, 2S	Renamed from "Cloud_Condensation_Nuclei_Ocean"
Optical_Depth_by_models_Ocean	X, Y, 9M	
Aerosol_Cloud_Fraction_Ocean	X, Y	Renamed from "Cloud_Fraction_Ocean"
Number_Pixels_Used_Ocean	X, Y, 10 λ	Separate tally for each of ten wavelength
Mean_Reflectance_Ocean	X, Y, 10 λ	Added 3 wavelengths
STD_Reflectance_Ocean	X, Y, 10 λ	Added 3 wavelengths
Quality_Assurance_Ocean	X, Y, 5B	
Wind_Speed_Ncep_Ocean	X, Y:	New diagnostic

X,Y refers to a 2-dimensional array along/across the swath (at a particular wavelength λ).

Some parameters have a third dimension.

A dimension of "# λ " refers to # wavelengths

= 7: 0.47, 0.55, 0.65, 0.86, 1.24, 1.63 and 2.11 μm .

= 10: 0.47, 0.55, 0.65, 0.86, 1.24, 1.63, 2.11, 0.41, 0.44 and 0.76 μm .

A dimension of "5B" refers to the number of bytes (5) of the QA Flags.

A dimension of "9M" is number of modes (9).

A dimension of "2S" is two solutions ("average" and "best").

The Collection 6 MODIS aerosol products over land and ocean

R. C. Levy et al.

Table 4. C5/C6 Comparison of DT-ocean statistics for Aqua, January and July 2008.

Month: C	Granule count	Pixel count	Valid count	QA0	QA1	QA2	QA3	Filtered count	Mean AOD Filtered
Jan: C5	4158	114005610	13229672	258096	10124022	2	2847552	12971576	0.1379
Jan: C6	4158	114005070	13661286	254624	9321301	2	4085359	13406662	0.1149
Jul: C5	4132	113292675	14943305	328372	11579972	100	3034861	14614933	0.1328
Jul: C6	4132	113292000	16130632	228965	11217509	113	4684045	15901667	0.1086

Title Page

Abstract

Introduction

Conclusions

References

Tables

Figures

◀

▶

◀

▶

Back

Close

Full Screen / Esc

Printer-friendly Version

Interactive Discussion



The Collection 6 MODIS aerosol products over land and ocean

R. C. Levy et al.

Title Page

Abstract

Introduction

Conclusions

References

Tables

Figures

◀

▶

◀

▶

Back

Close

Full Screen / Esc

Printer-friendly Version

Interactive Discussion

Table 5. C6 joint land and ocean data products that are changed from C5.

C5 SDS	C6 SDS	C6 dimension	Noted changes from C5 to C6
Optical_Depth_Land_And_Ocean	Optical_Depth_Land_And_Ocean	X, Y	Revised QA filtering: Land QAC=3 Ocean QAC \geq 1 Deleted
Optical_Depth_Ratio_Small_Land_And_Ocean	Land_Sea_Flag Land_Ocean_Quality_Flag	X, Y X, Y	New parameter: Integer land and sea New parameter: Integer value for QA

The Collection 6 MODIS aerosol products over land and ocean

R. C. Levy et al.

Title Page

Abstract

Introduction

Conclusions

References

Tables

Figures

◀

▶

◀

▶

Back

Close

Full Screen / Esc

Printer-friendly Version

Interactive Discussion

Table 6. New “aerosol” cloud Products.

C6 SDS	C6 dimension	New parameter description
Aerosol_Cldmsk_Land_Ocean	X(500 m), Y(500 m):	500 m resolution cloud mask used in retrieval
Cloud_Distance_Land_Ocean	X(500 m), Y(500 m):	Distance each pixel to nearest cloudy pixel (pixels)
Average_Cloud_Distance_Land_Ocean	X(10 km), Y(10 km):	Average distance to cloud in 10 km box

X,Y refers to a 2-dimensional array along/across the swath, with the spatial resolution in parantheses.

The Collection 6 MODIS aerosol products over land and ocean

R. C. Levy et al.

Title Page

Abstract

Introduction

Conclusions

References

Tables

Figures

◀

▶

◀

▶

Back

Close

Full Screen / Esc

Printer-friendly Version

Interactive Discussion

Table 7. C6 New combined Dark Target/Deep Blue SDSs.

C6 SDS	C6 dimension	New parameter description
Dark_Target_Deep_Blue_Optical_Depth_550_Combined	X, Y	“best of” AOD
Dark_Target_Deep_Blue_Optical_Depth_550_Combined_QA	X, Y	QAC assignment
Dark_Target_Deep_Blue_Optical_Depth_550_Combined_AlqFlag	X, Y	Which product?

The Collection 6 MODIS aerosol products over land and ocean

R. C. Levy et al.

Table A1. MODIS band number, central wavelengths (CW) and Rayleigh optical depths (ROD) for C6 compared to C5.

Band #	C5 CW (μm)	C5 ROD Ocean	C5 ROD Land	C6 CW (μm)	C6 ROD
1	0.644	0.0521	0.0509	0.645	0.05086
2	0.855	0.0165	0.0164	0.856	0.01623
3	0.466	0.1954	0.1948	0.466	0.19260
4	0.553	0.0963	0.0963	0.553	0.09480
5	1.243	0.0037	0.0038	1.242	0.00362
6	1.632	0.0012	0.0013	1.629	0.00122
7	2.119	0.0004	0.0005	2.113	0.00043

[Title Page](#)
[Abstract](#)
[Introduction](#)
[Conclusions](#)
[References](#)
[Tables](#)
[Figures](#)
[⏪](#)
[⏩](#)
[◀](#)
[▶](#)
[Back](#)
[Close](#)
[Full Screen / Esc](#)
[Printer-friendly Version](#)
[Interactive Discussion](#)


The Collection 6 MODIS aerosol products over land and ocean

R. C. Levy et al.

Table A2. C6 gas absorption correction coefficients.

Wavelength	$K_{0,\lambda}^{\text{H}_2\text{O}}$	$K_{1,\lambda}^{\text{H}_2\text{O}}$	$K_{2,\lambda}^{\text{H}_2\text{O}}$	$\overline{\tau}_{\lambda}^{\text{H}_2\text{O}}$	$K_{0,\lambda}^{\text{O}_3}$	$K_{1,\lambda}^{\text{O}_3}$	$\overline{\tau}_{\lambda}^{\text{O}_3}$	$\overline{\tau}_{\lambda}^{\text{other}}$
0.47					1.975×10^{-05}	7.416×10^{-06}	2.399×10^{-03}	2.397×10^{-03}
0.55				1.029×10^{-04}	2.299×10^{-04}	8.952×10^{-05}	2.930×10^{-02}	1.239×10^{-03}
0.65	-5.772	0.993	-0.041	8.630×10^{-03}	2.935×10^{-04}	7.128×10^{-05}	2.335×10^{-02}	4.601×10^{-03}
0.86	-5.375	0.855	-0.028	1.130×10^{-02}				
1.24	-6.659	1.201	-0.054	4.340×10^{-03}				1.844×10^{-02}
1.63	-7.899	1.115	-0.012	1.210×10^{-03}				1.189×10^{-02}
2.11	-4.069	0.928	-0.047	4.390×10^{-02}				3.470×10^{-02}

Note that the K -coefficients are used when NCEP data are valid, whereas the global average optical depths are used when NCEP data are missing. In case of “other” gases, global average optical depth is assumed.

Title Page

Abstract

Introduction

Conclusions

References

Tables

Figures

◀

▶

◀

▶

Back

Close

Full Screen / Esc

Printer-friendly Version

Interactive Discussion



Table A3. SDSs and attributes contained in C6 MxD04_L2 file.

SDS Name	units	scale	valid(1)	valid(2)	DimList	Long_Name
Longitude #	Deg East	1	-180	180	X,Y	Geodetic Longitude
Latitude #	Deg North	1	-90	90	X,Y	Geodetic Latitude
Scan_Start_Time #	Secs 1993	1	0	3.16E+05	X,Y	TAI Time at Start of Scan replicated across the swath
Solar_Zenith #	Degrees	0.01	0	18 000	X,Y	Solar Zenith Angle, Cell to Sun
Solar_Azimuth #	Degrees	0.01	-18 000	18 000	X,Y	Solar Azimuth Angle, Cell to Sun
Sensor_Zenith #	Degrees	0.01	0	18 000	X,Y	Sensor Zenith Angle, Cell to Sensor
Sensor_Azimuth #	Degrees	0.01	-18 000	18 000	X,Y	Sensor Azimuth Angle, Cell to Sun
Scattering_Angle #*	Degrees	0.01	0	18 000	X,Y	Scattering Angle
Land_sea_Flag #	None	1	0	1	X,Y	Land_sea_Flag(based on Wisconsin cloud mask 0 = Ocean, 1 = Land)
Aerosol_Cldmask_Land_Ocean	None	1	0	1	X,500,Y,500	Aerosol Cloud Mask 500 meter resolution 0= cloud 1= clear
Cloud_Distance_Land_Ocean	None	1	0	60	X,500,Y,500	Distance (number of pixels) to nearest pixel identified as cloudy (500 m resolution)
Land_Ocean_Quality_Flag #	None	1	0	3	X,Y	Quality Flag for Land and ocean Aerosol retrievals 0= bad 1 = Marginal 2= Good 3=Very Good
Optical_Depth_Land_And_Ocean #*	None	0.001	-100	5000	X,Y	AOT at 0.55 micron for both ocean (Average) (Quality flag=1,2,3) and land (corrected) (Quality flag=3)
Image_Optical_Depth_Land_And_Ocean #	None	0.001	-100	5000	X,Y	AOT at 0.55 micron for both ocean (Average) and land (corrected) with all quality data (Quality flag=0,1,2,3)
Average_Cloud_Distance_Land_Ocean *	Pixels	1	0	60	X,Y	Average Distance (number of pixels) to nearest pixel identified as cloudy from each clear pixel
Aerosol_Type_Land #	None	1	1	5	X,Y	used for Aerosol Retrieval in 10 km retrieval box Aerosol Type: 1 = Continental, 2 = Moderate Absorption Fine, 3 = Strong Absorption Fine, 4 = Weak Absorption Fine, 5 = Dust Coarse
Fitting_Error_Land #	None	0.001	0	1000	X,Y	Spectral Fitting error for inversion over land
Surface_Reflectance_Land #	None	0.001	0	1000	X,Y,SoL2_Land	Estimated Surface Reflectance at 0.47,0.65 and 2.11 micron
Corrected_Optical_Depth_Land #*	None	0.001	-100	5000	X,Y,SoL3_Land	Retrieved AOT at 0.47, 0.55,0.65 micron
Corrected_Optical_Depth_Land_wav2p1 #	None	0.001	-100	5000	X,Y	Retrieved AOT at 2.11 micron
Optical_Depth_Ratio_Small_Land #	None	0.001	0	1000	X,Y	Fraction of AOT (at 0.55 micron) contributed by fine dominated model
Number_Pixels_Used_Land #*	None	1	1	400	X,Y,Band_Extra	Number of pixels used for land retrieval at 0.47,0.55,0.65,0.86,1.24,1.64,2.11 Microns (plus extra bands for NPP: 0.41,0.44,0.75 microns)
Mean_Reflectance_Land #	None	0.0001	0	10000	X,Y,Band_Extra	Mean reflectance of pixels used for land retrieval at 0.47,0.55,0.65,0.86,1.24,1.64,2.11 microns (plus extra bands for NPP: 0.41,0.44,0.75 Micron)
STD_Reflectance_Land #	None	0.0001	0	20 000	X,Y,Band_Extra	Standard deviation of reflectance of pixels used for land retrieval at 0.47,0.55,0.65,0.86,1.24,1.64,2.11 microns (plus extra bands for NPP: 0.41,0.44,0.75 Micron)
Mass_Concentration_Land #*	$\mu\text{g cm}^{-2}$	1	0	1000	X,Y	Estimated Column Mass (per area) using assumed mass extinction coefficients
Aerosol_Cloud_Fraction_Land #	None	0.001	0	1000	X,Y	Cloud fraction from Land aerosol cloud mask from retrieved and overcast pixels not including cirrus mask
Quality_Assurance_Land #	None	1	0	255	X,Y,QA_Byte	Runtime QA flags
Solution_Index_Ocean_Small #	None	1	1	4	X,Y,SoL_Ocean	index identifying fine mode from Look Up Table for "best" solution
Solution_Index_Ocean_Large #	None	1	5	9	X,Y,SoL_Ocean	index identifying coarse mode from Look Up Table for "best" solution

The Collection 6 MODIS aerosol products over land and ocean

R. C. Levy et al.

Title Page

Abstract

Introduction

Conclusions

References

Tables

Figures

◀

▶

◀

▶

Back

Close

Full Screen / Esc

Printer-friendly Version

Interactive Discussion

Table A3. Continued. SDSs and attributes contained in C6 MxD04_L2 file.

SDS Name	units	scale	valid(1)	valid(2)	DimList	Long_Name
Effective_Optical_Depth_Best_Ocean #	None	0.001	-100	5000	X,Y,Band,Ocean	Retrieved AOT for "best" solution at 0.47, 0.55,0.65,0.86,1.24,1.63,2.11 um
Effective_Optical_Depth_Average_Ocean *#	None	0.001	-100	5000	X,Y,Band,Ocean	Retrieved AOT for "average" solution at 0.47, 0.55,0.65,0.86,1.24,1.63,2.11 um
Optical_Depth_Small_Best_Ocean #	None	0.001	-100	5000	X,Y,Band,Ocean	Retrieved AOT of small mode for "best" solution at 0.47, 0.55,0.65,0.86,1.24,1.63,2.11 um
Optical_Depth_Small_Average_Ocean *#	None	0.001	-100	5000	X,Y,Band,Ocean	Retrieved AOT of small mode for "average" solution at 0.47, 0.55,0.65,0.86,1.24,1.63,2.11 um
Optical_Depth_Large_Best_Ocean #	None	0.001	-100	5000	X,Y,Band,Ocean	Retrieved AOT of large mode for "best" solution at 0.47, 0.55,0.65,0.86,1.24,1.63,2.11 um
Optical_Depth_Large_Average_Ocean *#	None	0.001	-100	5000	X,Y,Band,Ocean	Retrieved AOT of large mode for "average" solution at 0.47, 0.55,0.65,0.86,1.24,1.63,2.11 um
Mass_Concentration_Ocean *#	µg cm ²	1	0	1000	X,Y,Sol,Ocean	Estimated Column Mass (per area) using assumed mass extinction coefficients for "best" (1) and "average" (2) solutions
Aerosol_Cloud_Fraction_Ocean #	None	0.001	0	1000	X,Y	Cloud fraction from Ocean aerosol cloud mask from retrieved and overcast pixels not including cirrus mask
Effective_Radius_Ocean *#	µm	0.001	0	5000	X,Y,Sol,Ocean	Effective_Radius at 0.55 micron for "best" (1) and "average" (2) solutions
PSML003_Ocean *#	#/cm ²	1	0	1.00E+11	X,Y,Sol,Ocean	Inferred column number concentration (number per area) of particles larger than 0.03 micron for "best" (1) and "average" (2) solutions
Asymmetry_Factor_Best_Ocean #	None	0.001	0	3000	X,Y,Band,Ocean	Inferred Asymmetry_Factor for "best" solution at 0.47, 0.55,0.65,0.86,1.24,1.63,2.11 um
Asymmetry_Factor_Average_Ocean #	None	0.001	0	3000	X,Y,Band,Ocean	Inferred Asymmetry_Factor for "average" solution at 0.47, 0.55,0.65,0.86,1.24,1.63,2.11 um
Backscattering_Ratio_Best_Ocean #	None	0.001	0	3000	X,Y,Band,Ocean	Inferred Backscattering_Ratio for "best" solution at 0.47, 0.55,0.65,0.86,1.24,1.63,2.11 um
Backscattering_Ratio_Average_Ocean #	None	0.001	0	3000	X,Y,Band,Ocean	Inferred Backscattering_Ratio for "average" solution at 0.47, 0.55,0.65,0.86,1.24,1.63,2.11 um
Angstrom_Exponent_1_Ocean #	None	0.001	-1000	5000	X,Y,Sol,Ocean	Calculated Angstrom Exponent for 0.55 vs 0.86 micron for "best" (1) and "average" (2) solutions
Angstrom_Exponent_2_Ocean #	None	0.001	-1000	5000	X,Y,Sol,Ocean	Calculated Angstrom Exponent for 0.86 vs. 2.11 micron for "best" (1) and "average" (2) solutions
Least_Squares_Error_Ocean #	None	0.001	0	1000	X,Y,Sol,Ocean	Residual of least squares fitting for inversion over land for best (1) and average (2) solutions
Optical_Depth_Ratio_Small_Ocean_0.55micrn #	None	0.001	0	1000	X,Y,Sol,Ocean	Fraction of AOT (at 0.55 micron) contributed by fine mode for "best" (1) and "average" (2) solutions
Optical_Depth_by_models_ocean *#	None	0.001	-100	5000	X,Y,Sol,Index	Retrieved AOT (at 0.55 micron) partitioned by mode index (for XXX solution)
Number_Pixels_Used_Ocean *#	None	1	1	400	X,Y,Band,Extra	Number of pixels used for ocean retrieval at 0.47,0.55,0.65,0.86,1.24,1.64,2.11 Microns (plus extra bands for NPP: 0.41,0.44,0.75 microns)
Mean_Reflectance_Ocean #	None	0.0001	0	10000	X,Y,Band,Extra	Mean reflectance of pixels used for ocean retrieval at 0.47,0.55,0.65,0.86,1.24,1.64,2.11 microns (plus extra bands for NPP: 0.41,0.44,0.75 Micron)
STD_Reflectance_Ocean #	None	0.0001	0	20000	X,Y,Band,Extra	Standard deviation of reflectance of pixels used for ocean retrieval at 0.47,0.55,0.65,0.86,1.24,1.64,2.11 microns (plus extra bands for NPP: 0.41,0.44,0.75 Micron)

The Collection 6 MODIS aerosol products over land and ocean

R. C. Levy et al.

Title Page

Abstract

Introduction

Conclusions

References

Tables

Figures



Back

Close

Full Screen / Esc

Printer-friendly Version

Interactive Discussion

The Collection 6 MODIS aerosol products over land and ocean

R. C. Levy et al.

Title Page

Abstract

Introduction

Conclusions

References

Tables

Figures



Back

Close

Full Screen / Esc

Printer-friendly Version

Interactive Discussion



Table A3. Continued. SDSs and attributes contained in C6 MxD04_L2 file.

SDS Name	units	scale	valid(1)	valid(2)	DimList	Long_Name
Quality_Assurance_Ocean_#	None	1	0	255	X,Y,QA.Byte	Run time QA flags
Deep_Blue_Aerosol_Optical_Depth_550_Land	None	0.001	0	5000	X,Y	AOT at 0.55 micron for land with all quality data (Quality flag=1,2,3)
Deep_Blue_Aerosol_Optical_Depth_Land	None	0.001	0	5000	X,Y,Band_DeepBlue	AOT at 0.41, 0.47, and 0.65 micron for land with all quality data (Quality flag=1,2,3)
Deep_Blue_Angstrom_Exponent_Land	None	0.001	-500	5000	X,Y	Deep Blue Angstrom Exponent for land (0.41–0.47 micron) with all quality data (Quality flag=1,2,3)
Deep_Blue_Single_Scattering_Albedo_Land	None	0.001	700	1000	X,Y,Band_DeepBlue	Deep Blue Single Scattering Albedo at 0.41, 0.47, and 0.65 micron for land with all quality data (Quality flag=1,2,3)
Deep_Blue_Surface_Reflectance_Land	None	0.001	0	1000	X,Y,Band_DeepBlue	Deep Blue Surface Reflectance at 0.41, 0.47, and 0.65 micron for land with all quality data (Quality flag=1,2,3)
Deep_Blue_Mean_Reflectance_Land	None	0.0001	0	10000	X,Y,Band_DeepBlue	Average measured TOA reflectance after cloud screening at 0.41, 0.47, and 0.65 micron for land
Deep_Blue_Number_Pixels_Used_Land	None	1	0	100	X,Y,Band_DeepBlue	Number of pixels used for AOT retrieval at 0.41, 0.47, and 0.65 micron for land
Deep_Blue_Aerosol_Optical_Depth_550_Land_STD	None	0.001	0	10000	X,Y	Standard deviation of Deep Blue AOT at 0.55 micron for land with all quality data (Quality flag=1,2,3)
Deep_Blue_Aerosol_Optical_Depth_Land_STD	None	0.001	0	10000	X,Y,Band_DeepBlue	Standard deviation of Deep Blue AOT at 0.41, 0.47, and 0.65 micron for land with all quality data (Quality flag=1,2,3)
Deep_Blue_Cloud_Fraction_Land	None	0.001	0	1000	X,Y	Cloud fraction from Deep Blue Aerosol cloud mask over land
Deep_Blue_Usefulness_Flag	None	1	0	1	X,Y	Deep Blue Aerosol Usefulness Flag (0= Not Useful, 1= Useful)
Deep_Blue_Confidence_Flag	None	1	0	3	X,Y	Deep Blue Aerosol Confidence Flag (0= No Confidence (or fill), 1= Marginal, 2= Good, 3= Very Good)
AOD_550_Dark_Target_Deep_Blue_Combined *	None	0.001	-500	5000	X,Y	Combined Dark Target, Deep Blue AOT at 0.55 micron for land and ocean
AOD_550_Dark_Target_Deep_Blue_Combined_QA_Flag	1	0	3	X,Y	X,Y	Combined Dark Target, Deep Blue Aerosol Confidence Flag (0= No Confidence (or fill), 1= Marginal, 2= Good, 3= Very Good)
AOD_550_Dark_Target_Deep_Blue_Combined_QA_Flag	1	0	2	X,Y	X,Y	Combined Dark Target, Deep Blue AOT at 0.55 micron Algorithm Flag (0=Dark Target, 1=Deep Blue, 2=Mixed)
Glint_Angle_#	Degrees	0.01	0	18000	X,Y	Glint Angle
Wind_Speed_Ncep_Ocean_#	m s ⁻¹	0.01	0	8000	X,Y	Wind Speed based on NCEP reanalysis for Ocean
Topographic_Altitude_Land_#	km	0.01	0	1400	X,Y	Averaged topographic altitude (in km) for Land

X,Y refers to a 2-dimensional array along/across the swath. Some parameters have a third dimension, which is described in the “Long_Name”.

Note that most SDSs are stored as integer format, so the scale must be applied as a multiplier to derive the physical units.

Valid(1) and Valid(2) represent the minimum and maximum valid values for a particular SDS (usually in integer form).

* SDSs that are aggregated to Level 3 (from MxD04.L2 10 km files).

SDSs included in 3 km file (MxD04_3K).

The Collection 6 MODIS aerosol products over land and ocean

R. C. Levy et al.

[Title Page](#)

[Abstract](#) [Introduction](#)

[Conclusions](#) [References](#)

[Tables](#) [Figures](#)

[◀](#) [▶](#)

[◀](#) [▶](#)

[Back](#) [Close](#)

[Full Screen / Esc](#)

[Printer-friendly Version](#)

[Interactive Discussion](#)

Table A4. Product quality and retrieval processing QA flags over land.

Flag name	# of bits	Bit value	Description	Comments
Product quality QA summary flags				
Summary quality flag for aerosol optical thickness ("QA usefulness")	1	0	Not useful data	(0) All products are fill values
		1	Useful	(1) Valid products
Estimated quality flag of aerosol optical thickness "QA Confidence flag" (QAC)	3	0	Poor	
		1	Marginal	
		2	Good	
		3	Very Good	
		4–7	Not Used (TBD)	
Summary quality flag for aerosol optical thickness	1	0	Not useful data	Repeat of bit 0
		1	Useful	
Estimated quality flag of aerosol optical thickness	3	0	Poor	Repeat of bits 1–3
		1	marginal	
		2	Good	
		3	Very Good	
		4–7	Not Used (TBD)	
Retrieval processing QA flags – Processing path flags				
Part I: retrieving condition flags when inversion is performed - retrieved value will be output	4	0	Retrieval performed normally (no issues)	(0) QAC = 3
		1	Procedure 2 performed (semi-bright surface, $\rho_{2,11} > 0.25$)	(1) QAC=0
		2	Water pixels in 10 × 10 box	(2) QAC=0
		3	Possible Cirrus present	(3) QAC=0
		4	Fitting error $\varepsilon > 0.25$	(4) QAC=0
		5	$-0.1 < \text{Retrieved } \tau_g < 0.0$	(5) QAC=3
		6	# pixels between 12 & 20	(6) QAC=0
		7	# pixels between 21 & 30	(7) QAC=1
		8	# pixels between 31 & 50	(8) QAC=2
		9	Angstrom out of bounds	(9) QAC=0
		10	Retrieved $\tau < 0.2$	(10) QAC=3
		11	No Retrieval	(11) QAC=0
	12–15	Not used (TBD)	(12–15)	



The Collection 6 MODIS aerosol products over land and ocean

R. C. Levy et al.

[Title Page](#)
[Abstract](#) [Introduction](#)
[Conclusions](#) [References](#)
[Tables](#) [Figures](#)
⏪ ⏩
◀ ▶
[Back](#) [Close](#)
[Full Screen / Esc](#)
[Printer-friendly Version](#)
[Interactive Discussion](#)

Table A4. Continued. Product quality and retrieval processing QA flags over land.

Flag name	# of bits	Bit value	Description	Comments
Part II: retrieving condition flags when inversion is NOT performed-fill alues are output	4	0	No error	QAC=0
		1	Solar/sensor geometry out of bounds in LUT	QA Useful flag=0
		2	Apparent reflectance out of bounds in LUT	
		3	# pixels < 12	
		4	$\rho_{2,11} > 0.35$ (too bright)	
		5	Retrieved $\tau < -0.1$	
		6	Retrieved $\tau > 5.0$	
Aerosol Type	2	7–8	Not used (TBD)	
		0	All empty	Not currently filled
		1		
		2		
Thin cirrus or stratospheric aerosol index	2	0	All empty	Not currently filled
		1		
		2		
		3		
Retrieval processing QA flags – Input data resource flags				
Total ozone	2	0	TOVS	
		1	TOMS	
		2	Climatology	
		3	DAO	
Total perceptible water	2	0	NCEP/GDAS	
		1	MOD05 – NIR	
		2	Climatology	
		3	DAO	
Snow cover	2	0	MOD35-cloud mask	
		1	MOD10-L3 8 day product.	
		2–3	TBD	
Spare	6		TBD	



The Collection 6 MODIS aerosol products over land and ocean

R. C. Levy et al.

Title Page

Abstract

Introduction

Conclusions

References

Tables

Figures

⏪

⏩

◀

▶

Back

Close

Full Screen / Esc

Printer-friendly Version

Interactive Discussion



Table A5. Product quality and retrieval processing QA flags over ocean.

Flag name	# of bits	Bit value	Description	Comments
Product quality QA summary flags				
Summary quality flag for "best" solution: "QA usefulness" flag	1	0	Not useful	(0) products are fill values (1) valid products
		1	Useful	
Estimated quality of aerosol parameters of "best" solution "QA Confidence" or "QAC"	3	0	Poor	
		1	Marginal	
		2	Good	
		3	Very Good	
		4–7	Not Used (TBD)	
Summary quality flag for "average" solution: "QA usefulness" flag	1	0	Not useful	(0) products are fill values (1) valid products
		1	Useful	
Estimated quality of aerosol parameter of "average" solution "QA Confidence" or "QAC"	3	0	Poor	average solution is used for populating joint product
		1	Marginal	
		2	Good	
		3	Very Good	
		4–7	Not Used (TBD)	
Retrieval processing QA flags - Processing path flags				
Part I: retrieving condition flags when inversion is NOT performed - fill values are output	4	0	Retrieval is performed	(0) QAC defined by PartII (1) QAC=0 no retrieval, but some arrays filled. (2–10) QAC=0, and no arrays filled.
		1	Glitter present (GA < 40°)	
		2	Cloudy (less than 10 pixels)	
		3	*** Not used***	
		4	Number of valid VIS/SWIR channels (0.55–1.24 μm) is insufficient	
		5	Number of valid channels <3	
		6	Geometry out of bounds	
		7	Land pixels in 10 x 10 km box	
		8	Retrieved τg < -0.01	
		9	Retrieved τg > 5.0	
		10	No valid reflectance for any channel	
		11–15	TBD	

Table A5. Continued. Product quality and retrieval processing QA flags over ocean.

Flag name	# of bits	Bit value	Description	Comments		
Part II: retrieving condition flags when inversion is performed – retrieved value will be output	4	0	Retrieval performed normally	(0) QAC=3		
		1	Number of pixels within 10 × 10 km box is < 10 % (40 pixels)	(1) QAC=1		
		2	$\rho_{0.86} < 1.5\rho_{0.86}^{RAY}$. Signal enough to retrieve τ ; Set size distribution $\eta =$ fill value	(2) QAC=2		
		3	1.63 μm channel not used	(3) QAC=1		
		4	2.11 μm channel not used	(4) QAC=1		
		5	2.11 & 1.63 μm not used	(5) QAC=0		
		6	Variability of reflectance: Large uncertainty in both retrieved τ and aerosol type	(6) QAC=1		
		7	Variability of reflectance: Large uncertainty in retrieved τ , but aerosol type is stable.	(7) QAC=2		
		8	The best value of θ is larger than the threshold value (3%)	(8) QAC=1		
		9	$-0.01 < t(550 \text{ nm}) < 0$ but to avoid bias in level 3 product	(9) QAC=0		
		10	$30^\circ < \text{GA} < 40^\circ$ (will be overwritten by either #11 or #12)	(10) QAC=1		
		11	$\text{GA} < 40^\circ$. Glint (store only $\rho_{0.1}$, var, and number of pixels, unless #12)	(11) QAC=0		
		12	$\text{GA} < 40^\circ$ and $\rho_{0.47}/\rho_{0.66} < 0.95$. In glint thick dust	(12) QAC=0		
		13	$\rho_{1.38}$ & $\rho_{1.24}$ suggest possible cirrus contamination	(13) QAC=2		
		14	$\text{GA} > 40^\circ$ and $\rho_{0.47}/\rho_{0.66} > 0.75$. Off glint thick dust	(14) QAC=2		
		15	No retrieval performed	(15) QAC=0		
		16–19	TBD	(16–19)		
		20	$\rho_{0.86} < 1.1 \rho_{0.86}^{RAY}$. Not enough signal to retrieve anything (set $\tau = 0.0$ and size parameters to fill)	(20) QAC=1		
		Retrieval processing QA flags – Input data resource flags				
		Total ozone	2	0	TOVS	
1	TOMS					
2	Climatology					
3	DAO					
Total perceptible water	2	0	NCEP/GDAS			
		1	MOD05 – NIR			
		2	Climatology			
		3	DAO			
Snow cover	2	0	MOD35-cloud mask			
		1	MOD10-L3 8 day product.			
		2–3	TBD			
Spare	2		TBD			

**The Collection 6
MODIS aerosol
products over land
and ocean**

R. C. Levy et al.

[Title Page](#)
[Abstract](#) [Introduction](#)
[Conclusions](#) [References](#)
[Tables](#) [Figures](#)
◀ ▶
◀ ▶
[Back](#) [Close](#)
[Full Screen / Esc](#)
[Printer-friendly Version](#)
[Interactive Discussion](#)



**The Collection 6
MODIS aerosol
products over land
and ocean**

R. C. Levy et al.

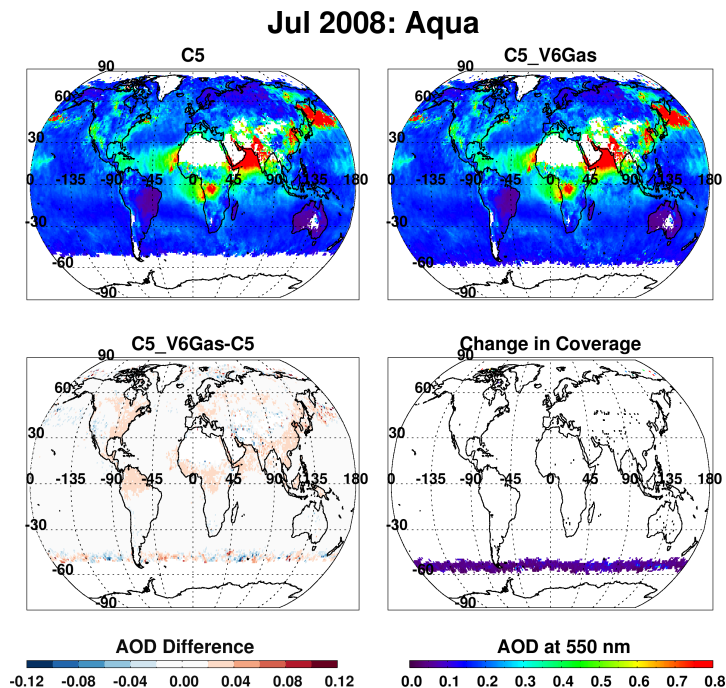


Fig. 1. Gridded, monthly averaged $1^\circ \times 1^\circ$ AOD (at $0.55 \mu\text{m}$) over land and ocean retrieved from Aqua for July 2008. The same C5-like retrieval algorithm is applied to both the C5 LUT (top left) and C6-like LUT (top right), with differences (New-Old) plotted in the bottom left. The changed (additional) pixel coverage is illustrated in the bottom right panel. Note that each gridded value is a simple average of all L2 data having sufficient quality ($\text{QAC} = 3$ for land and $\text{QAC} \geq 1$ for ocean) during the month.

Title Page

Abstract

Introduction

Conclusions

References

Tables

Figures

◀

▶

◀

▶

Back

Close

Full Screen / Esc

Printer-friendly Version

Interactive Discussion

**The Collection 6
MODIS aerosol
products over land
and ocean**

R. C. Levy et al.

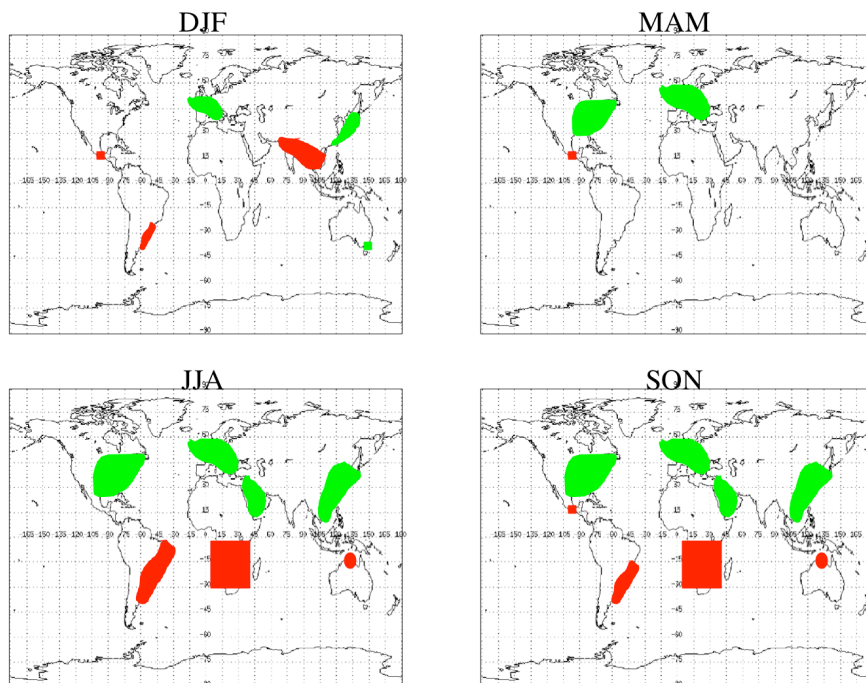


Fig. 2. New fine model map for four seasons: winter, spring, summer, fall. For each map, over land regions, red (green) mark where strongly absorbing (weakly absorbing) aerosol models are assumed. Areas with no color are assumed as moderately absorbing.

[Title Page](#)[Abstract](#)[Introduction](#)[Conclusions](#)[References](#)[Tables](#)[Figures](#)[◀](#)[▶](#)[◀](#)[▶](#)[Back](#)[Close](#)[Full Screen / Esc](#)[Printer-friendly Version](#)[Interactive Discussion](#)

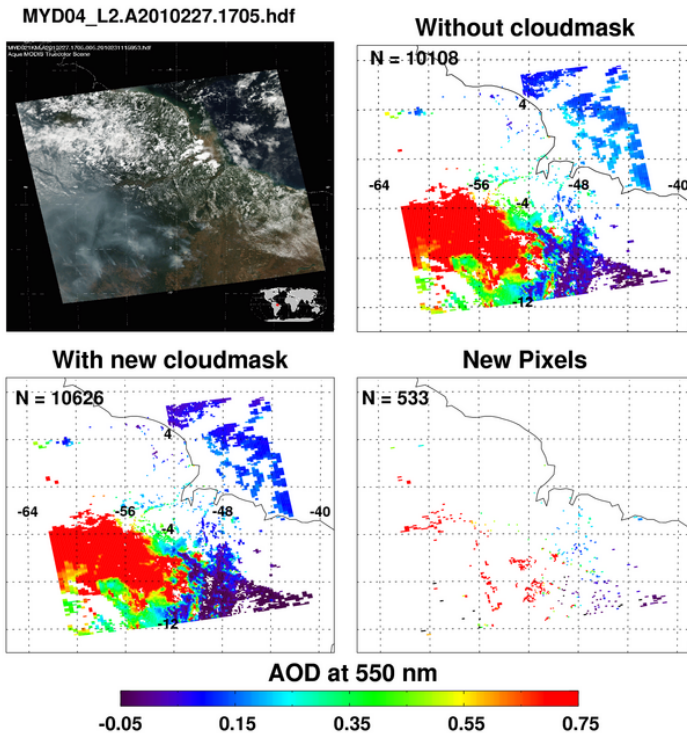


Fig. 3. Granule retrieved over northeastern South America from MODIS-Aqua on 15 August 2010 at 17:05 UTC. Top left: True-color (RGB) showing smoke and cloud scene taken from <http://modis-atmos.gsfc.nasa.gov>. Top right/bottom left: retrieved high quality (QAC = 3 over land and QAC \geq 1 over ocean) AOD at 0.55 μ m, without/with the 0.47 μ m cloud mask call-back (standard deviation test) over land. Bottom right: new (Smoke) pixels over land that have been reclaimed.

Title Page

Abstract

Introduction

Conclusions

References

Tables

Figures

◀

▶

◀

▶

Back

Close

Full Screen / Esc

Printer-friendly Version

Interactive Discussion

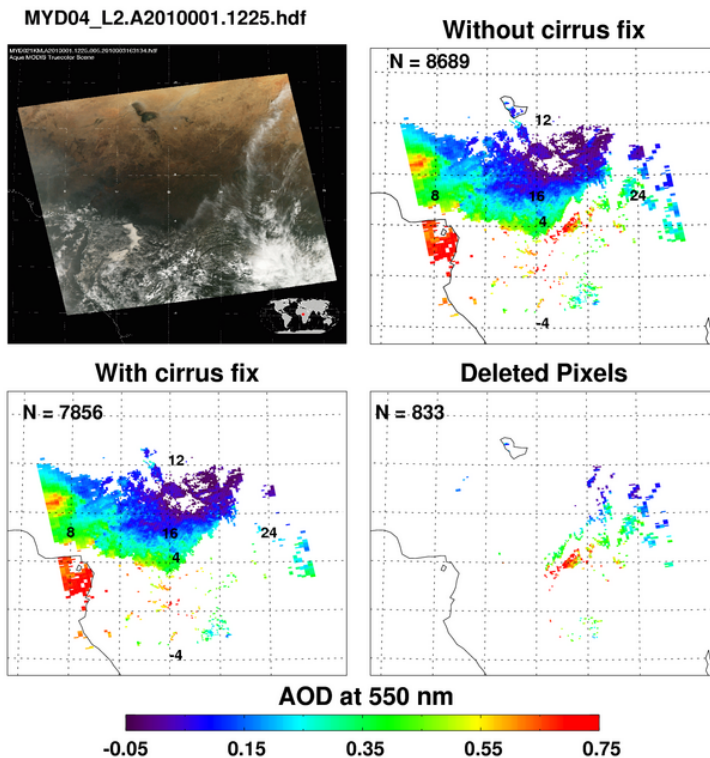


Fig. 4. MODIS-Aqua granule over central Africa, observed on 1 January 2010 at 12:25 UTC. Top left: true color image constructed from red/green/blue channels (modis-atmos.gsfc.nasa.gov). Top right/Bottom left: retrieved, high quality (QAC = 3 over land, QAC \geq 1 over water) AOD at 0.55 μm before/after the cirrus bug fix. Bottom right: Pixels that have been deleted over land as a result of degraded QAC.

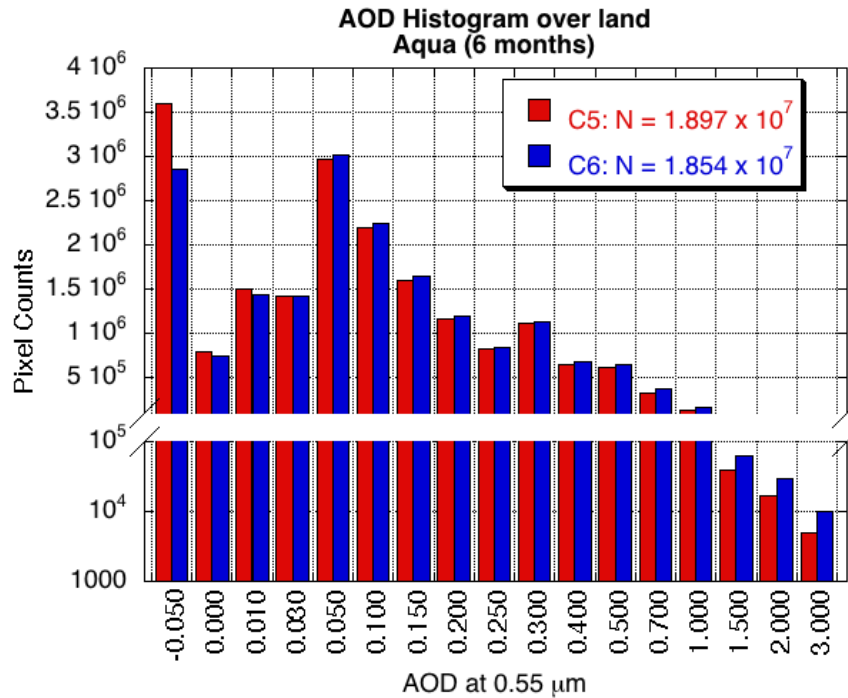


Fig. 5. Histograms for global retrieved Level 2 DT-land AOD (at 0.55 μm) from Aqua for six months. Plotted are data from C5 and C6.

[Title Page](#)
[Abstract](#) [Introduction](#)
[Conclusions](#) [References](#)
[Tables](#) [Figures](#)
[◀](#) [▶](#)
[◀](#) [▶](#)
[Back](#) [Close](#)
[Full Screen / Esc](#)
[Printer-friendly Version](#)
[Interactive Discussion](#)

The Collection 6 MODIS aerosol products over land and ocean

R. C. Levy et al.

Title Page

Abstract

Introduction

Conclusions

References

Tables

Figures

⏪

⏩

◀

▶

Back

Close

Full Screen / Esc

Printer-friendly Version

Interactive Discussion



DT-Land: Aqua 2008

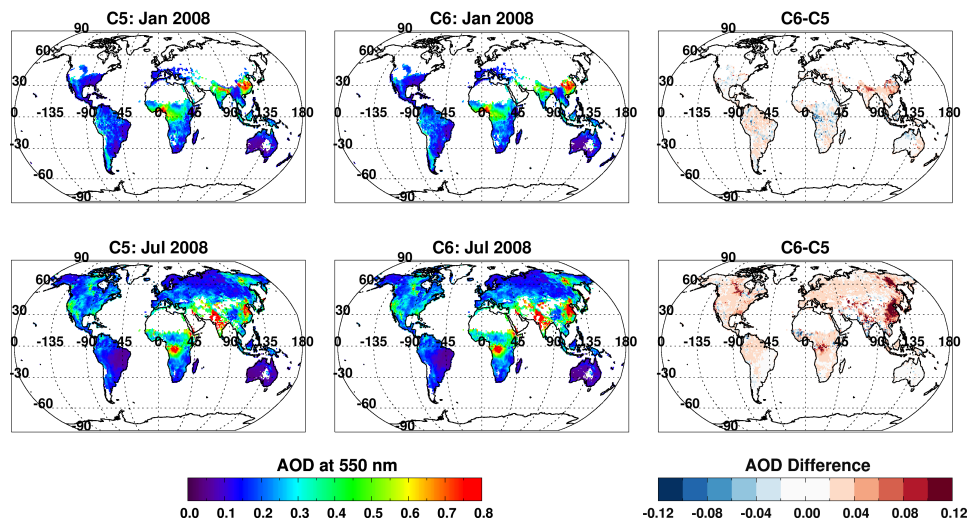


Fig. 6. Gridded, monthly averaged $1^\circ \times 1^\circ$ AOD (at $0.55 \mu\text{m}$) over land (QAC = 3) retrieved from Aqua for January 2008 (top row) and July 2008 (bottom row). For each row, the left panel is an aggregated product produced from C5, the middle panel is from C6, and the right panel is the differences C6-C5.

The Collection 6 MODIS aerosol products over land and ocean

R. C. Levy et al.

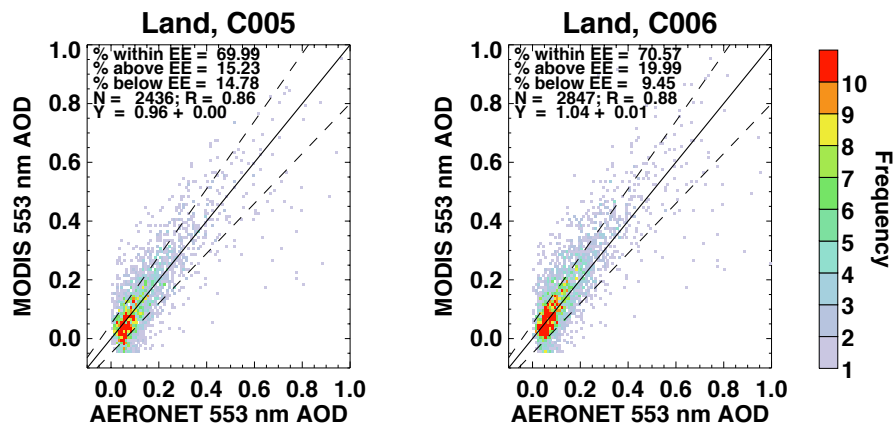


Fig. 7. Frequency scatterplots for AOD at $0.55\ \mu\text{m}$ over dark-land compared to AERONET, plotted from 6 months of Aqua (January and July, 2003, 2008 and 2010), computed with C5 algorithm (left) and C6 algorithm (right). One-one lines and EE envelopes $\pm(0.05 + 15\%)$ are plotted as solid and dashed lines. Collocation statistics are presented in each panel.

Title Page

Abstract

Introduction

Conclusions

References

Tables

Figures

◀

▶

◀

▶

Back

Close

Full Screen / Esc

Printer-friendly Version

Interactive Discussion

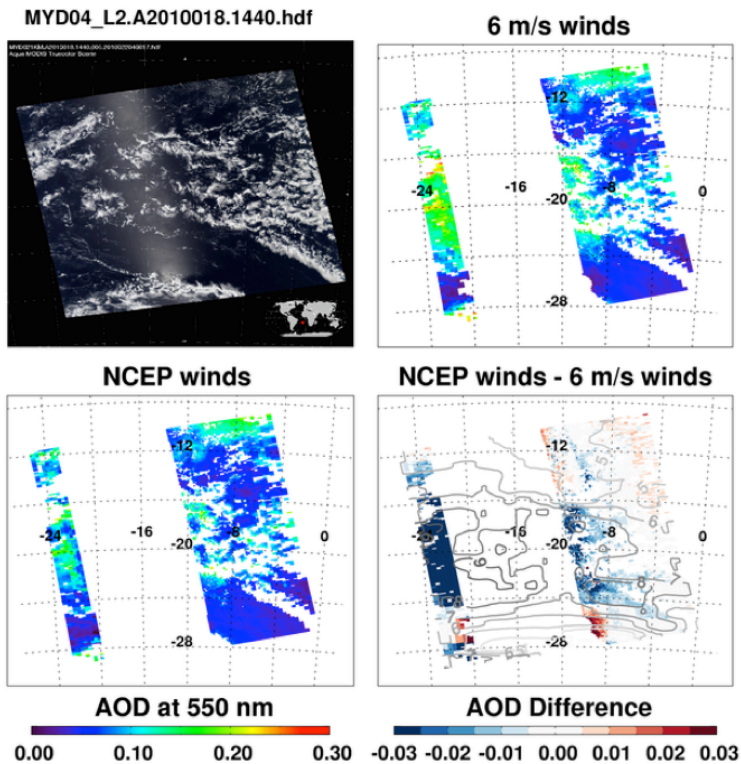


Fig. 8. Granule retrieved over the Atlantic Ocean from MODIS-Aqua taken on 18 January 2010 at 14:40 UTC. Top left: true color image (RGB) from <http://modis-atmos.gsfc.nasa.gov>. Top right/bottom left: retrieved high quality ($QAC \geq 1$ over ocean) AOD at $0.55 \mu\text{m}$, without/with use of NCEP surface wind speed. Bottom right: Change in AOD with use of wind information, with NCEP wind speeds overplotted in gray.

Title Page

Abstract

Introduction

Conclusions

References

Tables

Figures

⏪

⏩

◀

▶

Back

Close

Full Screen / Esc

Printer-friendly Version

Interactive Discussion



Aqua: 20080701

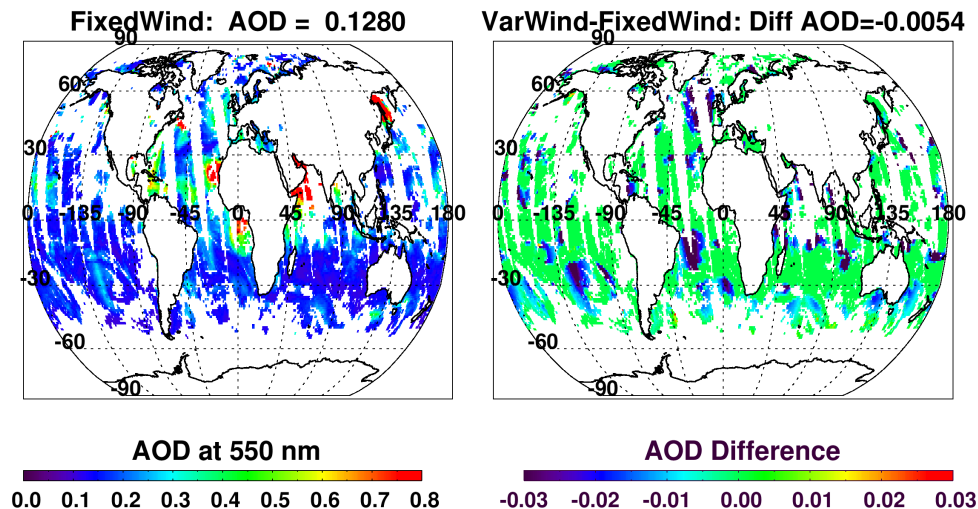


Fig. 9. Global, over-ocean AOD at $0.55 \mu\text{m}$, for MODIS-Aqua, 2008 day 183 (1 July). Left: AOD using fixed wind speed (6 m s^{-1}) LUT, and the corresponding mean AOD. Right: changes in AOD if using variable wind speed LUT (compared to fixed), with the global mean AOD difference reported in the title. Note that the largest differences are near the glint mask where the rough ocean surface model is sensitive to assumed wind speed.

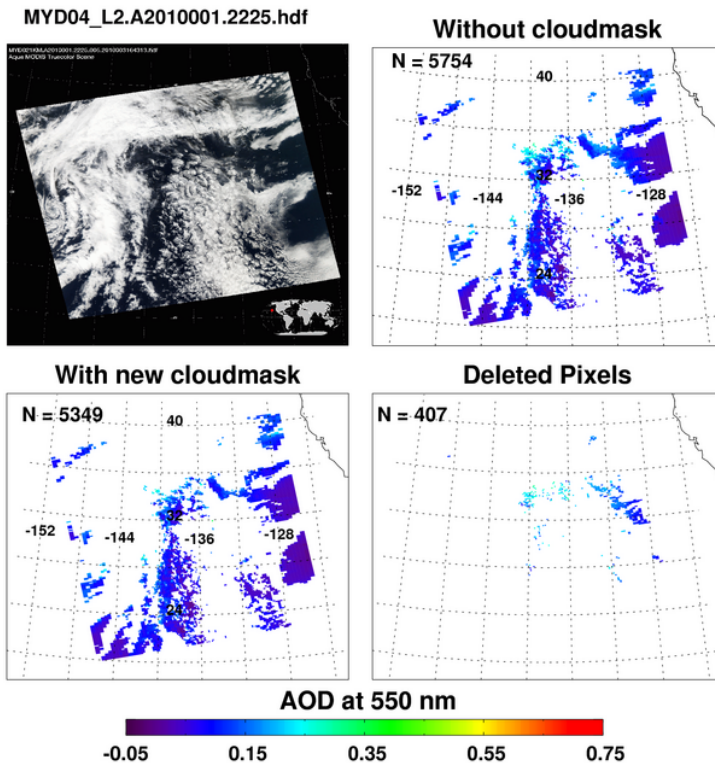


Fig. 10. Granule retrieved over the Pacific Ocean from MODIS-Aqua taken on 1 January 2010 at 22:25 UTC. Top left: true-color (RGB) showing scene taken from <http://modis-atmos.gsfc.nasa.gov>. Top right/bottom left: retrieved high quality (QAC ≥ 1 over ocean) AOD at 0.55 μm , without/with the revised 1.38 μm cloud mask test. Bottom right: cirrus contaminated pixels that have been removed over ocean.

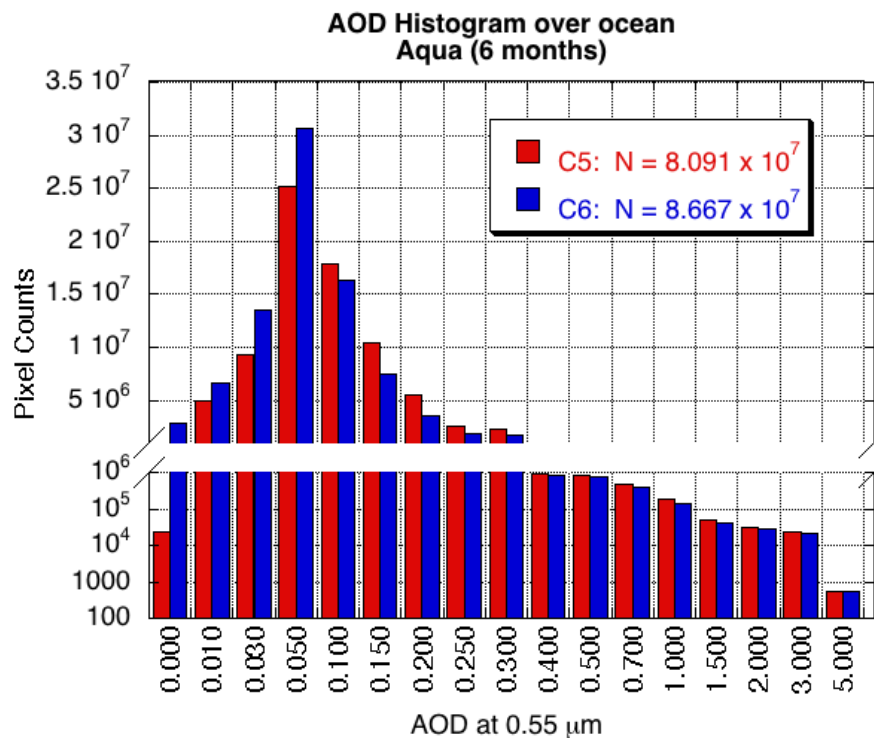


Fig. 11. Histograms for global retrieved Level 2 DT-ocean AOD (at 0.55 μm) from Aqua for six months. Plotted are data from C5 and C6.

[Title Page](#)
[Abstract](#)
[Introduction](#)
[Conclusions](#)
[References](#)
[Tables](#)
[Figures](#)
[◀](#)
[▶](#)
[◀](#)
[▶](#)
[Back](#)
[Close](#)
[Full Screen / Esc](#)
[Printer-friendly Version](#)
[Interactive Discussion](#)

The Collection 6 MODIS aerosol products over land and ocean

R. C. Levy et al.

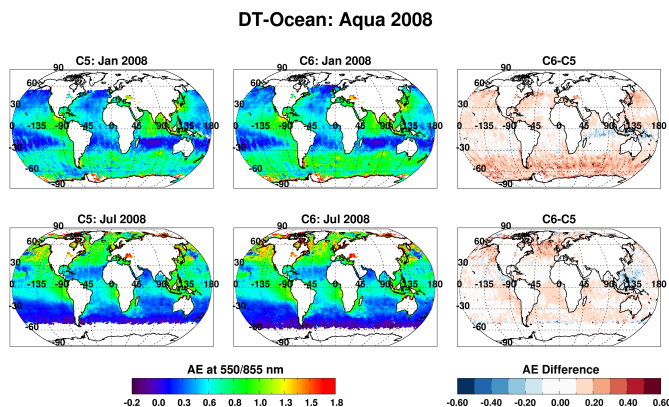
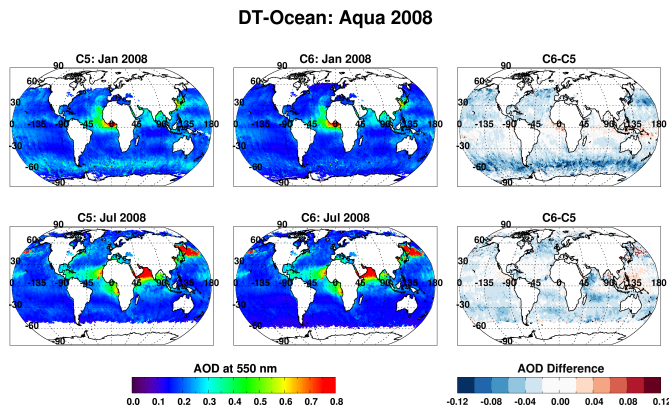


Fig. 12. Gridded, monthly averaged $1^\circ \times 1^\circ$ AOD/AE (at $0.55 \mu\text{m}$) over ocean retrieved from Aqua for January 2008 (top row) and July 2008 (bottom row). For each row, the left panel is an aggregated product produced from C5, the middle panel is from C6, and the right panel are differences C6-C5.

[Title Page](#)
[Abstract](#) [Introduction](#)
[Conclusions](#) [References](#)
[Tables](#) [Figures](#)
◀ ▶
◀ ▶
[Back](#) [Close](#)
[Full Screen / Esc](#)
[Printer-friendly Version](#)
[Interactive Discussion](#)



The Collection 6 MODIS aerosol products over land and ocean

R. C. Levy et al.

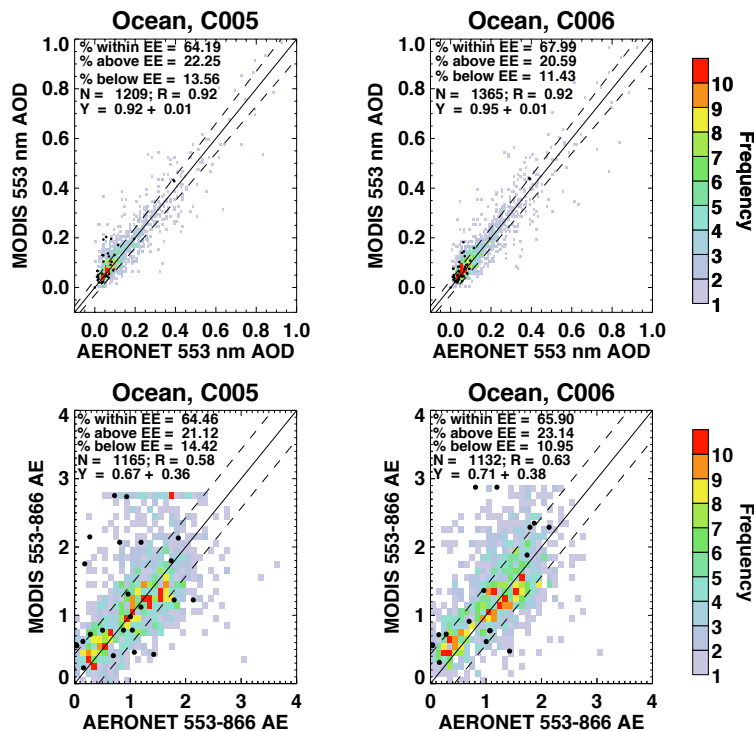


Fig. 13. Frequency scatterplots for AOD at 0.55 μm (top row), and AE at 0.86/0.55 (bottom row) over ocean compared to AERONET and MAN sunphotometers, plotted from 6 months of Aqua (January and July, 2003, 2008 and 2010). MODIS parameters are computed with C5 algorithm (left) and C6 algorithm (right). One-one lines and EE envelopes are plotted as solid and dashed lines, respectively. EE for AOD and AE is $\pm(0.03 + 5\%)$ and ± 0.4 , respectively. Comparisons with AERONET are plotted in colors (and gray for single points), whereas comparisons with MAN are black dots. Collocation statistics (with AERONET) are presented in each panel.

The Collection 6 MODIS aerosol products over land and ocean

R. C. Levy et al.

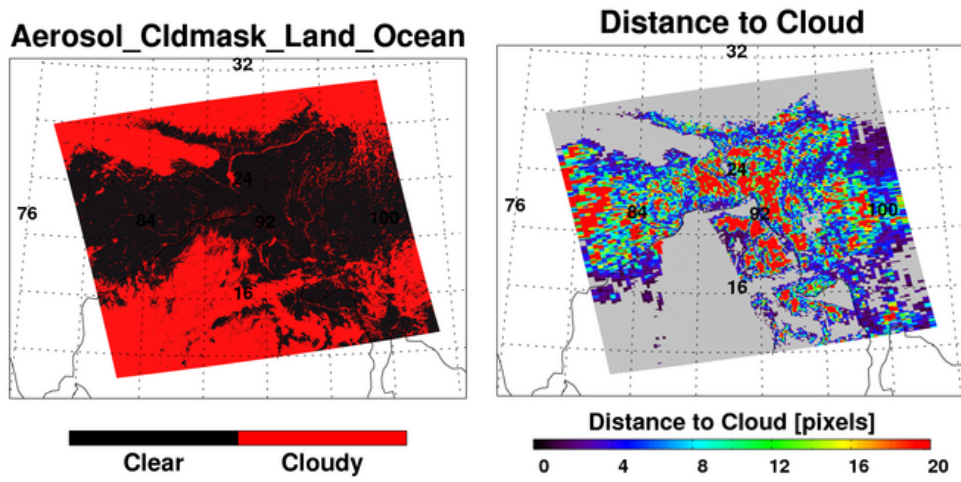


Fig. 14. New aerosol cloud mask variables, both from an AQUA granule on 03 January 2010 at 07:20 UTC. Left: aerosol cloud mask. Right: distance to cloud.

Title Page

Abstract Introduction

Conclusions References

Tables Figures

⏪ ⏩

◀ ▶

Back Close

Full Screen / Esc

Printer-friendly Version

Interactive Discussion



[Title Page](#)[Abstract](#)[Introduction](#)[Conclusions](#)[References](#)[Tables](#)[Figures](#)[Back](#)[Close](#)[Full Screen / Esc](#)[Printer-friendly Version](#)[Interactive Discussion](#)

DBDT Merge: Aqua 2008

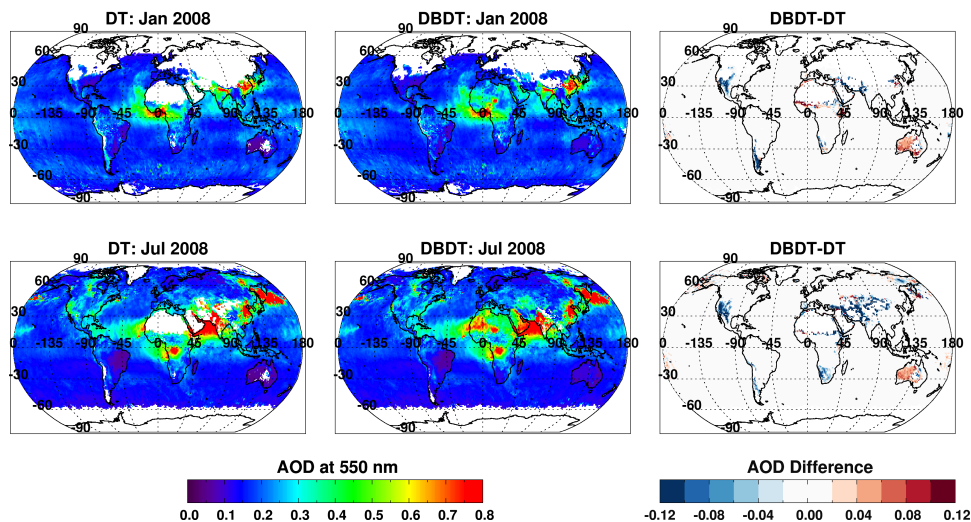


Fig. 15. Global map of Aqua-derived AOD (at $0.55\ \mu\text{m}$) for January (top) and July (bottom) 2008, for DT only (left), merged DT/DB (center), and differences between DTDB and DT, of grids where DT retrieves (right).

The Collection 6 MODIS aerosol products over land and ocean

R. C. Levy et al.

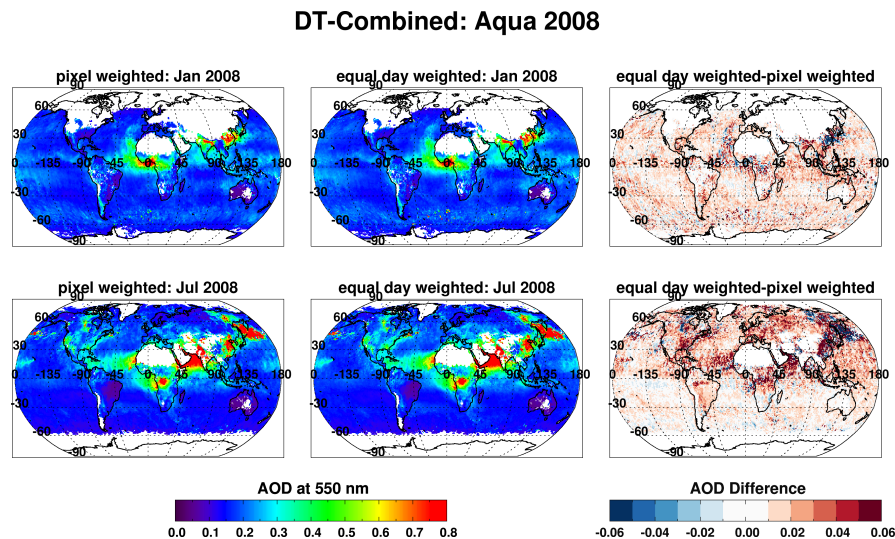
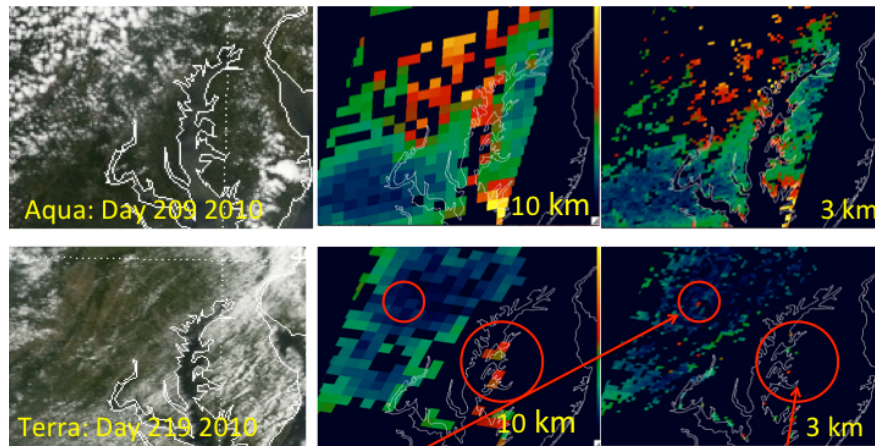


Fig. 16. Maps of gridded ($1^\circ \times 1^\circ$) monthly mean Level 3 (MxD08.M3) product (Optical_Depth_Land_And_Ocean_Mean), for January 2008 (top row) and July 2008 (bottom row). For each row, the left panel is the pixel-weighted product produced for C5, the middle panel is the equal-day weighted product for C6, and the right panel is the differences C6-C5.

The Collection 6 MODIS aerosol products over land and ocean

R. C. Levy et al.



- 3 km mirrors 10 km product (pattern and magnitude)
- 3 km introduces **noise**, but also can reduce spatial impact of **outliers**

Fig. 17. Plots of true-color RGB, 10 km AOD and 3 km AOD, derived from two granules observed over Maryland during the summer of 2010. The AOD scale ranges from 0.0 (dark blue) to 0.5 (yellow). One red circle identifies a noisy retrieval introduced by the 3 km product that does not exist at 10 km. The other circle identifies a region in which cloud effects are accentuated in the 10 km product but are put into better perspective in the finer resolution product.

[Title Page](#)
[Abstract](#)
[Introduction](#)
[Conclusions](#)
[References](#)
[Tables](#)
[Figures](#)
[◀](#)
[▶](#)
[◀](#)
[▶](#)
[Back](#)
[Close](#)
[Full Screen / Esc](#)
[Printer-friendly Version](#)
[Interactive Discussion](#)

**The Collection 6
MODIS aerosol
products over land
and ocean**

R. C. Levy et al.

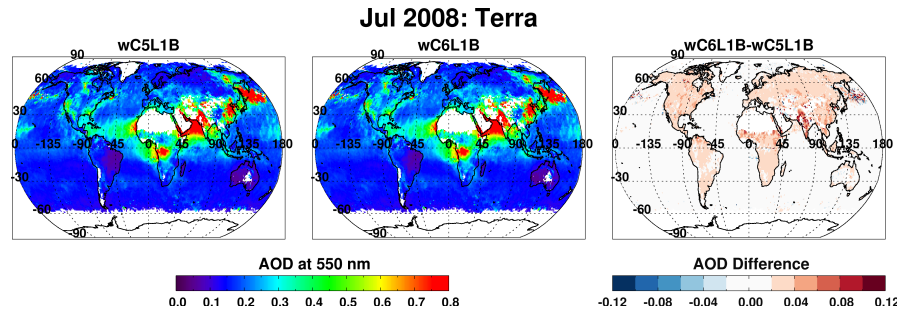


Fig. 18. Gridded, monthly averaged $1^\circ \times 1^\circ$ AOD (at $0.55 \mu\text{m}$) over land and ocean retrieved from Terra for July 2008. The same C6 retrieval algorithm is applied to both the C5 L1B (left) and the expected C6 L1B (center), with differences (New-Old) plotted on the right. Note that each gridded value is a simple average of all L2 data having sufficient quality (QAC = 3 for land and QAC ≥ 1 for ocean) during the month.

Title Page

Abstract

Introduction

Conclusions

References

Tables

Figures

◀

▶

◀

▶

Back

Close

Full Screen / Esc

Printer-friendly Version

Interactive Discussion